On the Non-Orthogonal Layered Broadcast Codes in Cooperative Wireless Networks

by

Payam Padidar

A thesis
presented to the University of Waterloo
in fulfillment of the
thesis requirement for the degree of
Doctor of Philosophy
in
Electrical and Computer Engineering

Waterloo, Ontario, Canada, 2020

Examining Committee Membership

The following served on the Examining Committee for this thesis. The decision of the Examining Committee is by majority vote.

External Examiner:	Dongkyun Kim Professor, School of Computer Science and Engineering, Kyungpook National University, Korea.
Supervisor:	Pin-Han Ho Professor, Dept. of Electrical and Computer Engineering, University of Waterloo
Internal Member:	Patrick Mitran Professor, Dept. of Electrical and Computer Engineering, University of Waterloo
Internal Member:	Liang-Liang Xie Professor, Dept. of Electrical and Computer Engineering, University of Waterloo
Internal-External Member:	Laura Sanità Associate Professor, Combinatorics & Optimization Department, University of Waterloo

Author's Declaration

I hereby declare that I am the sole author of this thesis. This is a true copy of the thesis, including any required final revisions, as accepted by my examiners.

I understand that my thesis may be made electronically available to the public.

Abstract

A multi-fold increase in spectral efficiency and throughput are envisioned in the fifth generation of cellular networks to meet the requirements of International Telecommunication Union (ITU) IMT-2020 on massive connectivity and tremendous data traffic. This is achieved by evolution in three aspects of current networks. The first aspect is shrinking the cell sizes and deploying dense picocells and femtocells to boost the spectral reuse. The second is to allocate more spectrum resources including millimeter-wave bands. The third is deploying highly efficient communications and multiple access techniques. Non-orthogonal multiple access (NOMA) is a promising communication technique that complements the current commercial spectrum access approach to boost the spectral efficiency, where different data streams/users' data share the same time, frequency and code resource blocks (sub-bands) via superimposition with each other. The receivers decode their own messages by deploying the successive interference cancellation (SIC) decoding rule. It is known that the NOMA coding is superior to conventional orthogonal multiple access (OMA) coding, where the resources are split among the users in either time or frequency domain.

The NOMA based coding has been incorporated into other coding techniques including multi-input multi-output (MIMO), orthogonal frequency division multiplexing (OFDM), cognitive radio and cooperative techniques. In cooperative NOMA codes, either dedicated relay stations or stronger users with better channel conditions, act as relay to leverage the spatial diversity and to boost the performance of the other users. The advantage of spatial diversity gain in relay-based NOMA codes, is deployed to extend the coverage area of the network, to mitigate the fading effect of multipath channel and to increase the system throughput, hence improving the system efficiency.

In this dissertation we consider the multimedia content delivery and machine type communications over 5G networks, where scalable content and low complexity encoders is of interest. We propose cross-layer design for transmission of successive refinement (SR) source code interplayed with non-orthogonal layered broadcast code for deployment in several cooperative network architectures. Firstly, we consider a multi-relay coding scheme where a source node is assisted by a half-duplex multi-relay non-orthogonal amplify-forward (NAF) network to communicate with a destination node. Assuming the channel state information (CSI) is not available at the source node, the achievable layered diversity multiplexing tradeoff (DMT) curve is derived. Then, by taking distortion exponent (DE) as the figure of merit, several achievable lower bounds are proved, and the optimal expected distortion performance under high signal to noise ratio (SNR) approximation is explicitly obtained. It is shown that the proposed coding can achieve the multi-input single-output (MISO) upper bound under certain regions of bandwidth ratios, by which the optimal performance

in these regions can be explicitly characterized. Further the non-orthogonal layered coding scheme is extended to a multi-hop MIMO decode-forward (DF) relay network where a set of DE lower bounds is derived.

Secondly, we propose a layered cooperative multi-user scheme based on non-orthogonal amplify-forward (NAF) relaying and non-orthogonal multiple access (NOMA) codes, aiming to achieve multi-user uplink transmissions with low complexity and low signaling overhead, particularly applicable to the machine type communications (MTC) and internet of things (IoT) systems. By assuming no CSI available at the transmitting nodes, the proposed layered codes make the transmission rate of each user adaptive to the channel realization. We derive the close-form analytical results on outage probability and the DMT curve of the proposed layered NAF codes in the asymptotic regime of high SNR, and optimize the end-to-end performance in terms of the exponential decay rate of expected distortion.

Thirdly, we consider a single relay network and study the non-orthogonal layered scheme in the general SNR regime. A layered relaying scheme based on compress-forward (CF) is introduced, where optimization of end to end performance in terms of expected distortion is conducted to jointly determine network parameters. We further derive the explicit analytical optimal solution with two layers in the absence of channel knowledge.

Finally, we consider the problem of multicast of multi-resolution layered messages over downlink of a cellular system with the assumption of CSI is not available at the base station (BS). Without loss generality, spatially random users are divided into two groups, where the near group users with better channel conditions decode for both layers, while the users in the second group decode for base layer only. Once the BS launches a multicast message, the first group users who successfully decoded the message, deploy a distributed cooperating scheme to assist the transmission to the other users. The cooperative scheme is naive but we will prove it can effectively enhance the network capacity. Closed form outage probability is explicitly derived for the two groups of users. Further it is shown that diversity order equal to the number of users in the near group is achievable, hence the coding gain of the proposed distributed scheme fully compensate the lack of CSI at the BS in terms of diversity order.

Acknowledgements

I would like to thank all the people who made this thesis possible, particularly my supervisor, Prof. Pin-Han Ho, for his continuous and precious support and insightful guidance throughout my studies at University of Waterloo.

I would also like to thank the members of my PhD advisory committee Prof. Dongkyun Kim, Prof. Laura Sanita, Prof. Patrick Mitran and Prof. Liang-Liang Xie for their time to review my thesis and their valuable comments that improved the quality of this thesis.

To

My parents,
Mahmoud Padidar, and Farahnaz Niknejad,

my wife,
Zahra Fiez Mahdavi,

my son,
Omid Padidar,

and my brother,
Peyman Padidar.

Table of Contents

List of Figures

Chapter 1

Introduction

1.1 Non-orthogonal layered broadcast codes for 5G network

The connectivity of massive number of devices in the paradigm of internet of things (IoT) for a wide range of new and emerging services like smart cities, smart grids, vehicular communications (V2X), health and environmental measuring and monitoring, and etc. is a challenging requirement for fifth generation (5G) wireless networks [1]. Several services, standards and technologies are envisioned to address the IoT communications in 5G networks including massive machine type communications (mMTC) of 5G new radio (5G-NR), narrow-band IoT (NB-IoT) and LTE-M [2]. The design of the IoT architectures needs to align with certain requirements and features of sensors and data collecting devices and networks including low cost and complexity, low power and wide range communications [3].

Along with the MTC and machine to machine (M2M) communications, the high throughput enhanced mobile broadband (eMBB) and ultra-reliable low latency communications (URLLC) services is envisioned for 5G networks [4]. These three core services create a heterogeneous network and coexistence of such diverse services within the same radio access network (RAN) requires highly spectral efficient multiple access techniques. Spectrum sharing is considered an effective strategy of improving overall network throughput in wireless communication systems. Several spectrum sharing techniques have been envisioned to be formally deployed in the cellular networks in order to meet the high requirements on throughput, low latency, and massive connectivity [5]. The non-orthogonal multiple access

(NOMA) is a promising spectrum sharing technique to boost the spectral efficiency [74]. By deploying the non-orthogonal layered broadcast coding and successive cancellation decoding, NOMA can serve multiple users/data-streams via a common frequency/time/code domain with different power levels.

It is widely studied and shown in the literature that NOMA can achieve higher spectral efficiency than that by the conventional orthogonal multiple access (OMA) systems. Similar implementations of NOMA have been devised for current wireless networks including the adoption of multi-user superposition transmission (MUST) by 3GPP for LTE-A and also layered division multiplexing (LDM) for next generation digital TV by ATSC 3.0. NOMA can be further improved in terms of reliability, throughput, and coverage by incorporating with a cooperative relaying scheme, where one or multiple dedicated relays and/or assisting users can be deployed to jointly forward the intended data to the recipients, [7] and [8].

The non-orthogonal layered broadcast code properly interplay with multi-resolution source codes for improved quality of service (QoS) [9], where the adaptive multi-resolution source codes like scalable video codes (SVC) used in H.264/MPEG-4 AVC standards can be overlayed with a non-orthogonal layered channel code.

In this dissertation, considering the multi resolution multimedia transmission and machine type communications where adaptive scalable content are transmitted by low complexity encoders with limited channel knowledge, we design and study the non-orthogonal layered broadcast codes in several cooperative network architectures. The contributions of this work are listed in following section.

1.2 Contributions

1.2.1 Layered Multi-Relay Non-Orthogonal Amplify-Forward Networks

In chapter 3, we consider a multi-relay network with the assumption of no channel state information (CSI) available at the transmitting node. We introduce a cross-layer coding scheme for transmission of successive refinement (SR) source code [10] interplayed with non-orthogonal layered broadcast code, deployed over a half-duplex multi-relay non-orthogonal amplify-forward (NAF) relaying network [11]. We have tackled the following tasks as the major contributions in this chapter:

- We introduce a novel power allocation strategy among the layers of the proposed

non-orthogonal layered code over NAF network and prove that it can achieve the optimal layered diversity multiplexing tradeoff (DMT) curve of the NAF network.

- Based on the derived layered DMT curve of the network, the optimal expected distortion performance of the proposed layered coding is characterized under a finite number of layers as well as asymptotically with an infinite number of layers in the high signal to noise ratio (SNR) scenario.

- We identify the regions on the bandwidth ratio, that the distortion exponent (DE) inner bounds are tight, where the optimal expected distortion performance of the proposed layered scheme over NAF network, in the high SNR regime is fully characterized.

- We extend the study of layered coding to the setup of multi-hop multi-input multi-output (MIMO) decode-forward (DF), where the layered DMT curve is derived along with its achievable DE lower bound.

- We verify the effectiveness of proposed layered coding under general SNR values via simulation, and compare it with a number of cooperative NOMA-based layered coding counterparts and also limited feedback networks.

1.2.2 Multi-layer NAF Cooperative NOMA Codes for uplink multiple access network

In chapter 4 we consider a multi-user uplink single cell scenario with focus on IoT enabling machine type communication over 5G network. The nature of MTC traffic, which is latency critical, sporadic, low data rate, low cost, diverse quality of service and massive number of devices requires a shift from the conventional centralized scheduling by the base station (BS) to reduce the latency, signaling overhead and complexity of the user encoders. Hence we consider a scenario where no feedback link is available from the BS to the users and the CSI is not available at the users. We design a cooperative layered non-orthogonal broadcast code over such network. The main contributions of this chapter are summarized as follows:

- A novel layered NAF cooperative NOMA code for uplink multi-user single cell wireless network, is proposed which matches the transmission rate of each node to channel condition with no CSI at the user equipment terminals.

- The DMT curve is explicitly derived for symmetric multi-layer NAF cooperative NOMA network and is shown to achieves the upper bound of multi-input single-output (MISO) system, hence the optimal performance in high SNR is proved.
- The proposed uplink channel coding is matched to multi-resolution SR source code and the end to end system performance in high SNR regime in terms of DE is fully characterized.
- The general SNR system performance is compared with OMA, non-cooperative NOMA code and available amplify-forward (AF) and DF based cooperative scheme and the superiority of the proposed coding in the setup of no CSI at transmitting nodes is confirmed by simulation results.

1.2.3 Non-orthogonal layered Compress-Forward over Single relay network

In chapter 5, we consider a network architecture of a source node transmitting to a destination node, while a single relay assists the transmission. We intend to analyze the system performance in general SNR regime. We propose a non-orthogonal layered broadcast scheme based on half-duplex compress-forward (CF) protocol. Our contributions in this chapter is summarized as follows

- We have proposed a non-orthogonal layered coding scheme deploying CF relaying strategy. Achievable rate for the proposed scheme is derived for general channel distributions.
- The proposed coding is further specialized for Gaussian networks and explicit achievable rate is derived.
- The system performance for the proposed coding is compared with several available cooperative NOMA codes in terms of achievable rates over Gaussian networks.
- We have analytically optimized the cross-layer performance of SR source code matched to non-orthogonal layered CF coding for a two state channel with no CSI at the source node. The optimal end to end distortion performance in terms of ED is compared to available cooperative NOMA schemes.
- Finally the system is analyzed for a Rayleigh fading channel. The simulation results confirm considerable gains in terms of end to end performance compared to conventional non-layered codes in the absence of CSI at the source node.

1.2.4 NOMA-based Distributed Cooperative Multi-layer Multicast with spatially random users

In chapter 6 we consider a cooperative multicast scenario. Assuming no CSI at the transmitting nodes, a novel distributed cooperative NOMA scheme is proposed. A circular cell with BS at the center, is assumed where users are randomly located in two groups, a circle close to the BS and a ring far away (cell-edge users). A multi resolution message is intended for all the users. The users with better channel condition decode more layers, hence reconstruct the source message with higher resolution, while the group of users with weak channel conditions decode only for the base layer. The main contributions of this chapter are

- We analyze the outage event of the proposed distributed non-orthogonal layered cooperative multicast code for spatially randomly located users and derive the explicit analytical outage probability.
- We provide asymptotic high SNR approximation and prove that diversity order, equal to the number of cooperating users is achievable, which is strictly improved over the available multicasting cooperative NOMA schemes in the case of no CSI at the BS and matches the performance of multicasting codes in case of CSI available at the BS.
- Simulation results is provided which confirms the validity of the analytical performance analysis.

1.3 Thesis Organization

The rest of this thesis is organized as follows. In chapter 2 we provide the background on the non-orthogonal layered broadcast coding. The expected distortion and its high SNR approximation as the end to end system performance metrics are introduced. In chapter 3 we deploy the SR source code concatenated to non orthogonal layered broadcast code over a L-relay NAF cooperative network and we analyze the end to end system performance in terms of DE. We study the deployment of NOMA code over cooperative uplink network in chapter 4 and provide system performance optimization in terms of end to end expected distortion. In chapter 5, a non orthogonal layered code deploying CF relaying scheme is proposed over a single relay network. Unlike other chapters the general SNR evaluation is performed in this chapter. In chapter 6 we analyze multicasting over a distributed

cooperative downlink network and propose the non-orthogonal layered broadcast coding. Outage probability and diversity order analysis is performed for this setup. Chapter 7 concludes this dissertation and some directions for future works is discussed.

Chapter 2

Background

2.1 Non-orthogonal layered Broadcast Code

In this section, we review the statistical channel models for wireless fading channels. We introduce the outage event analysis for the slowly fading channel model and review the layered coding schemes which can match the transmission scheme to the slow fading channel when there is no feedback link to the source node.

2.1.1 Channel Model

The wireless fading channel is a common model that captures the effects of the variations of the mobile wireless channel strengths in time and frequency. Fading effects are divided into two types of large-scale fading and small-scale fading. The former captures the path-loss of the signal due to the distance and shadowing of large objects which is of the order of cell size. As an instance in free space, the received power decreases with distance r as $\frac{1}{r^2}$. The latter is due to the multipath constructive and destructive interference and causes variations in the signal strength of the order of the carrier wavelength.

Statistical channel models are deployed to represent the small-scale fading. A fading multipath channel is modeled by a linear time varying system with impulse response $g(\tau, t)$, where t is the time variable and τ is the propagation delay. Its discrete time baseband equivalent model is given by l-tap filter $g[m, l]$. Coherence bandwidth W_c, and the coherence time T_c, are two key characterizing parameters of the channel. W_c is reciprocal to delay spread; the difference between propagation delay of different paths of the signal

in the channel. If the bandwidth of the input signal is considerably less than W_c, the channel is flat fading, and can be represented by single filter tap model, $g[m]$. In modern wireless mobile networks, multi carrier techniques like orthogonal frequency division multiplexing (OFDM) is implemented which divides the total available bandwidth into several sub bands, in each the bandwidth is of the order of W_c hence, flat fading single-tap channel model $g[m]$, properly model the channel [41]. The coherence time T_c, is defined as the time interval which the channel $g[m]$, changes significantly as a function of time m. If the delay requirement of the communication application is significantly shorter than T_c, the channel is categorized as slow fading and if longer is termed as fast fading. The transmission over a single-input single-output (SISO) channel for a single tap flat fading channel is modeled by

$$y[m] = g[m]x[m] + w[m], \tag{2.1}$$

where $x[m]$ is the transmit complex signal and $y[m]$ is the received symbol. $w[m]$ is additive white Gaussian noise, distributed according to $\mathcal{CN}(0, N_0)$ and is independent of the channel gain process $g[m]$. We adopt the Rayleigh fading channel model where $g[m]$ is circular symmetric with distribution $\mathcal{CN}(0, \sigma^2)$. Rayleigh fading model is a proper model for rich scatter environment and is widely adopted to model typical cellular networks. When there is a strong line of sight signal with uniform phase along with multiple independent paths, Rayleigh models is modified into Rician fading channel model.

2.1.2 Slow Fading Channel

In fast fading channels where the dynamics of the channel is shorter than the transmission block length, it is possible to encode over several coherence times and the ergodic capacity is well defined. In slow fading scenarios, assuming applications where there is no delay constraint, it is still possible to code over several channel coherence times, hence similar to the fast fading scenario the ergodic capacity is defined. In several scenarios like multimedia transmission or machine-type communications, there are certain stringent delay constraints on the coding, hence the code block length is in the order of channel coherence time and the channel is non ergodic and the capacity in Shannon sense is not defined.

Several alternative approaches are available in the literature for the slow fading scenario including compound channel model, outage capacity and broadcast strategy. In compound channel coding, the source node encodes against the worst channel case, hence it is very pessimistic coding approach and becomes impractical when fading causes very low channel

gains. In outage capacity approach a fixed transmission rate is assumed. Transmitted data is reliably decoded when the instantaneous channel realization supports the transmission rate, otherwise the channel is in outage and no data is decoded. Outage event is defined as the set of channel gains where the fixed transmission rate is not supported by the channel and the messages is not decodable at the destination. For the SISO channel. the outage set $\mathcal{O}$ is given by

$$\mathcal{O} = \{g : \log(1 + |g|^2\rho) < R\}, \tag{2.2}$$

where $\rho = \frac{P}{N_0}$ is the SNR, $P = E[|x|^2]$ and R is the rate of transmission in bits per channel use. The probability of the set $\mathcal{O}$ is the outage probability denoted by $P_{\mathcal{O}}$. For outage probability $P_{\mathcal{O}}$, the outage capacity is

$$C_{P_{\mathcal{O}}} = \max_{g:Pr[G<g]\leq P_{\mathcal{O}}} \log(1 + |g|^2\rho). \tag{2.3}$$

In slow fading scenario, CSI can be perfectly acquired at the receiving end through pilot and training symbols. Different scenarios on the feedback link from the receiver to the transmitting node determines the availability level of CSI at the transmitting node. Adaptive rate and power allocation can increase the capacity of the channel in case of availability of CSI at the transmitting node. Limited feedback models where partial CSI can be conveyed back to the transmitting node is also of interest in practical systems.

2.1.3 Broadcast code for SISO channel

To maximize the average achievable rate in slow fading scenario with no CSI at the transmitting node, [13] has proposed broadcast strategy, where the transmit signal is encoded into superimposed non-orthogonal layers. Broadcast strategy facilitates adaptive coding rate and matches the transmission rate to the instantaneous channel realization with no feedback link from the destination to the source node. This approach is in fact the extension of the superposition coding of broadcast channels over physically degraded Gaussian broadcast channel to the case of single user channel with unknown CSI at the transmitting node.

Message $m \in [1 : 2^{nR}]$, where n is the channel code length and R is the coding rate in bits per channel use, is intended to be transmitted over the SISO channel given in (2.1). A M-layer superposition code is constructed by rate splitting, where the message m is represented by M-tuple message vector $(m_1, m_2, ..., m_M)$, consisting of M independent

messages with rate vector $(R_1, R_2, ..., R_M)$. Message m_j for the layer $j \in [1 : M]$, is encoded by the rule

$$x_j^n : [1 : 2^{nR_j}] \to \mathcal{X}_j^n, \tag{2.4}$$

where for the Rayleigh fading channel of (2.1), the encoding functions of the layers are independent random Gaussian codes and $\mathcal{X}$ is the input alphabet for the Gaussian code. The superposition signal is constructed as follows

$$x^n(m_1, m_2, ...m_M) = \sum_{j=1}^{M} \sqrt{\alpha_j} x_j^n(m_j), \tag{2.5}$$

where $\alpha_j > 0, j \in [1 : M]$ are the power splitting parameters and $\sum_{j=1}^{M} \alpha_j = 1$. At the destination node, the decoder successively decodes each layer considering the higher layers as interference. Layer 1 is decoded first, considering the higher layers as interference. For the second layer, the message 1 is subtracted from the received signal and layer 2 is decoded considering layers 3 up to M as interference. Layer j is decoded after successful decoding of layers 1 to $j-1$ and considering the layers $j+1$ to M as interference. Finally layer M is decoded with no interference term. The signal to noise and interference (SINR) term of decoding layer j, deploying the successive interference cancellation (SIC) docoder described above is given by

$$\gamma_j = \frac{|g|^2 \rho \alpha_j}{1 + |g|^2 \rho \sum_{k=j+1}^{M} \alpha_k}, \tag{2.6}$$

and the rate of layer j is given by $\log(1 + \gamma_j)$. For the SISO Rayleigh fading channel, [13] has proposed an infinite-layer broadcast code, $M \to \infty$, where each layer corresponds to a fading channel power level $u = |g|^2$. In this case, the power allocation coefficient vector becomes a continuum power distribution function $\alpha(s)$. Each layer has a fractional rate

$$dR(u) = \log(1 + \frac{u\alpha(u)du}{1 + uI(u)}), \tag{2.7}$$

where ρ is set to 1 and $I(u)$ is the interference of the higher undecodable layers,

$$I(u) = \int_u^{+\infty} \alpha(v)dv. \tag{2.8}$$

For each power level realization u, rate $R(u) = \int_0^u dR(v)$ is achievable. The average achievable rate for different channel realizations is formulated as

$$R_{ave} = \int_0^{+\infty} R(v) p_{|G|^2}(v)dv, \tag{2.9}$$

where $p_{|G|^2}(v)$ is the probability distribution function of the channel fading power. Optimization of R_{ave} as a function $\alpha(u)$ (or I(u)) can be formulated as a functional of interference term $\alpha(u)$. The necessary condition for maximum $\alpha(u)$ can be derived by solving the corresponding Euler equation.

2.2 Successive refinement source code

Considering the problem of end to end system performance, we review the rate-distortion function of the source sequence encoding and introduce the successive refinement property for the source sequences in this section.

2.2.1 Rate-Distortion Function

Assuming a discrete memoryless source sequence s^k of length k source symbols, a source encoding function assigns a message m by mapping

$$m : \mathcal{S}^k \to [1 : 2^{kR^s}], \tag{2.10}$$

where $\mathcal{S}$ is the source symbol alphabet, and R^s is the source coding rate per source symbol. At the receiving side, a decoder assigns an estimation sequence $\hat{s}^k$ to each index m by the mapping

$$\hat{s}^k : [1 : 2^{nR_s}] \to \hat{\mathcal{S}}^k, \tag{2.11}$$

where $\hat{\mathcal{S}}$ is the reconstruction symbol alphabet. A per letter distortion measure d is defined as a mapping

$$d : \mathcal{S} \times \hat{\mathcal{S}} \to [0, +\infty), \tag{2.12}$$

which capture the closeness of the reconstruction symbol $\hat{s}$ to the source symbol s. The average distortion is defined as

$$d(s^k, \hat{x}^k) = \frac{1}{k} \sum_{i=1}^{k} d(s_i, \hat{s}_i). \tag{2.13}$$

The expected distortion for the source coding $(m, \hat{s}^k)$ is defined as

$$E[d(S^k, \hat{S}^k)] = \sum_{s^k} p(s^k) d(s^k, \hat{s}^k(m(s^k))), \tag{2.14}$$

For a source encoding function m and decoding function $\hat{s}^k$ with rate R^s, distortion D is said to be achievable if

$$\lim_{k\to+\infty} E[d(S^k, \hat{S}^k)] \leq D. \tag{2.15}$$

The rate distortion function $R(D)$ for the source sequence s^k is defined as the infimum of rates R^s for achievable distortion D. By the lossy source coding theorem, it is known that the rate-distortion function for a memoryless source S and distortion measure $d(s, \hat{s})$, is given by

$$R(D) = \min_{p(\hat{s}|s):E[d(S,\hat{S})]\leq D} I(S; \hat{S}) \tag{2.16}$$

Considering a Gaussian memoryless source $\{s\}_{k=1}^{\infty}$ generated independent and identically distributed (i.i.d) according to zero mean unit variance real valued Gaussian distribution, and for a squared error distortion measure, the rate distortion function is known to be

$$R(D) = \frac{1}{2}\log\frac{1}{D}. \tag{2.17}$$

2.2.2 SR Source Code

Consider an uncompressed source sequence is supposed to be transmitted to multiple users (or to a single user with unknown fading channel at the transmitting node). By SR source code, a coarse description of the source sequence is transmitted as the base layer, meanwhile refining layers which enhance the base layer description provide higher resolution reconstruction of the source sequence for users with better channel conditions (or when the receiver is experiencing better channel condition, in the single user scenario).

Two-layer SR source code for a source sequence s^k is defined as two descriptions (m_1, m_2) with rate (R_1^s, R_2^s) and two reconstruction functions $\hat{x}_1(m_1)$ and $\hat{x}_2(m_1, m_2)$. For the first estimation $\hat{x}_1$ only the first description m_1 is used and for the second estimation, m_2 is utilized to refine the first layer reconstruction and to achieve lower distortion. The rate distortion region is defined as the closure of the set of rate pairs (R_1^s, R_2^s) that

$$\lim_{k\to\infty} \sup E[d(S^k, \hat{S}_1^k(m_1))] \leq D_1, \tag{2.18}$$

$$\lim_{k\to\infty} \sup E[d(S^k, \hat{S}_2^k(m_1, m_2))] \leq D_2. \tag{2.19}$$

If pair (R_1, R_2) is achievable for distortion pair $(D_1, D_2), D_2 \leq D_1$, we have

$$R_1^s \geq R(D_1), \tag{2.20}$$

$$R_1^s + R_2^s \geq R(D_2), \tag{2.21}$$

where $R(D)$ is the rate distortion function of a single description code. It can be proved that for certain source sequences including Gaussian source with quadratic distortion measure and Bernoulli source with hamming distortion measure, there is no loss in optimality in describing the source by layers, in other words $R_1^s = R(D_1)$ and $R_1^s + R_2^s = R(D_2)$ are simultaneously achievable. This type of sources are termed as successively refinable source. The two-layer SR source code and the successive refinability property can be readily extended to M-layer coding. For a Gaussian source sequence with $R(D) = \frac{1}{2}\log\frac{1}{D}$, the successive refinability property indicates that M rate distortion functions,

$$\sum_{i=1}^{j} R_j(D_j) = \frac{1}{2}\log\frac{1}{D_j}, j \in [1:M], \tag{2.22}$$

are simultaneously achievable. The distortion is the reciprocal function to rate distortion and for layer $j \in [1:M]$ is given by

$$D_j = \exp(-2\sum_{i=1}^{j} R_j^s). \tag{2.23}$$

2.3 Source-Channel coding

The non-orthogonal layered broadcast channel coding properly matches to SR source codes where each of the descriptions of the M-layer SR source code is mapped onto a layer of the broadcast code. This technique is actually a source-channel separation approach where the parameters of the SR source code and broadcast channel code are jointly optimized. It is noted that joint source-channel coding schemes where source sequence s^k is directly map onto the channel sequences x^n, due to practical consideration of the coding in 5G networks where the source and channel coding are performed in different network layers is out of scope of this study.

First we consider a scenario where source sequence s^k is transmitted over a SISO fading channel, assuming channel has M finite number of fading states $g_i, i \in [1:M]$ with probability distribution function $p_G(g_i), i \in [1:M]$ and increasing order $|g_1|^2 < |g_2|^2 <$

$... < |g_M|^2$. The source sequence is encoded into M-tuple $(m_1, m_2, ..., m_M)$ index vector by an M-layer SR source code. The SR source encoder is matched to a M-layer non-orthogonal layered broadcast code given in (2.5), where each $m_i, i \in [1 : M]$ is channel encoded into channel sequence $x_i^n(m_i), i \in [1 : M]$, and the M-layer channel codes are superimposed according to (2.5). As the source sequence block length k can be different from channel code block length n, the source code rate and the channel code rate for each layer are related by the $R_i^s = bR_i, i \in [1 : M]$, where $b = \frac{n}{k}$ is defined as the bandwidth ratio. The distortion for decoding upto layer j is given by

$$D_j = \exp(-2b \sum_{i=1}^{j} R_j), \tag{2.24}$$

where

$$R_j = \frac{1}{2} \log(1 + \frac{|g|^2 \rho \alpha_j}{1 + |g|^2 \rho \sum_{k=j+1}^{M} \alpha_k}). \tag{2.25}$$

The distortion averaged over M realizations of the fading channel is

$$\begin{aligned} D &= \sum_{j=1}^{M} p_j D_j \qquad (2.26) \\ &= \sum_{j=1}^{M} p_j \exp(-2b \sum_{i=1}^{j} R_i) \\ &= \sum_{j=1}^{M} p_j \prod_{i=1}^{j} (1 + \frac{|g_i|^2 \rho \alpha_j}{1 + |g_i|^2 \rho \sum_{k=j+1}^{M}} \alpha_k)^{-b} \end{aligned}$$

The end to end expected distortion optimization problem is written as

$$\min D \tag{2.27}$$

$$\text{s.t.} \quad \alpha_i > 0, i \in [1 : M] \tag{2.28}$$

$$\sum_{i=1}^{M} \alpha_i \leq 1 \tag{2.29}$$

This optimization is not convenient problem due to its complicated form even in very simplified scenarios of SISO channel and for finite number of fading states. There are several suboptimal solutions for this problem in the literature to convexify it and sub-optimal solutions are proposed. This optimization problem gets intractable for more complex channels and network models. High SNR regime approximation is a common approach in the literature to simplify the optimization problem and to get to analytically tractable solutions. In the next section the high SNR approximation of the problem is presented for the SISO network.

2.4 Distortion Exponent Analysis

As noted in section 2.1.2, a channel in slow fading setup with no CSI at the transmitter is characterized by the outage probability as a function of target data rate. The outage probability captures the tradeoff between the data rate and the probability of error. In the high SNR regime, diversity-multiplexing curve is an approximation of the outage probability that captures the fundamental tradeoff of the data rate (degrees of freedom) and the reliability. Multiplexing gain r is defined as

$$R = r \log \rho, \tag{2.30}$$

and diversity gain is the SNR exponent of the outage probability [12]

$$d(r) = -\lim_{\rho \to +\infty} \frac{\log P_{\mathcal{O}}}{\log \rho}. \tag{2.31}$$

In other words the outage event probability is exponentially equal to $\rho^{-d(r)}$, denoted by $P_{\mathcal{O}} \doteq \rho^{-d(r)}$. Similarly, considering transmission of an uncompressed source over the channel, the SNR exponent of the expected distortion characterizes the end to end system performance in high SNR. Distortion exponent is defined as the exponential decay rate of expected distortion,

$$\Delta = -\lim_{\rho \to +\infty} \frac{\log D}{\log \rho}. \tag{2.32}$$

We consider single layer transmission of a Gaussian source with variance $\sigma_S^2 = 1$, over Rayleigh slowly fading SISO channel. The transmission rate is fixed at R_1 and the achievable distortion is given by $D_1 = \sigma_S^2 e^{-bR_1}$. Expected distortion can be written as

$$D = (1 - P_{\mathcal{O}})D_1 + P_{\mathcal{O}}\sigma_S^2. \tag{2.33}$$

in high SNR,

$$D \doteq D_1 + P_{\mathcal{O}}\sigma_S^2 \tag{2.34}$$

$$\doteq \rho^{-br} + \rho^{-d(r)} \tag{2.35}$$

The minimum expected distortion is achieved when both the terms has the same exponent, hence

$$\Delta = br = d(r). \tag{2.36}$$

The optimal rate assignment that maximize the distortion exponent is derived by $r = \frac{d(r)}{b}$.

Now we formulate the expected distortion analysis and the high SNR analysis of distortion exponent for the SR source code concatenated to the layered broadcast channel code for SISO Rayleigh fading channel. Assuming rate assignment vector $(R_1, R_2, ..., R_M)$ and power splitting vector $(\alpha_1, \alpha_2, ..., \alpha_M)$ for the M layers, outage event for each layer is defined as

$$\mathcal{O}_j = \{g : \log(1 + \frac{|g|^2\rho\alpha_j}{1 + |g|^2\rho\sum_{k=j+1}^{M}\alpha_k}) < R_j\}, \tag{2.37}$$

The expected distortion of the M-layer scheme is given by

$$D = \sum_{i=0}^{M}(P_{\mathcal{O}_{i+1}} - P_{\mathcal{O}_i})D_i, \tag{2.38}$$

where $D_0 = 0$, $P_{\mathcal{O}_{M+1}} = 1$ and $P_{\mathcal{O}_0} = 0$. Similar to non-layered scheme the diversity gain and multiplexing of each layer is defined based on the outage probability of each layer, where $R_i = r_i \log\rho$ and $P_{\mathcal{O}_i} = \rho^{-d(r_i)}$ for $i \in [1 : M]$. In high SNR regime the expected distortion expression is given by

$$D \doteq \sum_{i=0}^{M}(\rho^{-d(r_{i+1})} - \rho^{-d(r_i)})\rho^{-b\sum_{j=1}^{i} r_j} \tag{2.39}$$

$$\doteq \sum_{i=0}^{M}\rho^{-d(r_{i+1})-b\sum_{j=1}^{i} r_j}. \tag{2.40}$$

The expected distortion is dominated by the slowest decay rate

$$\min_{i\in[0:M]}\{d(r_{i+1}) + b\sum_{j=1}^{i} r_j\}. \tag{2.41}$$

Hence the DE optimization problem is given by

$$\Delta = \max_{\substack{(\alpha_1,\alpha_2,\ldots\alpha_M),\\ (r_1,r_2,\ldots,r_M)}} \min_{i\in[0:M]} \{d(r_{i+1}) + b\sum_{j=1}^{i} r_j\}. \tag{2.42}$$

We extend the DE optimization problem for different scenarios of cooperative wireless networks and provide resource allocation algorithms to optimize the end to end performance of each network.

Chapter 3

Layered Multi-Relay Non-Orthogonal Amplify-Forward Networks

3.1 Introduction

In this chapter we consider a fading multi-relay network, where an uncompressed Gaussian source sequence is observed at the source node and it is intended to be reconstructed at the destination node. L relay nodes assist in transmission of the source sequence to the destination. We adopt NAF relaying scheme as the cooperation protocol. Assuming no CSI is available at the source node, we propose a SR source code concatenated to a non-orthogonal layered broadcast channel code and optimize the end to end system performance.

As we mentioned in chapter 2, the fundamental theory of non-orthogonal multi-layer channel codes was firstly introduced in [13], aiming to adapt the transmission of a single user to a slow fading MIMO channel with no CSI at the transmitter. Since then, the non-orthogonal layered transmissions over several network architectures, including cooperative networks, have been extensively studied in the literature [14]-[38].

Expected distortion, as defined earlier, is the statistical difference between the source original sequence at the sender and reconstructed version at the destination node, averaged over multiple channel coherence times and channel blocks. It is a commonly employed measure that helps to capture the effects of both source and channel coding on the transmission

The results presented in this chapter have already been published in [39].

[14]. As shown in chapter 2, even for non-complex networks like SISO channel, the expected distortion evaluation with general channel SNR leads to a complex characterization.

It is common to consider the DE , the exponential decay rate of the expected distortion introduced in [15], as the figure of merit in the high SNR regime. [18] studies the distortion exponent in general MIMO channels. It proposes exponential power allocation among the layers which is shown to achieve successive refinable DMT curve and is optimal, in channels with one degree of freedom, but is suboptimal for general MIMO. [19] proposes more advanced power allocation which leads to better performance for low values of bandwidth ratio, b. [20] extends the analysis to relay channels and consider AF and DF relaying schemes and compare the system performance with multi-input single-output (MISO) upper bound. [21] and [22] extends the problem to multi relay channels and derive the achievable inner bound on the system performance for AF and DF repetition coding, relay selection coding and also space-time codes based on the network models of [23]. [24], [25] and [26] have considered the same problem in the presence of limited feedback and quantized channel state information at the transmitter. The two way relay channel is considered in [27] and achievable inner bounds are derived for distortion exponent. [28] has extended the problem to MIMO channel with side information, where upper bound on the distortion exponent and several inner bounds using superposition coding of layered codes is provided. [29] considered the parallel channel with asymmetric correlated channel gains and provided achievable distortion exponent for multiple description codes over such network. Nonetheless, general evaluation of expected distortion performance for more complex networks is still an open problem even in the high SNR regime.

3.2 System Model

We consider a multi-relay network as depicted in Fig. 3.1, in which the source node s is transmitting the message m to the destination node d, and the relay nodes $1, ..., L$ cooperate in transmission of the source message to the destination, with the assumption of no channel knowledge at the transmitter side.

The capacity of such multi-relay network is not known in general, and various suboptimal coding schemes are reported in literature [30]. We consider half-duplex multi-relay NAF setup, a variant of AF-based relaying scheme, where the relays process the received sequences and re transmit the linearly modified version of the noisy signal without further decoding the message. The term non-orthogonal is due to the fact that the source node continues to transmit subsequent messages while the relay nodes are forwarding the current ones. As depicted in Fig. 3.2, we consider $2L$ source node sequences $x_{s,i}^N, i \in [1 : 2L]$

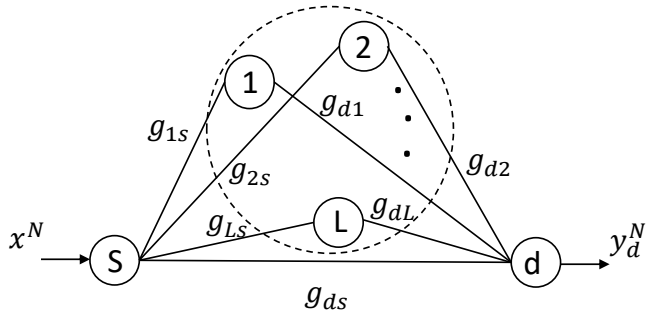

Figure 3.1: Multi-relay network

Slot	1	2	3	4	$\cdots$	$2L-1$	$2L$
Source	$x_{s,1}^N$	$x_{s,2}^N$	$x_{s,3}^N$	$x_{s,4}^N$		$x_{s,2L-1}^N$	$x_{s,2L}^N$
Relay 1		$x_{r,1}^N$					
Relay 2				$x_{r,2}^N$			
$\vdots$							
Relay L							$x_{r,L}^N$

Figure 3.2: Frame structure of half-duplex multi-relay NAF network.

$x_{s,i}^N =$ $i \in [1:2L]$	$\sum_{k=1}^{M} \sqrt{\rho_k} x_{i,k}^N(m_{i,k})$
Layer 1	$x_{i,1}^N(m_{i,1})$
Layer 2	$x_{i,2}^N(m_{i,2})$
$\vdots$	
Layer M	$x_{i,M}^N(m_{i,M})$

Figure 3.3: Non-orthogonal layered broadcast coding scheme.

each of length N channel uses to be transmitted by the source node in a multi-relay frame,

which consists of L relay frames, further consisting of 2 transmission slots each of length N channel uses. In each relay frame, one of the relays is active and the other $L-1$ relays are silent. In other words, the relays are active in turn during each relay frame.

Specifically, the received signals at relays $y_{i,j}^N, i \in [1, L], j \in [1:2L]$ in a multi-relay frame, consist of $2L$ transmission slots, which can be expressed as

$$y_{1,1}^N = g_{1,s} x_{s,1}^N + z_{1,1}^N, \tag{3.1}$$
$$y_{2,3}^N = g_{2,s} x_{s,3}^N + z_{2,3}^N, \tag{3.2}$$
$$\vdots$$
$$y_{L,2L-1}^N = g_{L,s} x_{s,2L-1}^N + z_{L,2L-1}^N, \tag{3.3}$$

where $g_{i,s}, i \in [1:L]$ is the Rayleigh fading gain of the source to relay-i channel. The channel gain realizations are assumed to be available at the receiving nodes while the transmitting node only have channel statistics knowledge. All the noise components $z_{i,j}$ are assumed to be i.i.d circularly-symmetric complex Gaussian random variables with zero mean and unit variance ($\mathcal{CN}(0,1)$). The received signal at the destination in a multi-relay frame, denoted as $y_{d,j}^N, j \in [1, 2L]$, is expressed as

$$y_{d,1}^N = \quad g_{d,s} x_{s,1}^N + z_{d,1}^N \tag{3.4}$$
$$y_{d,2}^N = \quad g_{d,s} x_{s,2}^N + g_{d,1} x_1^N + z_{d,2}^N \tag{3.5}$$
$$y_{d,3}^N = \quad g_{d,s} x_{s,3}^N + z_{d,3}^N \tag{3.6}$$
$$y_{d,4}^N = \quad g_{d,s} x_{s,4}^N + g_{d,2} x_2^N + z_{d,4}^N \tag{3.7}$$
$$\vdots$$
$$y_{d,2L-1}^N = g_{d,s} x_{s,2L-1}^N + z_{d,2L-1}^N \tag{3.8}$$
$$y_{d,2L}^N = \quad g_{d,s} x_{s,2L}^N + g_{d,L} x_L^N + z_{d,2L}^N, \tag{3.9}$$

where $g_{d,i}, i \in [1:L]$ is the Rayleigh fading gain of relay-i to destination channel. The transmit signal at relays $x_j, j \in [1:L]$, is set to be the linearly amplified version of the received signal at node j, hence

$$x_j = \beta_j y_j, j \in [1:L]. \tag{3.10}$$

With the half-duplex mode of the relays, the received message is transmitted in the next subsequent transmission slot, as shown in Fig. 3.2. The relaying coefficients need to meet

the transmission power constraint on each relay node, hence

$$\beta_j = \sqrt{\frac{\rho}{1 + |g_{j,s}|^2 \rho}}, \tag{3.11}$$

where ρ is the total transmit power at each node. Considering (3.1), (3.4) and (3.10), the transmission in each relay frame $j \in [1 : L]$ is modeled as

$$\mathbf{y}_{d,j}^N = \begin{bmatrix} g_{d,s} & 0 \\ \beta_j g_{j,s} g_{d,j} & g_{d,s} \end{bmatrix} \mathbf{x}_j^N + \begin{bmatrix} 0 & 1 & 0 \\ \beta_j g_{d,j} & 0 & 1 \end{bmatrix} \mathbf{z}_j^N \tag{3.12}$$

where

$$\mathbf{y}_{d_j}^N = \begin{bmatrix} y_{d,2j-1}^N \\ y_{d,2j}^N \end{bmatrix}, \mathbf{x}_j^N = \begin{bmatrix} x_{s,2j-1}^N \\ x_{s,2j}^N \end{bmatrix}, \mathbf{z}_j^N = \begin{bmatrix} z_{j,2j-1}^N \\ z_{d,2j}^N \\ z_{d,2j}^N \end{bmatrix}. \tag{3.13}$$

Defining the channel coefficient matrix and noise coefficient matrix of each relay frame as

$$G_j = \begin{bmatrix} g_{d,s} & 0 \\ \beta_j g_{j,s} g_{d,j} & g_{d,s} \end{bmatrix}, B_j = \begin{bmatrix} 0 & 1 & 0 \\ \beta_j g_{d,j} & 0 & 1 \end{bmatrix}, \tag{3.14}$$

The multi-relay frame of NAF network in a matrix form is given as

$$\mathbf{y}_d^N = G\mathbf{x}^N + B\mathbf{z}^N, \tag{3.15}$$

where

$$G = \text{diag}(G_1, G_2, ..., G_L), \tag{3.16}$$
$$B = \text{diag}(B_1, B_2, ..., B_L), \tag{3.17}$$

and

$$\mathbf{y}_d^N = \begin{bmatrix} \mathbf{y}_{d,1}^N \\ \mathbf{y}_{d,2}^N \\ \vdots \\ \mathbf{y}_{d,L}^N \end{bmatrix}, \mathbf{x}^N = \begin{bmatrix} \mathbf{x}_1^N \\ \mathbf{x}_2^N \\ \vdots \\ \mathbf{x}_L^N \end{bmatrix}, \mathbf{z}^N = \begin{bmatrix} \mathbf{z}_1^N \\ \mathbf{z}_2^N \\ \vdots \\ \mathbf{z}_L^N \end{bmatrix}. \tag{3.18}$$

An uncompressed discrete-time continuous-amplitude source sequence

$$s^K = (s(1), s(2), ..., s(K)), \tag{3.19}$$

assumed to be zero mean, unit variance, i.i.d Gaussian sequence, is considered to be transmitted over the NAF relay network. The ratio of channel block length to the source block length $b = \frac{N}{K}$, *bandwidth ratio*, as defined in chapter 2 is taken as the joint source-channel code rate. We intend to minimize the expected distortion, in the lack of channel knowledge at the transmitting side.

For transmission of the source sequence s^K over the NAF network, in the absence of CSI at the transmitter side, the proposed layered coding scheme with a SR source code concatenated to a non-orthogonal layered broadcast channel code is adopted. For the SR source code as defined in chapter 2, the source message s^K is encoded into M messages $(m_1, m_2, ..., m_M)$. Here, m_1 is the base layer, the higher layers are the refining layers. $2L$ source sequences, each are encoded into M messages, channel encoded and transmitted in a multi-relay NAF frame using a superposition coding as shown in Fig. 3.3. Denoting the transmit signal in a multi-relay frame for layer k as $\mathbf{x}_k^N$, the received signal vector at the destination is

$$\mathbf{y}_d^N = G \sum_{k=1}^{M} \sqrt{\rho_k} \mathbf{x}_k^N + B\mathbf{z}^N, \tag{3.20}$$

where ρ_k is the allocated power to layer k, $\sum_{k=1}^{M} \rho_k = \rho$ and $\mathbf{y}_d^N$ is a $2L$ by N matrix.

3.3 Diversity-Multiplexing Gain Analysis

We reviewed the DMT and DE analysis for layered coding in SISO channel in chapter 2. Here we specialized this analysis to the L-relay cooperative network. We analyze the DMT of the non-orthogonal layered channel code over the NAF network in this section. At the destination node a successive cancellation decoding scheme is assumed which iteratively decodes the received message up to layer $k-1$ while considering the signals of higher layers as interference. The achievable rate of layer k, is given by

$$\mathcal{I}^k = \frac{1}{2L} I(\mathbf{x}_k; \mathbf{y}_k | \mathbf{x}_1, ..., \mathbf{x}_{k-1}, G, B), \tag{3.21}$$

where

$$I(\mathbf{x}_k;\mathbf{y}_k|\mathbf{x}_1,...,\mathbf{x}_{k-1},G,B) =$$

$$\log\Big|I+(GK_{\mathbf{x}_k}G^h)(\sum_{i=k+1}^{M}GK_{\mathbf{x}_i}G^h+BK_{\mathbf{z}}B^h)^{-1}\Big| = \tag{3.22}$$

$$\sum_{j=1}^{L}\log\Big|I+(G_jK_{\mathbf{x}_{j,k}}G_j^h).$$

$$(\sum_{i=k+1}^{M}G_jK_{\mathbf{x}_{j,i}}G_j^h+B_jK_{\mathbf{z_j}}B_j^h)^{-1}\Big|, \tag{3.23}$$

G and B are given in (3.16), $K_{\mathbf{x}_k}$ and $K_{\mathbf{z}}$ are the covariance matrices of $\mathbf{x}_k$ and $\mathbf{z}$ given in (3.13) and (3.18), respectively, where $K_{\mathbf{x}_k}=\rho_k\mathbf{I}_{2L}$, $K_{\mathbf{z}}=\mathbf{I}_{2L}$ and $\mathbf{I}_n$ is an n-by-n identity matrix. Defining the aggregate power of layers $(k,k+1,...M)$ to be

$$\bar{\rho}_k=\sum_{i=k}^{M}\rho_i, \tag{3.24}$$

Mutual information term of (3.22) can be further simplified as

$$I(\mathbf{x}_k;\mathbf{y}_k|\mathbf{x}_1,...,\mathbf{x}_{k-1},G,B) =$$

$$\sum_{j=1}^{L}\log\frac{(1+g_{d,s}^2\bar{\rho}_k)^2+g_{d,j}^2\beta_j^2(1+(g_{d,s}^2+g_{j,s}^2)\bar{\rho}_k)}{(1+g_{d,s}^2\bar{\rho}_{k+1})^2+g_{d,j}^2\beta_j^2(1+(g_{d,s}^2+g_{j,s}^2)\bar{\rho}_{k+1})}. \tag{3.25}$$

The outage event for each layer is defined as

$$O_k=\big\{G:\mathcal{I}^k<R_k\big\}, \tag{3.26}$$

where R_k is the rate allocated to layer k and $\mathcal{I}^k$ is defined in (3.21). Aggregate outage event of layer k is defined as

$$\bar{O}_k=\cup_{i=1}^{k}O_i, \tag{3.27}$$

and the outage probability for layer k is denoted as $P_{\bar{O}_k}$. The multiplexing gain and the diversity gain of each layer is defined as

$$r_k=\lim_{\rho\to+\infty}-\frac{\log R_k}{\log\rho}, \tag{3.28}$$

$$d_k=\lim_{\rho\to+\infty}-\frac{\log P_{\bar{O}_k}}{\log\rho}. \tag{3.29}$$

The high SNR power allocation coefficient of layer k denoted as γ_k is defined as

$$\gamma_k = \lim_{\rho \to +\infty} \frac{\log \bar{\rho}_k}{\log \rho}. \tag{3.30}$$

We deploy the achievable rate of layer $k \in [1 : M]$, given in (3.25) to analyze the outage event and the diversity gain of the layers. The following theorem characterizes the layered DMT curve of the network.

Theorem 3.3.1. *The simultaneously achievable DMT curves of a non-orthogonal M-layer broadcast code over L-relay half-duplex network deploying NAF relaying protocol is*

$$d^k(r_k) = (1 - 2\sum_{i=1}^{k-1} r_i - r_k) + L(1 - 2\sum_{i=1}^{k} r_i)^+, \tag{3.31}$$

for $k \in [1 : M]$, where $(.)^+ = \max(0, .)$.

Proof: The proof is given in A.1.

To achieve the layered DMT given theorem 3.31, the aggregate power allocation coefficient of layer k, γ_k defined in (3.30), is set using the recursive power allocation of (A.13) given in the proof of theorem 3.31. It is noted that due to the lack of knowledge on the channel realizations, considering the outage event given in A.11, the transmitter cannot trace either the direct link or the relaying link for each relay is the dominant channel path, which can be taken as the worst case scenario in the coding stage. Considering a single bit feedback link for each $g_{j,s}$ and $g_{d,j}, j =\in [1 : L]$ the destination node sends the message

$$I_{fb,j} = \begin{cases} 1, & \text{if } u > v_j + w_j, \\ 0, & \text{otherwise} \end{cases} \tag{3.32}$$

for $j \in [1 : L]$, where u, v_j, w_j are defined in (A.5). The transmitter will be able to adapt the power allocation based on the stronger path as given in (A.23) and can achieve higher distortion gains. We outline the layered DMT curve of the one-bit feedback coding in the following theorem.

Theorem 3.3.2. *The simultaneously achievable DMT curve of M-layer non-orthogonal broadcast code over L-relay NAF network in the presence of 1-bit feedback per link is given by*

$$d^k_{fb}(r_k) = (1 - \sum_{i=1}^{k} r_i) + L(1 - 2\sum_{i=1}^{k} r_i)^+, \tag{3.33}$$

for $k \in [1 : M]$.

Proof: The proof is given in A.2.

3.4 Distortion Exponent (DE) Analysis

Having derived the achievable layered DMT curves, we study the DE performance of the proposed coding and compare its performance with limited feedback case in the section.

3.4.1 Rate Allocation for Non-Orthogonal Layered Coding

We defined the expected distortion for SISO channel in (2.38). Similarly the expected distortion of the proposed layered scheme over L-relay NAF network is

$$D = \sum_{k=0}^{M} (P_{\bar{O}_{k+1}} - P_{\bar{O}_k}) D_k, \tag{3.34}$$

where $D_k = \rho^{-b\sum_{j=1}^{k} r_j}$ is distortion-rate function of Gaussian source with k decoded layers, and $P_{\bar{O}_{M+1}} = 1 - \epsilon$, $P_{\bar{O}_0} = 0$, $D_0 = 1$. Assuming the high SNR regime, the expected distortion given in (3.34) becomes

$$\lim_{\rho \to +\infty} D = \sum_{k=0}^{M} P_{\bar{O}_{k+1}} D_i \tag{3.35}$$

$$= \sum_{k=0}^{M} \rho^{-d_{k+1}(r_{k+1}) - b\sum_{i=1}^{k} r_i}. \tag{3.36}$$

The next lemma demonstrates the optimal assignment of multiplexing gains, $r_i, i \in [1 : M]$, where the expected distortion in (3.35) is minimized.

Lemma 3.4.1. *Considering the proposed layered coding scheme over NAF network and the layered diversity gain derived in theorem 3.3.1, the optimal multiplexing gain assignment to minimize the expected distortion in (3.35) is given by*

$$b \sum_{i=k+1}^{M} r_i - d(r_k) = 0, k \in [1, M]. \tag{3.37}$$

Proof: The proof is given in A.3.

Now we are in a good position to derive the main result of this section, which is the cross-layer optimization of DE for the proposed scheme. By performing power allocation

according to (A.13) and the multiplexing gain assignment based on the result of lemma 3.4.1, we derive the achievable DE of the proposed layered coding as given in the following theorem.

Theorem 3.4.2. *The achievable DE of transmission of a M-layer SR source code over half duplex L-node NAF cooperative network is given by*

$$\Delta^M = \max\{\delta^1, \ldots, \delta^{M+1}\}, \tag{3.38}$$

where $\delta^k, k \in [1 : M+1]$ are defined as

$$\delta^k = \frac{(b-1)bC_k + bA_{k-1}\big(L+1+LbC_k\big)}{(b-1)(bC_k+1) + 2A_{k-1}\big(L+1+LbC_k\big)}, \tag{3.39}$$

A_k and C_k is defined as

$$A_k = 1 + \frac{2L+1}{b-1} + (\frac{2L+1}{b-1})^2 + ... + (\frac{2L+1}{b-1})^{k-1}, \tag{3.40}$$

$$C_k = 1 + (b-1) + (b-1)^2 + ... + (b-1)^{M-k}, \tag{3.41}$$

and $A_0 = 0$ and $C_{M+1} = 0$.

Proof: The proof is given in A.4.

Now we derive the achievable DE in the presence of 1-bit feedback per cooperating node. The proof for the 1-bit feedback case is a straightforward extension of the techniques deployed for the case of no feedback given in Theorem 3.4.2.

Theorem 3.4.3. *The achievable DE of transmission of M-layer code over L-node NAF network in the presence of 1-bit feedback per each cooperating node is given by*

$$\Delta_{fb}^M = \max\{\delta_{fb}^1, \ldots, \delta_{fb}^{M+1}\}, \tag{3.42}$$

where $\delta_{fb}^k, k \in [1 : M+1]$ are defined as

$$\delta_{fb}^k = \tag{3.43}$$

$$\frac{bA_{k-1}(L+1+LbC_k) + bC_k(b+LA_{k-1})}{(1+bC_k)(b+A_{k-1}+2LA_{k-1}) - A_{k-1}bC_k}, \tag{3.44}$$

A_k and C_k is defined as

$$A_k = 1 + \frac{2L+1}{b} + (\frac{2L+1}{b})^2 + ... + (\frac{2L+1}{b})^{k-1}, \tag{3.45}$$

$$C_k = 1 + b + b^2 + ... + b^{M-k}, \tag{3.46}$$

and $A_0 = 0$ and $C_{M+1} = 0$.

Proof: The proof is given in A.4.1.

3.4.2 Single Layer Coding with Limited Feedback link

As a special case, a single layer scheme over the NAF network is characterized. Similar to the layered case, the transmitter assigns the rate without CSI. The DE of the non-layered code applied over the NAF network is given in lemma 3.4.4.

Lemma 3.4.4. *The DE of a single layer code over NAF network in the absence of channel knowledge at the transmitter side is given by*

$$\Delta^{SL} = \begin{cases} \frac{b(L+1)}{b+2L+1}, & b \geq 1, \\ \frac{b}{1+b}, & b < 1. \end{cases} \tag{3.47}$$

proof: The proof is a special case of theorem 3.4.2 and is omitted.

Next we consider a single layer network in the presence of limited feedback link. For the network with limited feedback link, we assume a zero-delay, noiseless, fixed-rate feedback link from the receiver to the source node, where the quantized version of the CSI is conveyed back to the source node. The source node adapts its transmission based on partial channel knowledge. The achievable rate for single-layer transmission over NAF network for a given channel realization G defined in (3.16), is derived by letting $k = 1$ in (3.21), hence

$$\mathcal{I}^{SL}(G) = \mathcal{I}^{1}(G). \tag{3.48}$$

For the limited feedback setup, the value of $\mathcal{I}^{SL}(G)$ is quantized at the receiver side using Q-level scalar quantizer. The boundary values $\{b_k\}_{k=1}^{Q-1}$, reconstruction values $y_k, k \in [1:Q]$ and Q non overlapping intervals $\mathbf{I}_k = [b_{k-1}, b_k), k \in [1:Q]$ construct the quantizer. The quantizer is modeled as the mapping

$$\begin{cases} \Gamma_d : \mathbb{R} \to \{1, ..., Q\}, \\ \Gamma_s : \{1, ..., Q\} \to \{y_k\}_{k=1}^{Q}, \end{cases} \tag{3.49}$$

where $\mathbb{R}$ is the set of real numbers. The value of $\mathcal{I}^{SL}(G)$ for the realization of channel gain matrix G in each channel block, is mapped into the index set of size Q at the destination node. The quantizer index $k \in \{1, ..., Q\}$ is feedbacked to the source node through the limited rate feedback link. At the source node, the index of the quantizer is mapped into the reconstruction value $y_k, k \in [1:Q]$. The source node adjusts the rate of the transmission based on the value of y_k for each transmission block. Similar to [32], we set

the optimal reconstruction values of $\mathcal{I}^{SL}(G)$ by the rule of $y_k = b_{k-1}, k \in [1:Q]$. The expected distortion for a Q-level limited feedback system is given by,

$$ED^{SL-fb}(Q) = \sum_{i=1}^{Q} \big(P(y_i) - P(y_{i-1})\big).2^{-bR(y_{i-1})}, \tag{3.50}$$

where $P(x)$ represents the cumulative distribution function of achievable rate $\mathcal{I}^{SL}(G)$, and $R(y_k)$ is the rate of NAF code when the capacity lower bound is set to y_k. In the following lemma we provide the achievable DE curve of single layer NAF code, in the presence of Q-level feedback link.

Lemma 3.4.5. *The DE performance of a single layer code over NAF network with Q-level feedback link is given by*

$$\Delta^{SL-fb}(Q) = \max\{\delta^1, ..., \delta^Q\}, \tag{3.51}$$

where $\delta^k, k \in [1:Q]$ are defined as

$$\delta^k = \frac{(1+L)A_k^Q + (1+2L)^{k-1}C_1}{A_{k-1}^Q + (1+2L)^{k-1}C_0}, \tag{3.52}$$

$$\tag{3.53}$$

and

$$A_k^Q = \sum_{i=k}^{Q} b^i (1+2L)^{Q-i}, \tag{3.54}$$

$$C_j = \sum_{i=j}^{k} b^i, 0 \le j \le k. \tag{3.55}$$

proof: The proof is given in A.5.

3.5 Multi-Hop MIMO Relay Network

We extend the proposed layered SR source code concatenated to non-orthogonal layered channel coding scheme to the scenario where the source node, relay nodes, and the destination node are respectively equipped with $n_s, \{n_{r_i}\}_{i=1}^{L}, n_d$ antennas [33]. Similar to previous

section we assume CSI to be only available at the receiving nodes. We consider a multi-hop network, where the direct link from the source to the destination is not available (possibly due to shadowing) and the communications from the source to the destination is facilitated through the relay nodes. Although a single relay network is considered, the generalization to more relays is straightforward. We assume a multi-hop MIMO block fading channel, which is modeled as

$$\mathbf{y}_r[i] = G_{r,s}\mathbf{x}_s[i] + \mathbf{z}_r[i], i \in [1 : \alpha N], \tag{3.56}$$

$$\mathbf{y}_d[i] = G_{d,r}\mathbf{x}_r[i] + \mathbf{z}_d[i], i \in [\alpha N + 1 : N], \tag{3.57}$$

where $0 \leq \alpha \leq 1$, $\mathbf{x}_s$ and $\mathbf{x}_r$ are transmit vectors with n_s and n_r elements at source and relay node, respectively, while $G_{r,s}$ and $G_{d,r}$ are $n_r \times n_s$ and $n_d \times n_r$ channel gain matrices, respectively. We assume the source and destination have larger antenna arrays than that at the relay, hence $n_s > n_r$ and $n_d > n_r$. We assume that channels are independent frequency non-selective quasi static Rayleigh fading, hence the entries for $G_{r,s}$ and $G_{d,r}$ are i.i.d. complex Gaussian random variables with zero mean and unit variance. The additive white Gaussian vectors are assumed to have i.i.d. $\mathcal{CN}(0, 1)$ entries. $Y_i, i \in \{r, d\}$ are the received signal at the relay and the destination.

We assume a half-duplex DF relaying scheme, where the received signal at the relay is fully decoded before being re-encoded into a transmit signal $\mathbf{x}_r$. The transmission frame with N channel uses is divided between the source and relay node, where the source node transmits in the first αN time slots while the relay is silent. The relay node transmits in the following $(1 - \alpha)N$ channel uses. By deploying M-layer superposition coding, we have

$$\mathbf{x}_s = \sum_{i=1}^{M} \sqrt{\frac{\rho_i}{n_s}}\mathbf{x}_{s,i}, \tag{3.58}$$

where ρ_i is the allocated transmit power to layer i, and $\rho = \sum_{i=1}^{M} \rho_i$ is the SNR at source and relay nodes.

We analyze the expected distortion performance in the high SNR regime (i.e., $\rho \to \infty$) for the transmission of Gaussian source over the multi-hop MIMO DF relay network, deploying non-orthogonal layered broadcast scheme. Probability of outage event for each

layer $1 \leq k \leq M$, decoded at the relay O_k^r and destination O_k^d is

$$P_{O_k^j} = Pr\{G_{j,i} : \frac{1}{\beta_i} I(\mathbf{x}_k; \mathbf{y}) < r_k \log \rho\}, \tag{3.59}$$

$$(i,j) \in \{s,r\} \times \{r,d\} - \{(s,d)\},$$

$$\beta_i = \begin{cases} \alpha, & i = s \\ 1-\alpha, & i = r \end{cases} \tag{3.60}$$

The following lemma gives an achievable layered DMT analysis for the system.

Lemma 3.5.1. *The achievable layered DMT curve for a MIMO multi-hop DF relay channel deploying M-layer non-orthogonal broadcast code for layers $1 \leq k \leq M$ is given by*

$$d_k(r_k) = \max_{0 \leq \alpha \leq 1} \min \Big\{ n_s s_r (1 - \sum_{i=1}^{k-1} r_i) - (n_s + s_r - 1)\frac{r_k}{\alpha}),$$

$$n_d n_r (1 - \sum_{i=1}^{k-1} r_i) - (n_d + n_r - 1)\frac{r_k}{1-\alpha}) \Big\}. \tag{3.61}$$

For the case $n_s = n_d = m$, the layered DMT of layer $k \in \{1, ..., M\}$ is

$$d_k(r_k) = m n_r (1 - \sum_{i=1}^{k-1} r_i) - 2(m + n_r - 1) r_k. \tag{3.62}$$

proof: The proof is given in A.5.1.

Having derived the layered DMT curve for the system, we consider the DE performance analysis. With general values of (n_s, n_r, n_d), the DE maximization problem does not appear to be analytically tractable. The complexity arises from the non linear dependency of optimal α on the rate assignments $(r_1, ..., r_k)$. We consider the case of $n_s = n_d = m$, where the optimal α is equal to 0.5 as computed in the proof of lemma 5.1, and the DE can be derived in the following lemma:

Lemma 3.5.2. *The achievable DE curve of a Gaussian source with M-layer superposition coding over a block fading Rayleigh multi-hop MIMO DF relay channel with m antenna at source and destination and n_r antennas at the relay node is given by,*

$$\Delta^M = \begin{cases} \frac{bmn_r(A^M - C^M)}{mn_r A^M - bC^M}, & (m-2)(n_r-2) + 2 \leq b < mn_r \\ \frac{bMmn_r}{bM + 2(m+n_r-1)} & b \geq mn_r \end{cases} \tag{3.63}$$

where

$$A = 2(m + n_r - 1)$$
$$C = b - (m-2)(n_r - 2) + 2 \tag{3.64}$$

Proof: The proof is given in A.6.

The above analysis serves as a lower bound on the DE performance of MIMO relay channel. The analysis for more complex relaying protocols, e.g. dynamic protocols like DDF and the ones with a source-destination link, remains an open problem and is left for future research.

3.6 Performance Evaluation and Discussions

Fig. 3.4 provides a comparison in terms of the layered DMT curves among the proposed non-orthogonal layered broadcast code over NAF, denoted as NOL-NAF and NOL-NAF with one bit feedback (NOL-NAF-fb) given in theorem 3.3.1 and 3.3.2, respectively, and a number of counterparts including AF-based layered coding and non-layered coding schemes. For the AF coding, the relay-selection AF protocol given in [22] is employed. The result shows that the non-orthogonality property can effectively improve the DMT performance due to better utilization of the bandwidth resources by multiplexing more data on the same frequency band. In the meantime, the use of 1-bit feedback is observed to solidly improve the overall DMT performance by better exploring the available diversity gain of each layer $i \in [2 : M]$. For the first layer, interestingly, the performances of both with and without the feedback meet the optimal single layer curve, which demonstrates the optimality of the power allocation scheme in terms of the cancellation of inter-layer interference. Nonetheless, the feedback scheme eventually outperforms the non-feedback one due to a higher channel multiplexing gain, which leads to better performance curves of higher layers.

Next, we examine the DE performance of the proposed schemes, SR source code concatenated to non-orthogonal layered broadcast channel code deployed over NAF network, termed as SR-NOL-NAF and in the case of feedback link as SR-NOL-NAF-fb, as in theorem 3.4.2 and theorem 3.4.3. The result under an infinite number of layers is shown in Fig. 3.5, where a number of counterparts are also examined, including the single-layer NAF provided in lemma 3.4.4, the hybrid digital-analog transmission with layered source coding (HLS-AF/DF), hybrid layered dynamic DF (HLS-DDF) [36], and the DE upper

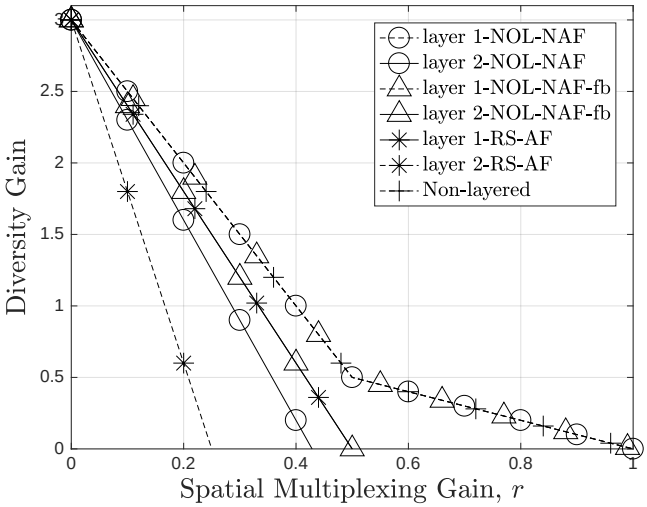

Figure 3.4: The DMT curve of non-orthogonal layered code over non-orthogonal AF network for $L = 2$ and two-layer coding, $r_1 = r_2 = r$ compared to RS-AF and non-layered code with rate $2r$.

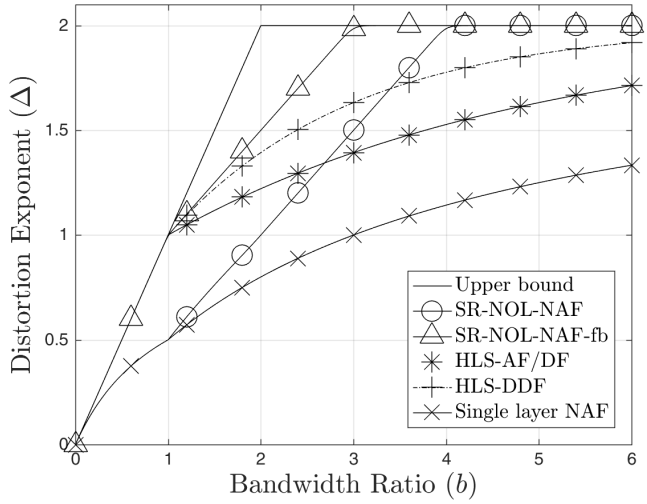

Figure 3.5: DE versus bandwidth ratio, b, for $L = 1$ and an infinite number of layers.

bound achieved by MISO with $L + 1$ transmit antenna given in [18],

$$\Delta_{MISO} = \min\{b, L + 1\}. \tag{3.65}$$

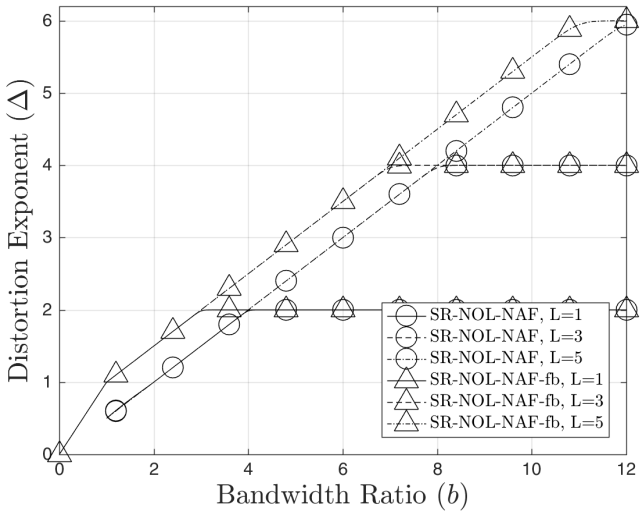

Figure 3.6: DE versus bandwidth ratio, b, under different numbers of cooperative nodes.

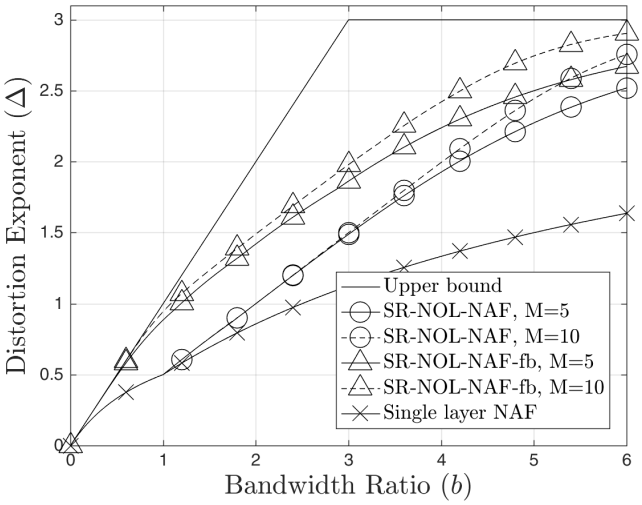

Figure 3.7: DE versus bandwidth ratio, b, for $L = 2$ and different numbers of layers.

Note that the DE analysis for HLS-AF and HLS-DDF was given in [20], which is taken as the best available AF and DF based hybrid layered scheme. All the multi-layer schemes were implemented with optimal DEs under infinite number of layers.

It is clearly shown in Fig. 3.5 that the proposed coding scheme, having infinite number

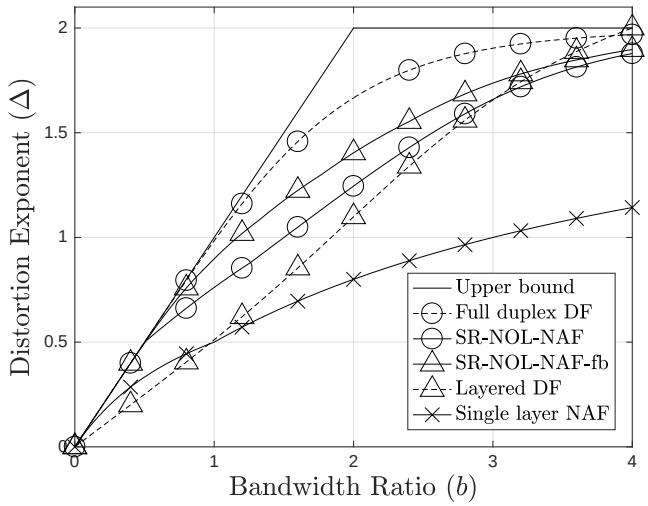

Figure 3.8: DE versus bandwidth ratio, b, for $L = 1$ and $M = 10$.

of layers with feedback can yield performance best approaching to the MISO upper bound curve under $0 \leq b \leq 1$ and $3 \leq b$, which demonstrates its optimality in this region. It also implies that the layered code with the proposed power allocation can properly match the transmission to the channel realization in this region. The non-feedback curve, on the other hand, can achieve the optimal curve when $b > 4$ and is sub-optimal for smaller values of b, due to the lower multiplexing gains of this scheme. The use of 1-bit feedback can enable better performance than that by HLS-AF and HLS-DDF for the entire range of b. Note that HLS based coding converges to the optimal curve with a rate lower than that of by SR-NOL-NAF, which demonstrates the superiority of non-orthogonal layered codes compared to the progressive codes in the regime of large b.

We then investigate the effect due to the number of relays, L, on the DE performance as shown in Fig. 3.6. It can be seen that the achievable DE converges to the maximum diversity gain of $L + 1$ as b increases. With small values of b (or, in the bandwidth limited region), the 1-bit feedback mechanism can dominantly boost the performance, thanks to the resultant higher bandwidth efficiency. The improvement, nonetheless, decays to zero as the bandwidth ratio increases. For the case of large values of b, both coding schemes can achieve the upper bound and are optimal in terms of DE performance.

We further consider more realistic cases of a finite number of layers. In Fig. 3.7, the DE performance of layered code on a 2-relay network, i.e., $L = 2$, with different numbers of layers of source codes is shown. With an improved adaptation of channel realization by adding more layers, the DE performance is significantly boosted against the non-layered

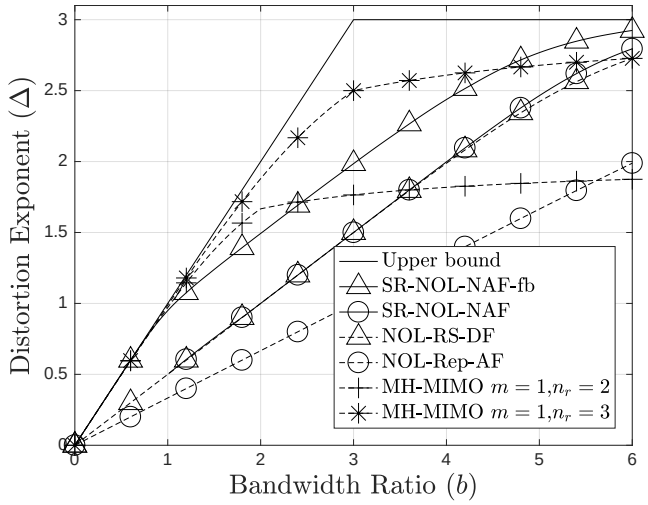

Figure 3.9: DE versus bandwidth ratio, b, for $L = 2$ and $M = 10$.

case, even with a small number of layers. Such improvement, nonetheless, is at the expense of higher complexity in the decoding process.

In Fig. 3.8 we compare the DE performance of 1-relay SR-NOL-NAF with the DF based cooperative schemes in both half-duplex and full-duplex modes under identical total power. The relaxation of the orthogonality constraint has affected the DE performance, where the gain of deploying the SR-NOL-NAF coding is significantly higher than the conventional DF code in half-duplex mode, especially under the low values of b. In contrast, the full-duplex DF coding dominantly outperforms SR-NOL-NAF since it enjoys additional degrees of freedom via simultaneous transmission and receiving at the relay nodes. Note that the full-duplex DF coding can achieve the optimal MISO upper bound for the entire range of bandwidth ratio in the asymptotic regime of infinite layers [20].

In Fig. 3.9 we consider the multi-relay network of $L = 2$ cooperating nodes and compare it with the repetition based AF codes and relay selection DF codes [22]. As the relay selection strategy requires one-bit feedback, the result of Theorem 3.4.3 is taken for comparison. It is observed that the NAF scheme exhibits higher gains compared to relay selection DF code with the one bit feedback and the repetition AF in the non-feedback mode; and the non-orthogonal layered code can better match to the non-orthogonal cooperative schemes compared with the conventional orthogonal counterparts. We also consider a more efficient method of distributed space-time codes for the conventional AF cooperation scheme as introduced in [40] in conjunction with non-orthogonal layered code in [22]. The

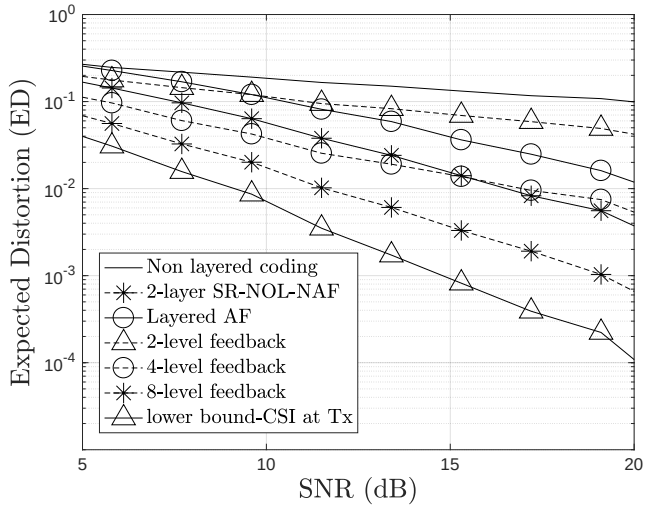

Figure 3.10: Expected distortion under different levels of SNR of SR-NOL-NAF for L=2 and $b = 4$, compared to non-layered coding, limited feedback network with 2, 4 and 8 levels of quantization, non-orthogonal layered code over AF network and the lower bound of full channel knowledge at transmitters.

space-time AF code achieves the same DE curve of relay selection DF code demonstrated in Fig. 3.9. Thus, compared with the NAF network, the space-time code achieves better DE performance compared with the non-feedback case, while the proposed feedback mode is superior to space-time code of [40]. It is concluded that the proposed SR-NOL-NAF code enjoys no worse performance than its counterparts while enjoying lower implementation complexity.

For the multi-hop MIMO system (denoted as MH-MIMO), we consider the case where the source and destination node is equipped with a single antenna, respectively, and the relay node has 2 or 3 antennas (i.e., n_r=2 or 3). It clearly shows that an L-relay single antenna NAF system yields very close performance to that by an $L + 1$-antenna single relay multi-hop MIMO system, mostly due to the same diversity orders. Specifically, the diversity of the former is achieved through independent nodes with single antenna, while the diversity of the later is achieved via a single node with multiple antennas. With low values of b, the MH-MIMO cases demonstrate better performance than that by multi-relay single antenna NAF, but become being outperformed when the value of b gets higher.

In order to demonstrate the effectiveness of the proposed low-complexity source-channel codes in the practical scenarios, we further demonstrate the expected distortion perfor-

mance of the layered code under general SNR setup, as shown in Fig. 3.10. A two-layer SR-NOL-NAF code is compared with a number of counterparts, including the non-layered code, the case of full channel knowledge at the transmitter, the AF based layered code and single-layer coding in the presence of limited feedback link studied in section IV.

We numerically optimize the expected distortion, $ED^{SL-fb}(Q)$ given in (3.50), by optimally adjusting the boundary values $b_k, k \in [1 : Q-1]$. It can be observed that the 2-layer SR-NOL-NAF code yields similar performance to that by four-level (2 bits) feedback link over a wide range of SNR values, which demonstrates how the layered scheme is able to effectively mitigate the lack of channel knowledge. The performance improvement compared to the non layered case and layered AF case is also clearly observed, which indicates a more efficient resource allocation of NAF compared to the conventional AF codes. The result confirms the effectiveness of the proposed SR-NOL-NAF coding for practical values of the SNR and finite numbers of layers.

3.7 Conclusions

In this chapter we consider the expected distortion performance of transmitting successive refinement Gaussian source over a multi-relay NAF network with the assumption that no CSI is available at the transmitter side. A novel low-complexity cross-layer design of source-channel codes is introduced, called SR-NOL-NAF, where the SR source codes and non-orthogonal layered broadcast channel codes are interplayed over the NAF network. By taking DE as the figure of merit, we have conducted in-depth analysis on the proposed codes under general values of bandwidth ratios in the high SNR regime, and further characterized the optimal performance of the proposed codes under certain regions of bandwidth ratio.

To gain deeper understanding on the performance of the proposed codes, extensive simulation was conducted for comparison of its counterparts with similar coding and network architecture available in the literature, including various DF and AF based layered broadcast codes, hybrid digital-analog codes, progressive code, distributed space-time codes, limited feedback codes, and multi-hop MIMO DF codes. We have also confirmed the superiority of the proposed SR-NOL-NAF codes in terms of the expected distortion performance under general SNR values.

Chapter 4

Uplink Multi-layer NAF Cooperative NOMA Codes

4.1 Introduction

As we discussed in chapter 1, power domain NOMA is a key enabling technique envisioned for 5G networks which unlike the OMA allows multiple data streams to be transmitted simultaneously over a resource block by using non-orthogonal layered broadcast code and is proved to achieve much higher spectral efficiency and enhanced user fairness compared to conventional OMA.

NOMA has attracted huge interest by research community in last few years. [51] has considered a downlink network of a base station transmitting to M users. It has shown that the superposition coding of the messages of the M users can highly improve the spectral efficiency in terms of ergodic sum rate compared to orthogonal allocation of the bandwidth to each user. [52] has proposed a pairing/grouping strategy to pair the M users into two-user groups and to use NOMA coding in each group. It is shown that pairing users with distinctive channel conditions (pairing a strong user with a cell edge user having poor channel gain) can boost the performance of the coding. Deployment of NOMA coding in MIMO systems is studied in several references including [58]-[61] and various precoding, beamforming, power allocation and clustering techniques is proposed. NOMA code is also incorporated into cooperative networks, where users with better channel conditions assist in transmission signals to weak users deploying forwarding strategies. It is shown that

The results presented in this chapter have already been published in [50].

cooperative NOMA schemes increase the range, reliability and system throughput, [7] and [8].

Most of the research on NOMA codes is dedicated to downlink network and there has been less attention to uplink scenario. [82] has firstly proposed an uplink NOMA code for orthogonal frequency division multiple access (OFDMA) where the users use the sub carriers without exclusivity and multi user detection is used for users' separation. suboptimal power and subcarrier allocation is proposed to boost the sum rate compared to OFDMA. Multiuser scheduling and power allocation for user fairness in NOMA over uplink OFMD is given in [87]. The same scenario of NOMA code for multicarrier system is studied in [85] and power and rate allocation is proposed for the non-asymptotic settings of practical block codes with finite length. [83] and [79] consider the power control strategy and decoding ordering problem in single carrier uplink to enhance the system outage event performance by minimize the inter-user interference, where [79] has proposed a dynamic ordering for SIC decoder based on the instantaneous received signal strength. While the work in [79] is limited to three users, [84] has extended the study to arbitrary number of users by approximating the interference term as a shifted-Gamma distribution and proper outage-constrained power allocation optimization is devised to achieve user fairness. Efficient clustering of users to boost the uplink NOMA performance is studied in [86]. [88] has considered a multicell uplink system with densely deployed cells. System throughput and outage probability is derived for randomly located users and in the presence of inter-cell interference.

Cooperative uplink NOMA coding has been investigated in terms of reliability, range and sum rate in the literature. [89] has proposed a coordinated direct and relay transmission in which a user has direct link to BS while the second user is connected through a relay node using DF scheme. Sum rate analysis is presented for both perfect and imperfect SIC decoding. A similar scenario with direct link available for both of the users is studied in [90]. A dedicated relay node deploying DF relaying protocol is assumed in [92], which facilitates the transmission of the far user to the base station and ergodic rate is derived for near and far users. Unlike the previous works, [93] has considered the full-duplex DF relaying scheme and sum rate and outage probability is provided in closed form. [94] has proposed a relay assisted network deploying AF scheme which does not rely on channel disparity among the paired user and prove to achieve the diversity order of two for each paired users.

In this chapter we propose a novel low-complexity layered cooperative NOMA scheme where the user equipment (UE) terminals cooperate with each other in transmission of their messages to the base station. Aiming to reduce the complexity at encoders to fit the requirements of machine type communications, we consider the NAF [11] scheme as

the cooperative scheme where each user deploy AF relaying scheme to forward the other users' messages with no need to decode the messages. Each user assists other users besides transmitting its own message by linearly amplifying its received signal. The messages of each user is encoded into several refining layers by deploying a non-orthogonal layered broadcast code and the layers are decoded at the BS, based on the instantaneous channel realization. The better the channel realization, the BS can decode more layers and achieve higher quality of service, hence adaptive quality of service is achieved. Outage probability of users is provided and unlike the previous studies on uplink cooperative NOMA which mainly rely on diversity order analysis for high SNR regime, we derive the more insightful DMT curve [12] of the proposed scheme.

Further to the outage and DMT analysis of channel coding, we consider transmission of uncompressed source messages at each user terminal. A layered SR [31] source code is matched to the multi-layer cooperative NOMA channel code. We define the notion of multi-user expected distortion and distortion exponent for the uplink network as an extension to single user network. Similar to previous chapter, the end to end performance of the system is derived in terms of expected distortion, the average distortion of the sources' messages reconstructed at the BS and the exponential decay rate of ED in high SNR. Although the analysis is valid for the asymptotically high SNR and long enough source/channel codes, it serves as an upper bound in facilitating the analysis of the performance of practical adaptive coding schemes for cooperative NOMA codes for machine type communications over uplink 5G networks.

4.2 System Model

We provide the system model for the cooperative multi user uplink system in this section and formulate the end to end system ED optimization problem for this network. As the optimization problem is intractable in general case, we subsequently reformulate the problem in high SNR regime.

4.2.1 SR Source Sequences Over Multi User Single Cell Cooperative Uplink Network

We consider an uplink single cell cellular network as shown in Fig. 4.1, where L user terminals communicate with a base station, all the nodes assumed to have single antenna. We assume a non-orthogonal multiple access scheme where all the users share the same

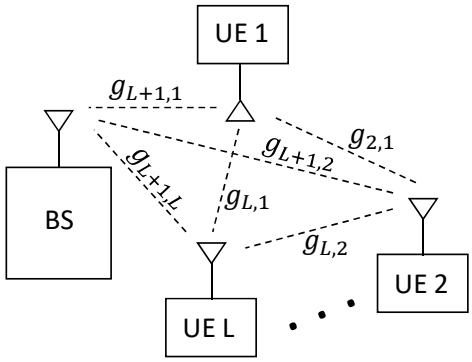

Figure 4.1: Multi-user cooperative uplink network.

frequency band resources. Every user $i \in [1 : L]$ intends to transmit its message m_i to the BS, termed as node $L+1$. The users are assumed to be able to cooperate with each other in transmission of their messages to the BS in half duplex mode. At user terminal i, the message $m_i \in [1 : 2^{NR_i}]$, where N is the channel code length and R_i is the coding rate in bits/s/Hz, is encoded into message sequence $\mathbf{x}_i = (x_i(n = 1), x_i(n = 2), ..., x_i(n = N))$, and $\mathbf{x}_i$ is transmitted over the network by user $i \in [1 : L]$. Each node besides transmission of its own message m_i encoded into sequence $\mathbf{x}_i$, cooperate in transmission of other nodes' messages $m_j, j \in [1 : L], j \neq i$, by encoding rule

$$(\mathbf{x}_i, \mathbf{y}_i) \rightarrow \mathbf{t}_i, \tag{4.1}$$

where $\mathbf{y}_i$, defined in (4.3) is the received vector of length N symbols at node i and $\mathbf{t}_i$ is the transmit vector with length N at node i, where the average energy available for transmission of a symbol at node i is given by

$$\frac{1}{N}\sum_{n=1}^{N} E[t_i^2(n)] = P, \tag{4.2}$$

for all nodes in the network. Assuming slowly Rayleigh flat fading channel, for links between each user to other users and to the BS node, the channel gain $g_{i,j}, i \in \{1, ..., L+1\}$, $j \in \{1, ..., , L\}$ are i.i.d complex Gaussian random variable with covariance equal to one, which remain constant over channel block length N. The received signal at each node $i \in [1 : L+1]$ is given by

$$\mathbf{y}_i = \sum_{\substack{j=1 \\ j\neq i}}^{L} g_{i,j}\mathbf{t}_i + \mathbf{z}_i, i \in [1 : L+1], \tag{4.3}$$

where $\mathbf{z}_i, i \in [1 : L+1]$ are additive white Gaussian noise vector of length N, having i.i.d elements with zero mean and unitary covariance. The SNR, ρ is defined as the ratio of average energy of a symbol to the variance of the noise observed at the receiving end. By setting σ_z^2 equal to 1, $\rho = \frac{P}{\sigma_z^2} = P$. Considering the mMTC services over 5G network, the signaling overhead and complexity of the encoders should be maintained as low as possible, hence we assume the CSI is only available at the BS node and no feedback link is deployed to convey such information to the transmitting nodes. The BS node's received sequence $\mathbf{Y}_{L+1}$ is decoded using SIC decoding rule to successively decode for messages $(m_1, ..., m_L)$ of the L users.

We assume data generated/collected at each user equipment node, including multimedia, measurement data, or etc. are supposed to be transmitted over the aforementioned 5G uplink network. Hence we model the source sequence at each node, by an uncompressed discrete-time continuous-amplitude data source sequence $s_i^K, i \in [1 : L]$ consisting of K source symbols. For the analysis, we assume the source sequences to be zero mean, unit variance, i.i.d Gaussian sequence. The source sequence s_i^K are mapped into the message m_i by source encoder $m_i(s_i^K)$, which is subsequently channel encoded by the channel encoder $\mathbf{x}_i(m_i)$ and sent over the cooperative NOMA uplink channel by the encoder $\mathbf{t}_i(\mathbf{x}_i, \mathbf{y}_i)$ as described above. The rate of the transmission of source sequence s_i^K is given by bR_i.

At the BS node, the SIC decoder, assigns estimate $(\hat{m}_1, \hat{m}_2, ..., \hat{m}_L)$, by successively decoding for the messages and then the source decoder reconstructs the source sequences by the estimation $(\hat{s}_1^K, \hat{s}_2^K, ..., \hat{s}_L^K)$.

Average distortion over K symbols for each source sequence is defined,

$$d(s_i^K, \hat{s}_i^K) = \frac{1}{K} \sum_{t=1}^{K} d(s_i^K(t), \hat{s}_i^K(t)), \tag{4.4}$$

and the *expected distortion* for user i is given by

$$D_i = E[d(s_i^K, \hat{s}_i^K)], \tag{4.5}$$

which is the statistical average of the end to end distortion, averaged over statistical random variables of the network including, random source sequences, AWGN noise at the nodes and channel fading gains. The overall network expected distortion is defined by

$$D = \max_{i \in [1:L]} D_i. \tag{4.6}$$

For the transmission of a Gaussian source over the Gaussian network, we assume the squared (quadratic) error distortion measure,

$$d(s, \hat{s}) = (s - \hat{s})^2. \tag{4.7}$$

We assume K is large enough to achieve the rate-distortion function of the source. The distortion of reconstruction of source sequence s_i^K by $\hat{s}_i^K$ at BS, is given by the inverse function of $R(D)$ where,

$$D_i = 2^{-bR_i}, \tag{4.8}$$

where R_i is the channel code rate for transmission of EU i. We intend to optimize the expected distortion of transmission of mMTC source sequence of L cooperating nodes over the uplink NOMA network described above, by devising the cooperative scheme $t_i, i \in [1 : L]$ and proper rate and power allocation to each node, hence the problem is formulated as follows

$$\begin{aligned} &\min_{\{t_i\}_{i=1}^L, \{R_i\}_{i=1}^L, \{\rho_i\}_{i=1}^L} \{D\} \\ &\text{s.t. } E[T_i^2] \leq \rho_i, \end{aligned} \tag{4.9}$$

with the assumption that CSI is only available at the BS node. This is a non-linear non-convex problem, which is not tractable in general case. We reformulate the problem in high SNR regime where $\rho \to \infty$, and consider the symmetric case, where the rate and power constraint of the nodes are assumed to be the same, hence $(R_i, \rho_i) = (R, \rho), \forall i \in [1 : L]$. We propose a novel sob optimal solution, where the source sequences at each node are encoded into refining layers, hence adapt the transmission to the channel state, with no CSI at the transmitting nodes and we propose a novel NOMA cooperative scheme based on NAF relaying protocol and prove that the proposed scheme is optimal for the symmetric network in high SNR. The achieved distortion serves as an lower bound on the general network in general SNR case.

4.2.2 High SNR approximation, DMT and DE analysis in multi-user case

The definition for DMT and DE given in 2.4 is extended to multi user case. Considering a slow fading network, the mutual information $\mathcal{I}_i$, corresponds to the supportable transmission rate of user i to the BS. It is a function of the random fading gains and other channel uncertainties, hence It is a random variable. Defining the channel fading gain vector $\mathbf{g} = \{g_{i,j}, i \in [1 : L+1], j \in [1 : L]\}$, the outage event, $\mathcal{O}_i$, for a fixed channel code rate R_i, is defined as $\mathcal{O}_i = \{\mathbf{g} | \mathcal{I}_i < R_i\}$ and probability of outage is $P_{\mathcal{O}_i} = Pr[\mathbf{g} | \mathcal{I}_i < R_i]$. In high SNR regime, defining the multiplexing gain, r_i as $R_i = r_i \log \rho$, the diversity gain

for user i is defined

$$d(r_i) = \lim_{\rho \to \infty} -\frac{\log P_{\mathcal{O}_i}(r_i)}{\log \rho}, \tag{4.10}$$

and $d(r_i)$ is the DMT curve for the channel. Similarly, DE for each user is defined as the exponential decay rate of the expected distortion for each UE,

$$\Delta_i = \lim_{\rho \to \infty} -\frac{\log D_i}{\log \rho}. \tag{4.11}$$

In high SNR the channel coding performance is captured by the $d(r_i)$ and DE fully characterizes the end to end performance of the source and channel coding scheme. For the problem of source sequence transmission over the cooperative uplink network, similar to the expected distortion, the overall network DE is defined as

$$\Delta = \min_{i \in [1:L]} \Delta_i \tag{4.12}$$

we assume the symmetric case, where $r_i = r, \forall i \in [1 : L]$. In high SNR regime the end to end performance optimization problem given in (4.9) is reformulated as

$$\begin{aligned} &\max_{\{t_i\}_{i=1}^L, r} \{\Delta\} \\ &\text{s.t. } E[T_i^2] \leq \rho_i. \end{aligned} \tag{4.13}$$

We outline the proposed suboptimal optimizing cooperative encoding rules $\{t_i\}_{i=1}^L$ and multiplexing gain, r, assignment for optimization problem (4.19), termed as layered NAF cooperative NOMA scheme in section 4.3. Subsequently in section 4.4 the performance analysis of the proposed coding in terms of DMT curve, and DE is presented.

4.3 Layered NAF Cooperative NOMA code

In this section we propose the layered coding scheme as a solution to optimize the end to end system performance. Also we provide the NAF cooperative uplink NOMA code as the proposed layered cooperative scheme.

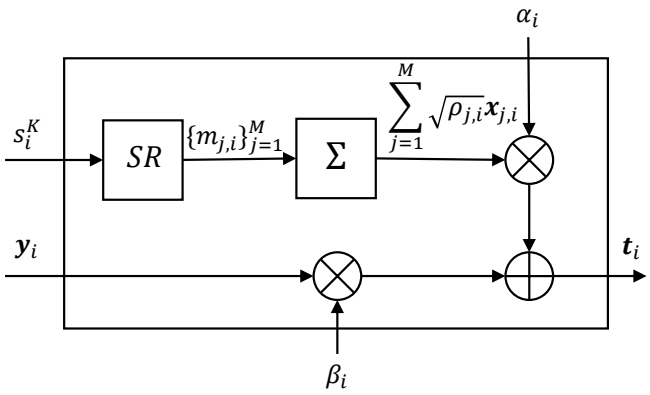

Figure 4.2: Proposed coding scheme for multi-layer NAF cooperative NOMA uplink code; Encoder, for user $i, i \in [1 : L]$.

4.3.1 Layered coding scheme

We consider a layered coding scheme, where the Gaussian source sequence s_i^K at node i is encoded into M refining descriptions $(m_{1,i}, ...m_{M,i})$, where the base layer description provides a coarse reconstruction of the source, while the refining descriptions of the upper layers can increase the resolution of the reconstruction, thus achieving lower distortions. Considering the SR property of the Gaussian source [31] under a common distortion measure d, there is no loss of optimality by successively describing layers of the source, hence the following M rate-distortion functions are simultaneously achievable,

$$\sum_{j=1}^{k} R_{j,i} = R(D_{k,i}), k \in [1 : M], \tag{4.14}$$

for each source sequence, where $R(D)$ is the rate-distortion function of the underlying source code defined in (2.17).

At each source node i, the sequence $s_i^K, i \in [1 : L]$ is compressed into M layers and channel encoded into superimposed sequences. At the destination node, the decoder decodes for layers $j \in [1 : M]$ for each source node $i \in [1 : L]$. Assuming j successfully decoded layers for each source message, the source sequence $s_i^K, i \in [1 : L]$ is reconstructed at the destination by $\hat{s}_i^K(m_{1,i}, ..., m_{j,i})$.

At source node i, the M successively refining layers of the source sequence are separately channel encoded and are superimposed. For each source sequence we have M channel sequences of rates $(R_{1,i}, R_{2,i}, ..., R_{M,i})$, where $R_i = \sum_{j=1}^{M} R_{j,i}$. The M-layer channel sequence

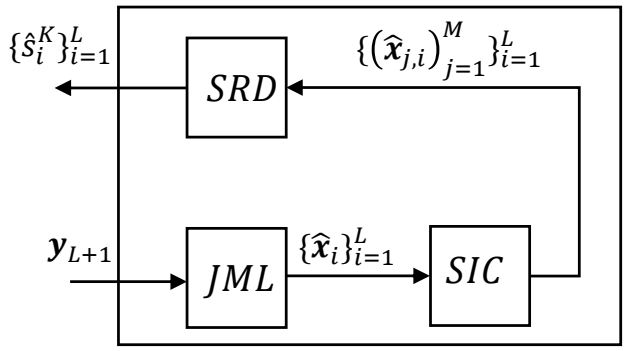

Figure 4.3: Proposed coding scheme for multi-layer NAF cooperative NOMA uplink code; Decoder at BS node, including joint maximum likelihood (JML), successive interference cancelation (SIC).

$\boldsymbol{t}_1^1$	$\boldsymbol{t}_2^1$	...	$\boldsymbol{t}_L^1$
$\boldsymbol{t}_1^2$	$\boldsymbol{t}_2^2$	...	$\boldsymbol{t}_L^2$
⋮			
$\boldsymbol{t}_1^P$	$\boldsymbol{t}_2^P$	...	$\boldsymbol{t}_L^P$

Figure 4.4: Proposed coding scheme for multi-layer NAF cooperative NOMA uplink code; Super frame structure.

at node i is given by

$$\big(\mathbf{x}_{1,i}(m_{1,i}), \mathbf{x}_{2,i}(m_{2,i}), ..., \mathbf{x}_{M_i,i}(m_{M,i})\big).$$

Based on the channel realization, the destination decodes as many layers as possible by considering the rest of the layers as interference. Based on the number of decoded

layers, the decoder reconstructs the source sequence with a distortion that is matched to the instantaneous channel realization.

At the source node i, channel sequence x_i^N, is constructed by superposition of the M layers,

$$\mathbf{x}_i(m_{1,i},...,m_{M,i}) = \sum_{j=1}^{M} \sqrt{\rho_{j,i}}\mathbf{x}_{j,i}(m_{j,i}), \tag{4.15}$$

where $\rho_{j,i}, j \in [1:M]$ defines the allocated power to layer j of transmitter i and $\sum_{j=1}^{M} \rho_{j,i} = \rho$.

The destination node decodes the received messages $(m_{1,i}, m_{2,i}, ..., m_{M,i})$ of source sequence $s_i^K, i \in [1:L]$ and recovers as many layers as possible for each transmitter based on the instantaneous fading status, channel realization and additive noise level. Based on the number of successfully decoded layers, $\hat{s}_i^K$ is reconstructed accordingly. For the case that k layers are decoded for source i, the distortion rate functions is given by,

$$D_{k,i} = 2^{-b\sum_{j=1}^{k} R_{k,i}}, k \in [1:M]. \tag{4.16}$$

The outage event for layer k, is denoted by

$$O_{k,i} = \{\mathbf{g} : \mathcal{I}_{k,i} < R_{k,i}\}. \tag{4.17}$$

where $\mathcal{I}_{k,i}, k \in [1:M]$ is the mutual information of the kth layer of node i, assuming the lower layers are decoded by SIC decoder and the higher layers are interference terms. For the case of layered coding, the expected distortion of node i is defined as

$$D_i^L = \sum_{j=0}^{M} (P_{O_{j+1,i}} - P_{O_{j,i}})D_{j,i}, \tag{4.18}$$

where $D_{j,i}$ is given by (4.16) and $P_{O_{M+1,i}} = 1-\epsilon$, $P_{O_{0,i}} = 0$, $D_{0,i} = 1$, $\epsilon > 0$.

By the high SNR assumption, $\rho \to +\infty$, the layered network overall expected distortion, D^L and distortion exponent, Δ^L, are defined as in (4.6) and (4.12), replacing D_i with D_i^L as given in (4.18). The distortion exponent optimization problem for layered code is,

$$\begin{aligned} &\min_{\{t_i\}_{i=1}^{L}, r} \{\Delta^L\} \\ &\text{s.t. } E[T_i^2] \leq \rho_i. \end{aligned} \tag{4.19}$$

4.3.2 NAF Cooperative uplink NOMA Code

We outline the proposed NAF based cooperative NOMA scheme for the uplink network which is matched to the layered coding scheme described above, in follows. We characterize the cooperative encoding functions $\mathbf{t}_i(\mathbf{x}_i, \mathbf{y}_i)$ which defines the cooperation scheme. Let a cooperation frame consists of L transmission blocks. In transmission block i, only node i is active and transmits its own layered messages $\{m_{j,i}\}_{j=1}^{M}$ encoded into $\mathbf{x}_i$, besides it assists in transmission of another node j. Hence the message sequences in cooperation frame p is

$$\mathbf{x}_1^p, \mathbf{x}_2^p, ..., \mathbf{x}_L^p. \tag{4.20}$$

We consider P consecutive cooperation frames, termed as super frame, during which the message sequences are expressed as

$$\begin{aligned} &\mathbf{x}_1^1, \mathbf{x}_2^1, ..., \mathbf{x}_L^1, \\ &\mathbf{x}_1^2, \mathbf{x}_2^2, ..., \mathbf{x}_L^2, \\ &\vdots \\ &\mathbf{x}_1^P, \mathbf{x}_2^P, ..., \mathbf{x}_L^P. \end{aligned} \tag{4.21}$$

During each super frame the cooperating node assignment for each transmitting node is based on the right circular shift of $1, 2, , ..., L$, where for super frame l, the cooperating node i for transmitter $j = 1, ..., L, j \neq i$ is assigned by

$$i = j + l \pmod{L}. \tag{4.22}$$

There are $L-1$ distinct configurations for the cooperation assignment, so $L-1$ consecutive super frame are considered, where in each super frame the cooperating node assignment is defined by the rule given in (4.22), and is fixed during the P cooperation frames of the super frame. This forms the transmission frame of length $LP(L-1)$ channel code blocks. In each transmission frame, in total $LP(L-1)$ messages are transmitted to the destination by L nodes, which provides $P(L-1)$ messages for each node.

The cooperating node i at cooperation frame p, relays the sequence $\mathbf{x}_j^{p'}(m_j)$, besides transmitting its own message sequence $\mathbf{x}_i^p(m_i)$ by linearly combining the two sequences. For each super frame l, p' is given by

$$p' = \begin{cases} p, \ j + l \pmod{L} > j \\ p - 1, \ j + l \pmod{L} \leq j. \end{cases} \tag{4.23}$$

Hence the encoding function of the cooperative scheme, $\mathbf{t}_i(\mathbf{x}_i, \mathbf{y}_i)$ is defined as the linear combination of the node i, message sequence and the received signal at node i,

$$\mathbf{t}_i^p = \alpha_{i,p}\mathbf{x}_i^p + \beta_{i,p}\mathbf{y}_{i,}^p, i \in [1:L]. \tag{4.24}$$

where the coefficients of $\alpha_{i,p}$ and $\beta_{i,p}$ in (4.24) are set such that the overall power limit of ρ is met by the nodes at each transmission block and $\mathbf{y}_{i,p}$ is the received signal at source node i in cooperation frame p defined as

$$\mathbf{y}_i^p = g_{i,j}\mathbf{t}_j^{p'} + \mathbf{z}_i^p, i \in [1:L]. \tag{4.25}$$

The received sequence at the BS node in each super frame is given by

$$\mathbf{y}_{L+1}^p = g_{L+1,i}\mathbf{t}_i^p + \mathbf{z}_i^p, i \in [1:L], p \in [1:P], \tag{4.26}$$

where $\mathbf{t}_i^p$ is given in (4.24) and the super frame structure is shown in Fig. 4.4.

The recursive cooperation relationship (4.24) and (4.25), along with the cooperating node assignment by (4.22), ensure all source nodes to be relayed by all the other $L-1$ nodes in every transmission frame.

The destination node decodes the $P(L-1)$ messages of each source node sent during the transmission frame, and in total it receives $LP(L-1)$ messages from all the senders during transmission frame of length $LP(L-1)$, hence the overall rate of the system is equal to R. The encoder and decoder for the proposed NAF cooperative NOMA code is given in Fig. 4.2 and Fig. 4.3.

4.4 high SNR Analysis for Layered NAF Cooperative Uplink NOMA Code

In this section we derive the achievable layered DMT curve for the proposed coding. Based on the achievable DMT curve, we also optimize the DE measure for the cooperative network.

4.4.1 Layered DMT curve analysis

In this section we analyze the DMT curve of the proposed layered NAF cooperative NOMA scheme. We provide a lower bound on the achievable diversity and show that it achieves

the upper bound of MISO network, hence prove the optimality of the layered scheme. Our approach follows the techniques used in [11], [12] and [18]. Assuming only a subset of sources $Q \subset [1:L]$ are transmitting messages and the rest are set to zero, we consider a suboptimal decoder which picks a partial observation vector, consist of only one observation for source $j \in Q$, in each transmission frame.

For the transmitted sequence $\mathbf{x}_j^{p'}, j \in Q$ which is relayed by the node i in cooperation frame p, the decoder picks the observation based on the following rule

- in case the cooperating node $i \notin Q$, the decoder picks either the transmit sequence of $g_{L+1,j}a_{j,p'}\mathbf{x}_j^{p'}$ or the relayed sequence $g_{L+1,i}b_i g_{i,j}a_j\mathbf{x}_j^{p'}$, deciding based on the more dominant channel gain of $g_{L+1,j}$ and $g_{L+1,i}$.
- In case $i \in Q$, the decoder picks the direct transmission of $g_{d,j}a_j\mathbf{x}_j^{p'}$ over the relayed signal.

The outage event for layer k of the sub optimal SIC decoder can be written as

$$O_k = \Big\{\frac{1}{|Q|P(L-1)}\log|I+ G\Sigma_{x_k}G^h(G\Sigma_{x_{k+1}}G^h+\Sigma_Z)^{-1}| < r_k\log\rho\Big\} \tag{4.27}$$

where G is square matrix of size $|Q|P(L-1)$, corresponds to the $|Q|$ observation per cooperation frame over a transmission frame of length $L-1$ super frames. It is a lower triangular matrix with nonzero elements of $g_{L+1,j}a_{j,p'}\mathbf{x}_j^{p'}$ or $g_{L+1,i}b_{i,p}g_{i,j}a_{j,p'}\mathbf{x}_j^{p'}$ based on the decoding rule of decoder. The matrix Σ_{x_k} is a diagonal matrix, where the non zero elements are set such that the transmit signals t_j^p meet the power constraints $E(|t_j^p|^2) \leq \rho$. Σ_Z is the covariance of the noise vector. With the high SNR regime, the channel gain exponents $v_i, u_{i,j}, i,j \in [1:L]$ are defined as $|g_{L+1,i}|^2 = \frac{1}{\rho^{v_i}}$,$|g_{i,j}|^2 = \frac{1}{\rho^{u_{i,j}}}$ and the channel gain exponent vector $\mathbf{u}$ is defined, $\mathbf{u} = \big(\{v_i\}_{i=1}^L, \{u_{i,j}\}_{i,j=1}^L\big)$. We define the set O' as the channel exponents set, where

$$O'_k = \Big\{\mathbf{u} : \log|I+ G\Sigma_{x_k}G^h(G\Sigma_{x_{k+1}}G^h+\Sigma_Z)^{-1}| < |Q|P(L-1)r\log\rho_k\Big\}. \tag{4.28}$$

The following theorem provides the achievable diversity gain for the multiplexing gain in the range $[0:1]$ for the symmetric layered NAF cooperative uplink NOMA code.

Theorem 4.4.1. *The DMT curve of a symmetric layered NAF cooperative uplink NOMA code of L nodes deploying M-layer coding is lower bounded by*

$$d^L(r_k) = L(1-r_1-...-r_k), k \in [1:M]. \tag{4.29}$$

Proof: We analyze the high SNR outage event for the layer k by considering the event O'_k in (4.28). Since the channel matrix G is a lower triangular matrix, the determinant is the multiplication of the diagonal elements. Based on the decoding rule, in case the cooperating node is in Q, the direct source signal is used by the decoder and in case of $i \notin Q$, the best link of $g_{L+1,j}$ and $g_{L+1,i}g_{ij}$ is chosen. Also the noise covariance in high SNR can be shown to be $\Sigma_Z \leq I$. Hence, the outage event of layer k, O'_k, in (4.28), can be written as

$$O'_k = \big\{\mathbf{u} : \log \frac{|G\Sigma_{x_k} G^h|}{|G\Sigma_{x_{k+1}} G^h + I|} < |Q|P(L-1)r_k \log \rho\big\} \tag{4.30}$$

The aggregate power allocated to layers $(k, k+1, ...M)$, $\sum_{i=k}^{M} \rho_i$ is set to

$$\bar{\rho}_k = \sum_{i=k}^{M} \rho_i = \rho^{\gamma_k}. \tag{4.31}$$

Replacing the values of channel gains of G by the corresponding values, given by the decoding rule, and further simplification, the term $|G\Sigma_{x_k} G^h|$ in (4.30) in terms of power allocation exponent γ_k and channel gain exponents $\{v_i\}_{i=1}^{L}, \{u_{i,j}\}_{i,j=1}^{L}$ is

$$|G\Sigma_{x_k} G^h| = \rho^{\eta_k},$$

where

$$\begin{aligned} \eta_k &= |Q|(L-1)P\gamma_k - \\ &\sum_{j\in Q}\Big((|Q|-1)Pv_j + \sum_{i\notin Q}\big(\min\{v_j, u_{ij}+v_i)\}(P-1)+v_j\big)\Big) \end{aligned} \tag{4.32}$$

Hence O'_k can be written as

$$O'_k = \big\{\mathbf{u} : \rho^{\eta_k} - \rho^{\eta_{k+1}+|Q|P(L-1)r_k} < \rho^{|Q|P(L-1)r_k}\big\} \tag{4.33}$$

We set the power allocation coefficients recursively as

$$\gamma_{k+1} = \gamma_k - r_k - \epsilon, \tag{4.34}$$

for some $\epsilon > 0$. Hence

$$\begin{aligned} O'_k &= \big\{\mathbf{u} : \rho^{\eta_k}(1-\rho^{-\epsilon}) < \rho^{|Q|P(L-1)r_k}\big\} \Rightarrow \\ O'_k &= \big\{\mathbf{u} : \rho^{\eta_k} < \rho^{|Q|P(L-1)r_k}\big\} \end{aligned} \tag{4.35}$$

Replacing the value for η_k given in (4.32), the outage event for layer k is

$$O'_k = \Bigg\{ \mathbf{u} : \sum_{j \in Q} v_j > |Q|(1-r), \\ \sum_{j \in Q} (|Q|-1)v_j + \sum_{i \notin Q} u_{ij} + v_i > \\ |Q|(L-1)(1-r) \Bigg\} \tag{4.36}$$

The probability of outage is

$$P_{O'_k} = \int_{O'_k} p_{\mathbf{u}}(\mathbf{u}) d\mathbf{u} \tag{4.37}$$

Deploying the typical outage event method of [11, Result 5], the probability of the outage event in the high SNR , $P_{O'_k}$, is given by

$$P_{O'_k} \doteq \rho^{-d_k(r_k)} \tag{4.38}$$

where $\doteq$ denotes high SNR exponent equality, and $d_k(r_k)$ is given by

$$d_L(r_k) = \inf_{\mathbf{u} \in O'} \sum_{j=1}^{L} v_j + \sum_{i<j} u_{ij} \tag{4.39}$$

The infimum is achieved by the lower bounds given in (4.36). Replacing the values of v_j and u_{ij} we have

$$\begin{aligned} d^L(r_k) &= |Q|(1 - \sum_{i=1}^{k} r_i) \\ &\quad + (L-1)(1 - \sum_{i=1}^{k} r_i) - (|Q|-1)(1 - \sum_{i=1}^{k} r_i) \\ &= L(1 - \sum_{i=1}^{k} r_i) \end{aligned} \tag{4.40}$$

which proves the achievable diversity order given in 4.29.

This provide the achievable lower bound on the diversity gain of the proposed coding. An upper bound on the system performance is derived by assuming that all the L nodes form an antenna array of length L and jointly transmitting to BS node with one antenna, hence form a MISO system. The layered MISO system diversity gain is given in [18] and by (4.29) it is shown that MISO upper bound is achieved by the proposed coding. Hence indeed the achieved curve is the optimal DMT curve for cooperative uplink NOMA code.

4.4.2 End to end performance Analysis; DE optimization

Having derived the DMT curve of symmetric layered NAF cooperative uplink NOMA system, where the M layers of the L transmitting nodes are assumed to have the same diversity gains $r_{j,i} = r_j, i \in [1:L], j \in [1:M]$, we now provide the achievable average DE of end to end system. The conditions on the optimal multiplexing gain assignment $\{r_j\}_{j=1}^{M}$ are firstly derived in the following lemma.

Lemma 4.4.2. *The multiplexing gain assignment, r_j of the layers $[1:M]$ of the L transmitting nodes over a layered NAF cooperative NOMA network, which optimize the achievable expected distortion in the high SNR regime in (4.19) is given by*

$$b\sum_{i=k+1}^{M} r_i - d^L(r_k) = 0, k \in [1, M]. \tag{4.41}$$

$$\begin{aligned} &-\min -b\sum_{i=1}^{M} r_i \\ &\text{s.t. } b\sum_{i=1}^{M} r_i \le d^L(r_k) + b\sum_{i=1}^{k} r_i, k \in [0:M]. \end{aligned} \tag{4.42}$$

We form the Lagrangian

$$L = -b\sum_{i=1}^{M} r_i + \sum_{k=0}^{M} \mu_k \big(b\sum_{i=k+1}^{M} r_i - d^L(r_k)\big) \tag{4.43}$$

Considering the complementary slackness condition [44], the optimal solution satisfies the

$$\begin{cases} \nabla L = 0 \\ \mu_k \big(b \sum_{i=k+1}^{M} r_i - d(r_k)\big) = 0, k \in [0, M] \\ \mu_k \geq 0, k \in [0, M] \end{cases} \tag{4.44}$$

solving $\partial L / \partial r_i = 0$ for $i \in [0, M]$, the coefficients μ_k are

$$\mu_{k+1} = \frac{L}{b} \mu_k, \tag{4.45}$$

where $\mu_0 = \frac{b^M}{\sum_{k=0}^{M} b^{M-k} L^k}$. Hence for $b > 0$ the $\mu_k, k \in [0, M]$ are strictly positive. Therefore the optimal multiplexing gain vector $(r_1, r_2, ..., r_M)$, satisfies

$$b \sum_{i=k+1}^{M} r_i - d(r_k) = 0, k \in [1, M] \tag{4.46}$$

This completes the proof of lemma 4.4.2.

Now we derive the optimal DE for the layered NAF cooperative NOMA code, deploying the multiplexing gain of each layer according to the results of lemma 4.4.2. The following theorem characterizes the DE for the finite number of layers and in the case of asymptotic approximation of infinite number of layers.

Theorem 4.4.3. *The achievable DE of L Gaussian sources with unit covariance, each observed at a source node $i \in [1 : L]$ and encoded into M layers concatenated to a symmetric NAF cooperative uplink NOMA code, is given by*

$$\Delta^M = \frac{bLA_M}{L + bA_M} \tag{4.47}$$

where A_M is given by

$$A_M = \sum_{i=0}^{M-1} (\frac{b}{L})^i. \tag{4.48}$$

The optimal DE of the layered NAF cooperative NOMA code in the limit of infinite number of layers, $M \to \infty$, is given by

$$\Delta^{+\infty} = \min\{b, L\}. \tag{4.49}$$

Proof: Considering the layered diversity gain of (4.29), the expected distortion equation of (4.18) for layered code, and the optimal diversity gain assignment given in lemma 4.4.2, the optimal multiplexing gain of each layer is computed as

$$r_k = (\frac{b}{L})^{k-1} r_1, \tag{4.50}$$

and for the last layer we have

$$r_M = \frac{L}{b + LA_M}, \tag{4.51}$$

where A_M is given by (4.48). The distortion exponent can be written as

$$\begin{aligned} \Delta^M &= b(r_1 + r_2 + ... + r_M) \\ &= bA_M r_M, \end{aligned} \tag{4.52}$$

further simplification for Δ gives the equation of (4.47).

In the case of the infinite number of layers, A_M simplifies to $\frac{L}{L-b}$ and the DE given in (4.47) is equal to b for $b < L$, and the DE simplifies to L for $b > L$.

This completes the proof. □

It can be seen that the layered NAF cooperative NOMA code achieves the MISO upper bound [18] in terms of DE in the asymptotic regime of infinite number of layers. This implies that the proposed layered code is indeed optimal in the considered network setup.

In order to compare the result of the layered scheme with the single layer case, we formulate the DE of a single layer code over uplink network which is given in the following lemma.

Lemma 4.4.4. *The DE of a single layer NOMA code over an uplink network is given by*

$$\Delta^{SL} = \frac{Lb}{L + b}. \tag{4.53}$$

Proof: The DMT curve of the single layer uplink network is given in [11]

$$d(r) = L(1 - r) \tag{4.54}$$

The expected distortion in terms of outage event and source distortion-rate function for a single layer code is

$$ED = (1 - P_O)D + P_O \tag{4.55}$$

In the high SNR region, we have

$$\lim_{\rho\to\infty} ED = \rho^{-br} + \rho^{d(r)} \tag{4.56}$$

Hence the optimal multiplexing gain is

$$br = L(1-r) \tag{4.57}$$

Therefor, the DE is

$$\Delta = \frac{bL}{L+b} \tag{4.58}$$

This completes the proof. □

4.5 Simulation Results

To gain deeper understanding of the performance of the proposed layered cooperative NOMA code, a case study is conducted on transmission of Gaussian sources over a 5-layer NAF cooperative NOMA uplink code, termed as NAF-NOMA (i.e., $M = 5$). The network DE versus bandwidth ratio b is illustrated in Fig. 4.5 under different number of cooperating nodes L. It can be seen that the diversity gain and consequently the achievable DE are proportional to L. With small values of b, the performance of all the cases is close to each other disregard of the number of cooperating nodes. As b increases, the effect of number of cooperating nodes becomes more dominant, and the DE tends to the value of L as b is very large. In practical applications, users can be clustered into groups and cooperative scheme can be deployed within each group. The optimal number of user per cluster is designed by a tradeoff between the ED performance and the complexity of SIC decoder and is subject to further research.

Fig. 4.6 shows the inference due to the number of layers upon the DE performance of the proposed NAF-NOMA uplink coding with 3 cooperating nodes, where the proposed code is compared with a non-layered code and also the MISO upper bound. It can be seen that even with a limited number of layers, the DE performance is considerably improved against the non-layer coding case.

It is also observed that by increasing the number of layers, the performance of the proposed code is getting closer to the upper bound of L MISO system. As proved in Theorem 4.4.3, the case of infinite numbers of layers can achieve the MISO upper bound and is thus optimal in terms of DE.

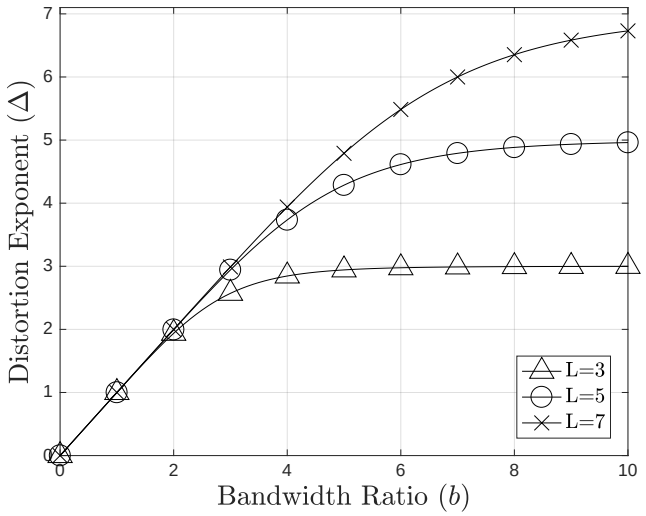

Figure 4.5: DE versus bandwidth ratio (b) for the proposed for layered cooperative NAF-NOMA uplink code under different numbers of cooperating nodes and five layers (i.e., $M = 5$).

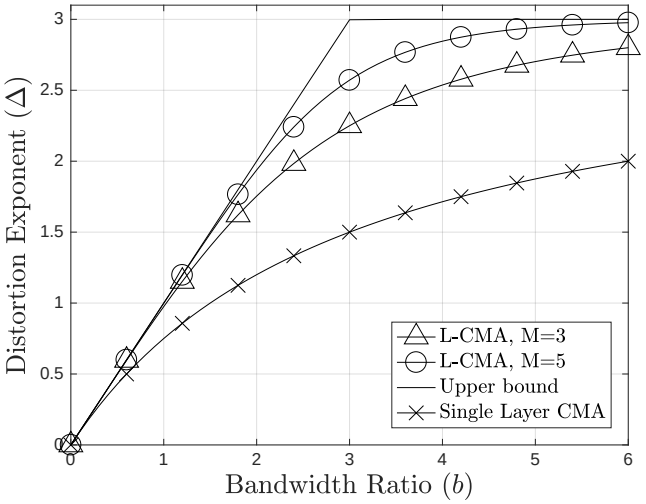

Figure 4.6: DE versus bandwidth ratio (b) for layered cooperative NAF-NOMA uplink code with 3 cooperating nodes (i.e., $L = 3$) and different numbers of layers M.

In Fig. 4.7, we examine the performance of the proposed coding in general SNR values. We compare the expected distortion of a two-layer NAF-NOMA with the schemes of AF

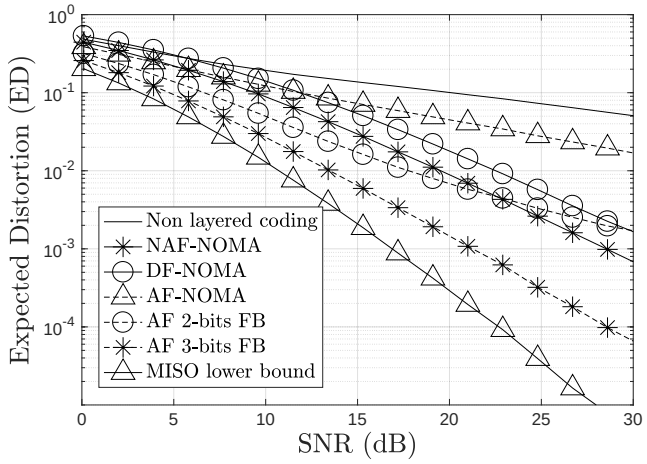

Figure 4.7: DE versus bandwidth ratio (b) for the proposed layered CMAN under different numbers of cooperating nodes and five layers (i.e., $M = 5$).

and DF NOMA codes available in the literature, for case of CSI is not available at the transmitting nodes. Also, we consider a limited feedback non-layered AF scheme where partial CSI is feedbacked to the transmitting nodes. It can be seen that the layered NAF-NOMA scheme provide significant SNR gain compared to non-layered scheme and improves performance over the layered AF-NOMA and DF-NOMA. Based on the number of layers deployed, it matches the performance of a limited feedback network and in the asymptotic case of infinite number layers it matches the full CSI at the transmitting nodes. It should be noted that, to facilitate a tractable analytical result, our analysis considers the case of asymptotic high SNR symmetric network, hence the results serves as an lower bound on the outage probability and upper bound on the expected distortion of practical scenarios.

4.6 Conclusions

In this chapter a novel layered NAF cooperative NOMA code has been proposed for uplink multi-user cellular transmission. It is shown that layered scheme matches the performance of the users to channel conditions with no CSI at the transmitting node, and the NAF cooperative NOMA scheme outperforms the AF and DF based coding in terms of expected distortion. The low complexity encoders with low signaling overhead make it a proper solution for mMTC of uplink IoT communications over 5G network.

Chapter 5

Finite SNR Analysis of Non-orthogonal Layered Compress-Forward Coding

5.1 Introduction

In this chapter we consider a single relay network with the same assumption of no CSI at transmitting node and analyze the end to end performance in terms of expected distortion. We propose a layered coding scheme which delivers an adaptive rate coding with no CSI at the transmitter. We consider a two state fading channel and propose a two layer coding scheme matched to the channel. Unlike the previous two chapters we analyze the system performance in general SNR values. We develop a non-orthogonal layered coding scheme based on CF relaying strategy, where the base layer is assisted by the relay node deploying CF coding and the refining layer is transmitted through the direct link.

We consider a scenario where a base station (source node) is transmitting messages to a mobile user equipment (destination node) under the assistance of a relay node. This architecture forms a relay-assisted network as depicted in Fig. 5.1. The channel can be modeled as

$$p_{Y_2Y_3|XX'}(y_2, y_3|x, x'), \tag{5.1}$$

where x and x' are the input symbols at the source node and the relay node, respectively, which are chosen from finite-alphabet input sets $\mathcal{X}$ and $\mathcal{X}'$. The y_2 and y_3 are received

The results presented in this chapter have already been published in [73].

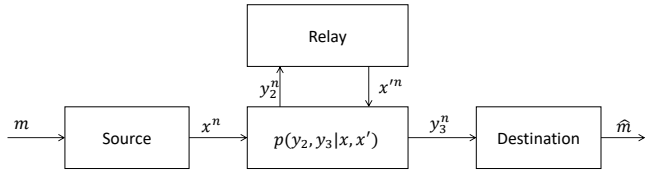

Figure 5.1: Channel model for relay-assisted network

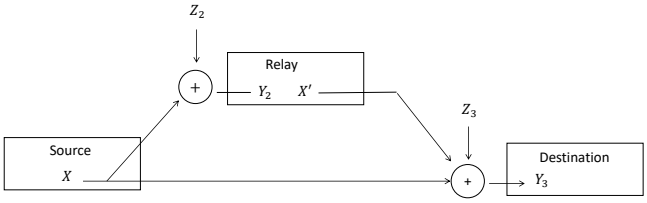

Figure 5.2: Gaussian relay-assisted network

symbols at the relay and destination nodes. Considering coding over n channel uses at the rate of R bits per channel uses, message $m \in [1 : 2^{nR}]$, is encoded into the channel codewords at the source node, denoted as $x^n(m)$. The set of codewords $x^n(m), m \in [1 : 2^{nR}]$, forms the codebook $\mathcal{C}$. The channel sequence $x^n(m)$ at the source node is sent over the channel. The relay and the destination nodes receive noisy sequences of y_2^n and y_3^n, respectively. The relay transmits the message x'^n, containing information on the message m, in the next transmission block. At the destination node, the decoder assigns an estimate of $\hat{m}$ to each received sequence y_3^n, which is a function of x^n and x'^n.

For this channel coding setup, it is intended to make the average probability of error in decoding the message m at the destination node, denoted as $P_{error}(\mathcal{C}) = Pr(M \neq \hat{M})$, close to zero in the asymptotic regime of n,

$$\lim_{n \to +\infty} P_{error}(\mathcal{C}) = 0. \tag{5.2}$$

For the special case of Gaussian network, the network is modeled as

$$\begin{cases} Y_2 &= g_{12}X + Z_2, \\ Y_3 &= g_{13}X + g_{23}X' + Z_3, \end{cases} \tag{5.3}$$

which is shown in the Fig. 5.2. We assume a slowly fading, frequency non-selective channel, where the channel gain of each of the links is represented by a single discrete-time complex filter tap, $g_{i,j}$,$i \in \{1, 2\}$ and $j \in \{2, 3\}$. The noise terms Z_2 and Z_3 are i.i.d

zero-mean, circularly-symmetric complex Gaussian random variables with power spectral density equal to 1.

5.2 Non-orthogonal Layered Broadcast CF Coding

We develop a non-orthogonal layered broadcast coding scheme based on CF relaying strategy, where the base layer is assisted by the relay node deploying CF coding and the refining layer is transmitted through the direct link. In the following theorem, the achievable inner bound of the proposed layered coding is presented.

Theorem 5.2.1. *The layered CF inner bound on the capacity of relay channel modeled by (5.1), when the channel state information is not available at the source node is given by*

$$C \geq \max_{p(x_2,x_1)p(x')p(u|x',y_2)} \min\{R', R''\}, \tag{5.4}$$

where,

$$\begin{aligned} R_r &= I(X_2; Y_3|X', X_1, U), \\ R' &= I(X_1; U, Y_3|X') + R_r, \\ R'' &= I(X_1, X'; Y_3) - I(U; Y_2|X_1, X', Y_3) + R_r, \end{aligned}$$

for a probability mass function,

$$p(x_2, x_1)p(x')p(u|x', y_2).$$

Proof:

We deploy block Markov coding to encode q 2-layer message sets $(m_{1,j}, m_{2,j})_{j=1}^{q}$ into q blocks, each of length n channel uses. Similar to classical CF coding, Wyner-Ziv coding is used to compress the description U of the received message Y_2 at the relay, and to transmit its compressed version, X' to the destination. The refining layer X_2 is superimposed over the base layer message X_1. The destination node jointly decodes for U and X_1, and then successively decodes for the refining layer X_2. The sketch of the proof is given as follows.

Codebook Generation:

For each $j \in [1 : q]$, generate 2^{nR_1} sequences $x_1^n(m_{1,j})$ each according to $\prod_{t=1}^{n} P_{X_{1,j}}(x_{1,j,t})$.

For each $m_{1,j}$ generate 2^{nR_2} sequence $x_2^n(m_{2,j}|m_{1,j})$, each according to the conditional distribution

$$\prod_{t=1}^{n} P_{X_{2,j}|X_{1,j}}(x_{2,j,t}|x_{1,j,t}).$$

Generate $2^{nR'}$ sequences $x'^n(l_{j-1})$ each according to

$$\prod_{t=1}^{n} P_{X'(x'_t)}. \tag{5.5}$$

For each $l_{j-1} \in [1 : 2^{nR'}]$, generate $2^{n\tilde{R}'}$ sequences $u^n(k_j)$ each according to the conditional distribution $\prod_{t=1}^{n} P_{U|X'}(u_t|x'_t)$.

Partition the set of $[1 : 2^{n\tilde{R}'_j}]$ into $2^{nR'}$ equal-sized bins $\mathcal{B}(l_j), l_j \in [1 : 2^{nR'}]$. The following codebooks and the bin assignments are revealed to all three nodes in the relay network,

$$\begin{aligned}\mathcal{C}_j = \Big\{ & x_1^n(m_{1,j}), x_2^n(m_{2,j}|m_{1,j}), x'^n(l_{j-1}), u^n(k_j|l_{j-1})), \\ & u^n(k_j) \in \mathcal{B}(l_j), \\ & m_{1,j} \in [1 : 2^{nR_1}], m_{2,j} \in [1 : 2^{nR_2}], \\ & k_j \in [1 : 2^{n\tilde{R}'}], l_j \in [1 : 2^{nR'}] \Big\}. \end{aligned} \tag{5.6}$$

Source and Relay Encoding:

At the transmitter side the sequence $x_2^n(m_{1,j}, m_{2,j})$ is sent over the channel.

At the end of block j and upon receiving the signal $y_2^n(j)$, the relay finds the index $\tilde{k}_j$ such that

$$\big(u^n(\tilde{k}_j), x'^n(l_{j-1}), y_2^n(j)\big) \in \mathcal{T}_\epsilon^n. \tag{5.7}$$

At the next block $j+1$, it transmits $x'^n(l_j)$, where $\tilde{k}_j \in \mathcal{B}(l_j)$.

Decoding

At the destination node, after receiving two signals $y_3^n(j)$ and $y_3^n(j+1)$ in two consecutive blocks j and $j+1$, the receiver first finds the estimate $\hat{l}_j$, such that

$$(y_3^n(j+1), x'^n(\hat{l}_j)) \in \mathcal{T}_\epsilon^n. \tag{5.8}$$

Then it jointly finds the unique $(\hat{k}_j, \hat{m}_{1,j})$ such that,

$$(y_3^n(j), x'^n(\hat{l}_{j-1}), u^n(\hat{k}_j), x_1^n(\hat{m}_{1,j})) \in \mathcal{T}_\epsilon^n,$$
$$\text{for some } \hat{k}_j \in \mathcal{B}(\hat{l}_j). \tag{5.9}$$

After successfully decoding $m_{1,j}$, the decoder successively decodes for $\hat{m}_{2,j}$ such that,

$$\big(y_3^n(j), x'^n(\hat{l}_{j-1}), u^n(\hat{k}_j), x_1^n(\hat{m}_{1,j}), x_2^n(\hat{m}_{2,j}, \hat{m}_{1,j})\big) \in \mathcal{T}_\epsilon^n. \tag{5.10}$$

Error probability analysis

It can be shown that the relay successfully finds the description $u^n(\tilde{k}_j)$ based on the received sequence $y_2^n(j)$ according to the condition (5.7), if

$$\tilde{R}' > I(U; Y_2|X'), \tag{5.11}$$

At the end of block $j+1$, the destination node successfully decodes $x'^n(\tilde{l}_j)$ for the unique $\tilde{l}_j$ based on the joint typical decoding rule of (5.8), if the following condition is met

$$R' < I(X'; Y_3). \tag{5.12}$$

At the end of block j, the receiver can find the unique $(\hat{k}_j, \hat{m}_{1,j})$ in (5.9) if the following holds

$$R_1 + \tilde{R}' - R' < I(U; Y_3, X', X_1) + I(X_1; Y_3|X'), \tag{5.13}$$

Also the refinement layer message $m_{2,j}$ is decoded correctly in (5.10) if the following holds

$$R_2 < I(X_2; Y_3|X', X_1, U). \tag{5.14}$$

Considering the conditions (5.11), (5.12),(5.13) and (5.14), eliminating R' and $\tilde{R}'$, and further simplification of the inequalities, the rate limits of (5.4) is derived.

5.2.1 Non-orthogonal layered CF coding for Gaussian Network

For the Gaussian network as given in (5.3) and depicted in Fig. 5.2, we specialize the two-layer CF code of theorem 5.2.1. The following lemma provides the achievable rates of this scheme.

Lemma 5.2.2. *The achievable rates of a two-layer non-orthogonal CF coding deployed on a half-duplex Gaussian network, modeled in (5.3), with power constraint of P for both of the source an relay nodes is given by*

$$\begin{aligned}
&\mathcal{I}^1_{NOL-CF} = \\
&\log\big(1+\frac{\alpha S_{12}S_{23}+\alpha S_{13}(1+S_{12}+S_{13}+S_{23})}{\bar{\alpha}S_{12}S_{23}+(1+\bar{\alpha}S_{13})(1+S_{12}+S_{13}+S_{23})}\big),\\
&\mathcal{I}^2_{NOL-CF} = \\
&\log\big(1+\frac{\bar{\alpha}S_{13}(1+S_{12}+S_{13}+S_{23})}{S_{12}S_{23}\bar{\alpha}+(1+S_{12}+S_{13}+S_{23})}\big),
\end{aligned} \tag{5.15}$$

for some $\alpha \in [0:1]$ and $S_{ij} \triangleq g_{ij}^2 P$.

Proof:

We apply the results of Theorem 5.2.1 to the Gaussian case, where X_1, V and Z' are assumed to be independent Gaussian random variables defined as follows,

$$\begin{aligned}
X_1 &\sim \mathcal{CN}(0,\alpha P),\\
V &\sim \mathcal{CN}(0,\bar{\alpha}P),\\
U &= Y_2 + Z',\\
Z' &\sim \mathcal{CN}(0,Q),
\end{aligned} \tag{5.16}$$

where

$$X_2 = X_1 + V. \tag{5.17}$$

The mutual information terms of (5.4) given in Theorem 5.2.1, can be calculated as follows,

$$\begin{aligned}
&I(X_1,X';Y_3) = \log\big(\frac{1+S_{13}+S_{23}}{1+\bar{\alpha}S_{13}}\big),\\
&I(Y_2,U|X_1,X',Y_3) = \log\big(\frac{1+Q}{Q}+\frac{\bar{\alpha}S_{12}}{Q(1+\bar{\alpha}S_{13})}\big),\\
&I(X_1;U,Y_3|X') = \log\big(\frac{1+Q+S_{12}+(1+Q)S_{13}}{1+Q+S_{12}\bar{\alpha}+\bar{\alpha}S_{13}(1+Q)}\big),\\
&I(X_2;Y_3|X',X_1,U) = \log(1+\frac{\bar{\alpha}(1+Q)S_{13}}{1+Q+\bar{\alpha}S_{12}}),
\end{aligned} \tag{5.18}$$

where $S_{ij} \triangleq g_{ij}^2 P$. Replacing the rate values of (5.18) into the (5.4), the achievable rates can be further simplified for the Gaussian case to

$$\begin{aligned} R' &= \frac{Q(1+S_{13}+S_{23})}{(Q+1)(1+S_{13}\bar{\alpha})+S_{12}\bar{\alpha}}, \\ R'' &= \frac{(1+Q)(1+S_{13})+S_{12}}{(Q+1)(1+S_{13}\bar{\alpha})+S_{12}\bar{\alpha}}, \\ R_r &= 1+\frac{\bar{\alpha}(1+Q)S_{13}}{1+Q+\bar{\alpha}S_{12}}. \end{aligned} \tag{5.19}$$

We optimize the achievable rate on the values of Q to evaluate:

$$\max_{p(x_1,x_b)p(x_2)p(u|x_2,y_2)} \min\{R', R''\}.$$

It can be shown that the optimal Q^* for the above maximization is given by,

$$Q^* = \frac{1+S_{12}+S_{13}}{S_{23}}. \tag{5.20}$$

Replacing the value for Q^* given in (5.20) into (5.19) and further simplifications, we obtain the result of Lemma 5.2.2 for the achievable rates of each layer.

5.3 Cross-layer Expected Distortion Analysis

We consider the end-to-end system performance of the proposed cross-layer design of SR source code concatenated to no-orthogonal layered CF channel code, outlined in the previous section. We optimize the system performance in terms of ED given in (2.27), by manipulating the operational parameters and adjusting the power allocation and rate of layers for each coding scenario.

5.3.1 End to end non-orthogonal layered CF Code Optimization

We consider a two-state channel model where the source-destination channel is a two-state channel with power spectral density (x_1, x_2), and probability mass function $(p_1, 1-p_1)$. We consider a fixed channel for the source-relay and relay-destination channels. We assume the bandwidth ratio to be equal to one, i.e., $b = 1$. The ED analysis of concatenation of the two-layer SR source code and the non-orthogonal layered CF system is given in the following optimization problem.

Lemma 5.3.1. *The optimal power allocation for cross-layer design of SR source code concatenated to a two-layer non-orthogonal layered CF code over a two states channel with spectral density (x_1, x_2) and parameter p_1, with no CSI at the source node is given by*

$$\begin{aligned}\alpha^* = &\frac{1}{M_2} \\ &- \frac{\sqrt{M_1(M_2 - M_1)(M_2T - Q)(p_1M_2 + p_2Q)p_2}}{M_2(p_1M_1M_2 + p_2M_1Q)},\end{aligned} \tag{5.21}$$

where M_1, M_2, T and Q in (5.25) are defined as

$$\begin{aligned}M_i &= \frac{B + Ax_i + x_i^2}{A + \alpha B + (1 + \alpha A)x_i + \alpha x_i^2}, i \in \{1, 2\} \\ T &= \frac{A + B + x_2}{A + \alpha B + (1 + \alpha A)x_2 + \alpha x_2^2}, \\ Q &= \frac{B}{A + \alpha B + (1 + \alpha A)x_2 + \alpha x_2^2},\end{aligned} \tag{5.22}$$

and

$$\begin{aligned}A &\triangleq 1 + S_{12} + S_{23}, \\ B &\triangleq S_{12}S_{23}.\end{aligned} \tag{5.23}$$

Proof:

We apply the expected distortion optimization given in (2.27) to the two layers NOL-CF code,

$$\begin{aligned}ED_{NOL-CF} &= \min D_{NOL-CF}(\alpha) \\ &= \min_{0 \le \alpha \le 1} p_1 2^{-R_1} + p_2 2^{-(R_1 + R_2)},\end{aligned} \tag{5.24}$$

where R_1 and R_2 are given in (5.15) and can be written as

$$\begin{aligned}R_1 &= \frac{1}{2}\log\left(\frac{1}{1 - M_1\alpha}\right), \\ R_2 &= \frac{1}{2}\log\left(\frac{1 - M_2\alpha}{T - Q\alpha}\right),\end{aligned} \tag{5.25}$$

where M_1, M_2, T and Q are defined in (5.22). Replacing the R_1 and R_2 into (5.24), the optimization problem is written as

$$\begin{aligned} ED &= \min_{0\leq\alpha\leq 1} D_{NOL-CF}(\alpha), \\ D_{NOL-CF}(\alpha) &= p_1 e^{-2R_1} + p_2 e^{-2(R_1+R_2)} \\ &= p_1(1-M_1\alpha) + p_2\frac{1-M_1\alpha}{1-M_2\alpha}(T-Q\alpha) \end{aligned} \tag{5.26}$$

We apply the KKT conditions [44] to the optimization problem of (5.26). The Lagrangian, L of the cost function D_{NOL-CF} is

$$\begin{aligned} L(\alpha,\mu_1,\mu_2) &= p_1(1-M_1\alpha) \\ &\quad + p_2\frac{1-M_1\alpha}{1-M_2\alpha}(T-Q\alpha) \\ &\quad - \mu_1\alpha + \mu_2(\alpha-1), \end{aligned}$$

setting the gradient of L equal to zero,

$$\bigtriangledown L = 0, \tag{5.27}$$

and applying the complementary Slackness condition

$$\begin{cases} \mu_1(-\alpha) = 0, \\ \mu_2(\alpha-1) = 0 \end{cases} \tag{5.28}$$

It can be shown that both of the constraints are inactive and the optimal α^* is computed as (5.21) and this completes the proof.

Hence the $R_1(\alpha^*)$ and $R_2(\alpha^*)$, where α^* is given in (5.21), are the optimal rate/power allocation to minimize the expected distortion of a 2-layer non-orthogonal layered CF coding. We investigate numerical results of this optimization in the next section.

5.3.2 Expected Distortion for Rayleigh Fading Channel Model

Considering a more general channel model, we assume Rayleigh fading channel gain for each of the links in the network. Hence g_{12}, g_{13} and g_{23} are independent identically distributed complex Gaussian random variables with covariances ρ_{12}, ρ_{13} and ρ_{23}. In order to keep the computational complexity of the SIC decoder at a moderate level and suitable for real

networks applications we consider a two-layer code. We formulate the ED optimization problem of the cross-layer design of SR source code matched to non orthogonal layered CF code in follows.

Assuming the rate of layers to be R_1 and R_2, the outage event probability for each layer is defined as

$$P_{\mathcal{O}_1} = Pr\{R_1 > \mathcal{I}_1\}, P_{\mathcal{O}_2} = Pr\{R_2 > \mathcal{I}_2\}, \tag{5.29}$$

where the achievable rates of layers $(\mathcal{I}_1)$ and $(\mathcal{I}_2)$ are given by lemma 5.2.2. The expected distortion can be written as

$$\begin{aligned} ED = P_{\mathcal{O}_1} &+ (1 - P_{\mathcal{O}_1}) P_{\mathcal{O}_2} 2^{-bR_1} \\ &+ (1 - P_{\mathcal{O}_1})(1 - P_{\mathcal{O}_2}) 2^{-b(R_1+R_2)} \end{aligned} \tag{5.30}$$

The ED should be optimized over the rates of layers R_1, R_2 and the power allocation coefficient $\alpha \in [0 : 1]$ for each case. We provide the numerical optimization for these two problems in the next section.

5.4 Numerical results and discussions

We derived the optimal power allocation among the layers for non-orthogonal layered CF coding given in (5.21) under different channel conditions in Fig. 5.3. We compare the results with a DF based scheme given in [71]. As can be seen in high SNR regime, more power is allocated to the base layer. It demonstrates that in high SNR regime, the system is mainly limited by the interference of the higher layer, hence the optimal scheme suppresses the power allocated to this layer. For low value of source-destination SNR, the additive noise is the dominant limiting factor of the rate, hence higher multiplexing gains by deploying more power to the higher layer can increase the overall system performance. It is also observed that for the NOL-CF scheme, when the relay link becomes the dominant link comparing to the direct link, the majority of the power is allocated to the base layer; while as the direct link becomes stronger, the second layer becomes more effective and more power is allocated to this layer.

We compare the achievable rates of the proposed NOL-CF scheme for the Gaussian network, with several available NOMA relaying schemes in Fig. 5.4. The achievable rate for NOL-CF schemes for a Gaussian network is given in (5.15). The achievable rates of NOMA-DF coding given in [7], and the broadcast relay channel CF (BRC-CF) coding

given in [70], are plotted. In these two schemes, unlike the proposed NOL codes, both layers are relayed through the relay link. As explained before, for the proposed NOL code, the refining layer is transmitted through the direct link. It can be seen that the first layer rate and sum rate performance of NOL codes outperforms the counterparts. The improvement for the sum rate is due to the first layer better performance. It shows that, the NOL-CF code is more robust to the interference effect of the higher layers, comparing to the NOMA-DF and BRC-CF counterparts. The second layer rate performance remains the same for the NOL codes comparing to the counterpart schemes.

In Fig. 5.5, we examine the ED performance of two-layer NOL-CF code under two different channel conditions. The optimal expected distortion of the two-layer case, matched to the two-state source-destination channel, is compared with the one-layer coding with no channel knowledge at the source node. In addition, the curve for the optimal expected distortion when the full CSI is available at the source node and the transmission can be optimally matched to each channel realization is plotted as the lower and higher bounds. The system performance is compared to the BRC-CF code. For all the plotted curves, the power gain of the high quality channel realization is assumed to be 20 dB higher than the low quality case, and the probability of high-gain state of the channel is assumed to be $p_2 = 0.5$. We have compared the performance of the two-layer NOL-CF under such a scenario to the non-layered case and the case of CSI at transmitter (CSIT) and BRC-CF. As illustrated, the NOL-CF coding outperforms BRC-CF code in terms of the ED and is closer to the CSIT lower bound. The improvement is more dominant in high SNR cases. It demonstrate that the better achievable rates of NOL-CF shown in Fig. 5.4, is also reflected in the end to end performance measure of ED.

We observe the effectiveness of the proposed layered coding in reducing the expected distortion by utilizing the second layer for the refinement. In case of low SNR regime, the performance of layered coding is degraded and approaches to that of the one-layer coding because the system is limited in terms of power instead of the throughput. As SNR gets higher, the effectiveness of the layered coding becomes more significant. Comparing to the NOMA-DF code and the AF based NOMA code given in [68], we can see that the proposed NOL-CF can better match the rates to the instantaneous channel conditions.

Comparison of the proposed NOL-CF code with BRC-CF, NOMA-DF and NOMA-AF in Fig. 5.5 demonstrates that for the Gaussian channel, transmitting the refining layer through the direct link, is a more effective strategy to utilize the relay link resources, while reducing the interference of the higher layer in CF cases.

We analyze the adoption of NOL codes over Rayleigh fading channel in follows. We numerically optimize the ED given in (5.30) for both of the proposed NOL codes deploying

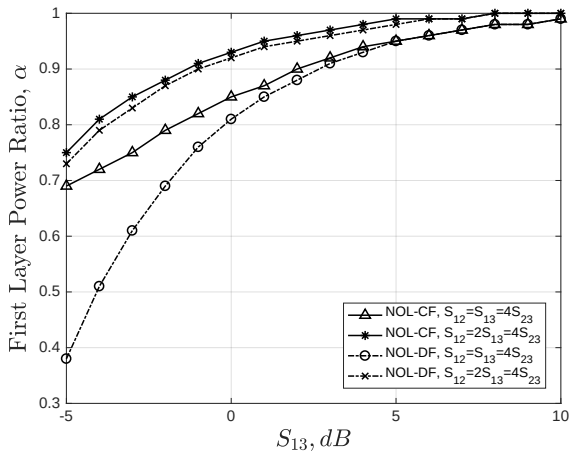

Figure 5.3: Optimal power allocation for the proposed NOL-CF code

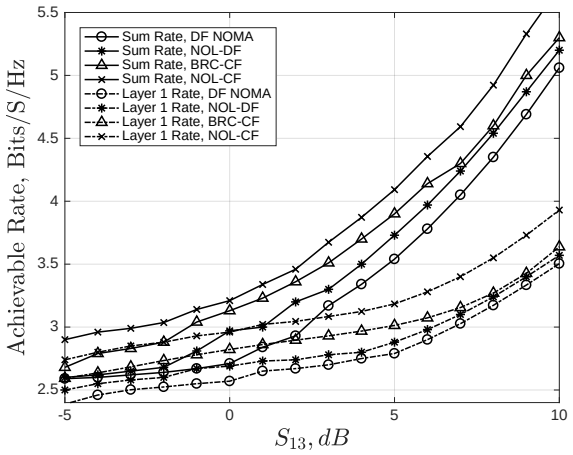

Figure 5.4: Achievable sum rate and first layer rate for the Gaussian channel gains given for NOL-CF, NOL-DF, NOMA DF and BRC-CF code.

Monte Carlo method and exhaustive search for optimal power and rate allocation. We assume the g_{13} to be Rayleigh fading process with mean equal to one and the covariance to be in the range of $[0 : 30]$ dB, g_{23} is assumed to be a Rayleigh fading process with covariance proportional to the SNR of source-destination link and SNR of g_{12} is assumed to be fixed. The ED versus SNR of source-destination link for the proposed NOL-DF and NOL-CF scheme is given in Fig. 5.6 and is compared to the non-layered schemes. We have plotted the ED graphs for different values of bandwidth ratio b. As observed, the NOL

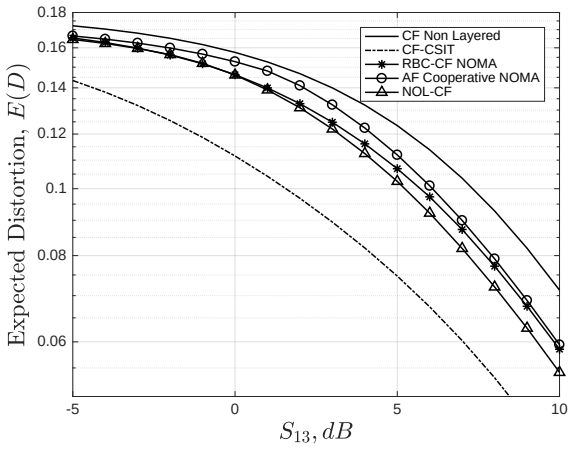

Figure 5.5: ED of the proposed two-layer NOL-CF coding as a function of source-destination SNR, compared to the non-layered coding without channel knowledge at the source node, RBC-CF code and the case of CSI is available at the source node (CSIT)

codes dominantly improve the performance over the non-layered coding for the Rayleigh fading channel. Increasing the bandwidth ratio provides more sub bands to the system, hence improve the overall performance. The best performance is evident for the NOL-CF. It turns out that the gain of NOL-CF scheme over non-layered codes is more dominant for lower values of b, which demonstrates the diversity gain impact, when we are in low bandwidth regime.

In the next figure we plot the ED curves of NOL-CF over Rayleigh channel, for different values of source-relay link SNR and compare with non layered scheme. We compare it with results of DF based code given in [71]. As can be seen the improvement of NOL codes over the non-layered schemes is more dominant when we have stronger source-relay link. The source-relay gain directly impact the ability of each scheme in mitigating the fading effect. For lower values of SNR_{12}, NOL-DF achieves higher gains comparing to the NOL-CF coding and for high values of SNR_{12} this is reversed. In fact, this observation can lead to designing hybrid NOL-CF-DF codes, which will be covered in our next research.

5.5 Conclusions

This chapter studied the cross-layer design of non-orthogonal layered coding scheme coupled with successive refinement source code with application of multi resolution multimedia

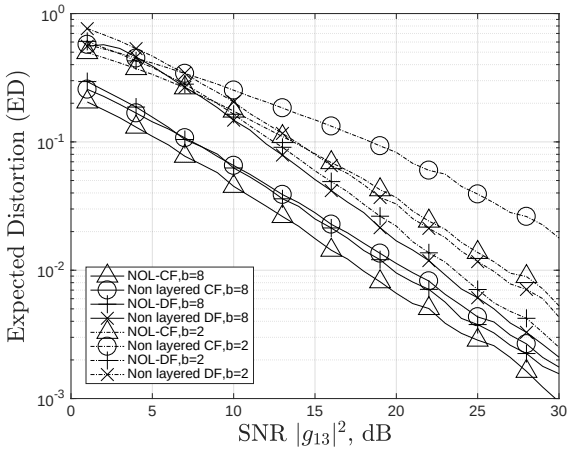

Figure 5.6: ED as a function of SNR for proposed NOL-CF and NOL-CF codes compared to non-layered scheme for bandwidth values of $b = 1$ and $b = 4$.

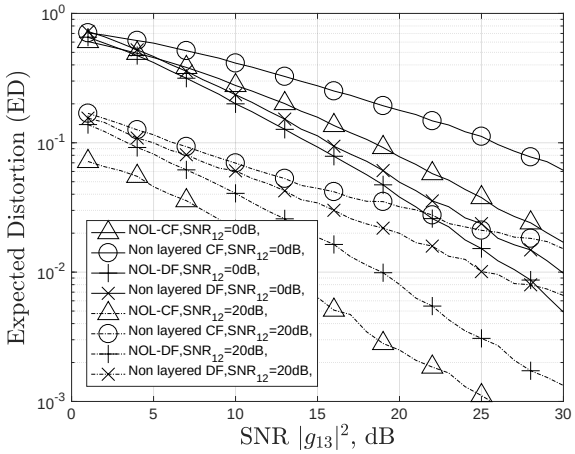

Figure 5.7: ED as a function of SNR for the proposed NOL-CF and NOL-CF codes compared to non-layered scheme for the cases of $SNR_{12} = 10$ dB and $SNR_{12} = 100$ dB.

content transmission over downlink of cellular network, when CSI is not available at the source node. We introduced a layered relaying strategies and derived their achievable rates that are taken as inner bounds on the capacity of the relay channel. Explicit analytical solutions for achieving optimal expected distortion under NOL-CF coding were obtained. Superiority of the two proposed coding schemes in terms of achievable rate and ED performance in comparison to available NOMA-DF and BRC-CF codes has been demonstrated

for Gaussian network. Numerical results showed the effectiveness of the coding in mitigating the fading of the channel for the Rayleigh fading scenarios.

Chapter 6

NOMA-based Distributed Cooperative Multi-layer Multicast with spatially random users

6.1 Introduction

Several technologies including massive MIMO, millimeter-wave spectrum, NOMA and cognitive radio (CR) are envisioned for 5G wireless networks, in order to boost the spectral efficiency and to meet the ever increasing demand in data traffic and massive user connectivity [6]. NOMA codes are promising technique, where unlike the conventional OMA, the users share bandwidth resources (time/frequency/code) and can achieve higher spectral efficiency at lower cost and latency [72].

Cooperative NOMA has been an active area of research in recent years. In this technique users with better channel condition, having prior information on the messages of the other users, act as relay and support the transmission to other users. Diversity gain achieved through cooperative scheme, further enhances the reliability and throughput of NOMA codes [7]. The capacity analysis for cooperative relaying system is provided in [62] for a single user, and it is further generalized to more users with application of coordinated direct and relay transmission (CDRT) in [63].

The main concentration of research on NOMA codes has been focused on unicasting to users. Recently implementation of NOMA technique for multicast problem, where

The results presented in this chapter have already been published in [77].

a common data/video stream is simultaneously transmitted to a group of users, with increasing demand in applications like IPTV, live streaming, etc. has been considered by researchers [60]-[78]. A mixed non-cooperative multicast-unicast problem for single antenna BS is considered in [60], and similar problem of multi resolution multicast problem for multi antenna BS is studied in [61]. Outage behavior and diversity order analysis is performed by proper power allocation among the layers and beamforming for the multi antenna case. [8], [75] and [76] have extended the idea of multi resolution multi cast to cooperative NOMA codes, where two transmission phases are defined, in the first phase the NOMA codes is transmitted by the BS, and in the second phase, the successful nodes in decoding the messages in phase one, are selected to relay and retransmit the messages to other users. Assuming the CSI to be available at the source node, several power allocation and selection of best user criteria are devised in these papers. It is shown that the diversity order equal to the number of cooperating nodes is achievable in the above scenarios. In this chapter we consider a multicast scenario over downlink network. We propose a cooperative NOMA code which adapts the transmission with the assumption of no CSI at the transmuting node.

6.2 System Model

We consider a cellular downlink multicast transmission scenario as depicted in Fig. 6.1. The users are grouped into two clusters by the criteria of average received power, i.e., EUs and RUs. Without loss of generality, the EUs are assumed to be located in a disk denoted by A_E with radius R_E, while the RUs are in a ring denoted by A_R with inner radius of R_R and outer radius of R_D. All nodes in the network are equipped with single antenna and operate in half-duplex mode, and all the users share the same bandwidth resources.

We assume that all the wireless links between the nodes in the network are subject to narrowband quasi-static Rayleigh fading, path loss, and additive white Gaussian noise (AWGN). The channel gain between the BS and the user at distance r from the BS, is modeled by $\sqrt{r^{-\eta}}\tilde{g}$, where $\tilde{g}$ denotes the Rayleigh fading channel coefficient, distributed according to $\mathcal{CN}(0,1)$ and η is the propagation path loss exponent. The additive noise term, n, is assumed to have covariance of N_0. The received power at the node is proportional to $r^{-\eta}|\tilde{g}|^2$. At each node, the long-term average SNR, $\frac{1}{N_0}E[r^{-\eta}|\tilde{g}|^2] = \frac{r^{-\eta}}{N_0}$, is compared to the predefined power level threshold γ_0, and the user is considered as an EU if it has a higher average gain than the threshold and is grouped as RU otherwise. We assume the users are randomly located based on a uniform distribution within each group.

We assume there are M enhanced users $E_i, 1 \leq i \leq M$ located within the disc A_E,

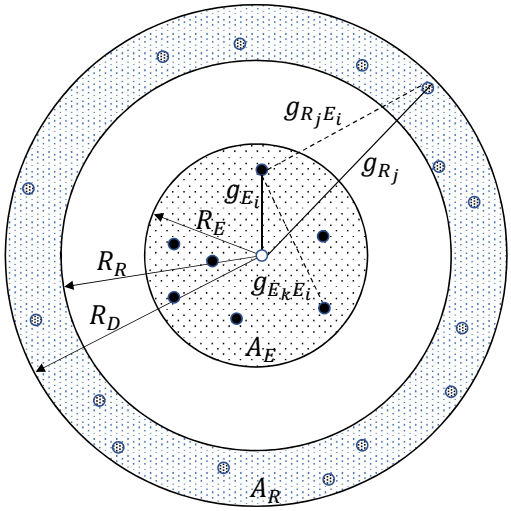

Figure 6.1: System model for distributed cooperative NOMA code for multicasting of multi-resolution message to spatially random users over downlink wireless network.

with location vectors independently and identically distributed (i.i.d) according to uniform probability distribution function,

$$f(r,\theta) = \frac{r}{\pi R_E^2}, 0 \leq r \leq R_E, 0 \leq \theta \leq 2\pi, \tag{6.1}$$

where r and θ are the radial and angular coordinates of each of the users with respect to the BS node, in a polar coordination. The location vector for the M enhanced users is denoted by $\mathbf{L}_E = \{(r_{E_i}, \theta_{E_i})\}_{i=1}^{M}$. Similarly, N regular users $R_i, 1 \leq i \leq N$, i.i.d distributed within the ring A_R are assumed as cell edge users and each uniformly distributed according to its probability distribution function

$$f(r,\theta) = \frac{r}{\pi(R_D^2 - R_R^2)}, R_R \leq r \leq R_D, 0 \leq \theta \leq 2\pi. \tag{6.2}$$

The location vector for RUs is denoted by $\mathbf{L}_R = \{(r_{R_i}, \theta_{R_i})\}_{i=1}^{N}$.

The channel gain between the BS and the M EUs located at distance $0 \leq r_{E_i} \leq R_E, i \in [1:M]$ is modeled by $g_{E_i} = \sqrt{r_{E_i}^{-\eta}}\tilde{g}_{E_i}$, Similarly, the link between BS to the RUs, the link

between E_i to $E_k, k \in \{1, ..., M\} - \{i\}$, and the link between the E_i to $R_j, j \in \{1, ..., N\}$ are respectively modeled by $g_{R_j} = \sqrt{r_{R_j}^{-\eta}}\tilde{g}_{R_i}$, $g_{E_kE_i} = \sqrt{r_{E_kE_i}^{-\eta}}\tilde{g}_{E_kE_i}$ and $g_{R_jE_i} = \sqrt{r_{R_jE_i}^{-\eta}}\tilde{g}_{R_jE_i}$, where $r_{NE_i}, N \in \{E_k, R_j\}$ is given by $r_{E_i}^2 + r_N^2 - 2r_{E_i}r_N\cos(\theta_{E_i} - \theta_N)$.

Considering a layered multicast scenario over cellular downlink network, without loss of generality a two-layer NOMA scheme is deployed where the BS transmits the superimposed signal in each transmission block,

$$x_s = \sqrt{\alpha P_s}s_b + \sqrt{\bar{\alpha}P_s}s_r, \tag{6.3}$$

where P_s is the power available at the BS, s_b is the base layer signal encoded by rate R_b bits per channel uses, s_r is the refining layer with rate R_r and $0 \leq \alpha \leq 1$ is the power splitting parameter. The EUs enjoying better channel due to the proximity to the BS, decode for both base and refining layers, and the RUs only decode for the base layer message. In the next section we present a two-phase distributed cooperative scheme where the AU nodes which successfully decoded the messages s_b and s_r, assist other EUs and the RUs in transmission of the messages.

6.3 Distributed cooperative multicast scheme

We consider a two-phase transmission consisting of broadcast phase where the BS transmits the NOMA code over the network and a cooperation phase where the successful EU nodes participate in re-transmission of the messages to other nodes. The transmission block is partitioned into $M + 1$ subchannels. The broadcast phase is performed in the first time slot and the next M time slots are allocated to each of the cooperating nodes. For the broadcast phase the received signal at the AUs and RUs is defined as

$$y_{E_i} = g_{E_i}x_s + n_{E_i}, i \in [1 : M], \tag{6.4}$$
$$y_{R_j} = g_{R_j}x_s + n_{R_j}, j \in [1 : N], \tag{6.5}$$

where x_s is defined in (6.3), n_{E_i} and n_{R_j} are i.i.d AWGN terms with distribution $\mathcal{CN}(0, N_0)$. We consider a SIC decoding scheme for the EUs, where the base layer is decoded first, considering the higher layer as interference and then the refining layer is decoded. The RUs decode only for the base layer. Defining $\rho = \frac{P_s}{N_0}$, the SINR of the EU $E_i, i \in [1 : M]$ in decoding the base layer in broadcast phase is given by

$$\gamma_{E_i,b}^B = \frac{\alpha r_{E_i}^{-\eta}|\tilde{g}_{E_i}|^2}{\bar{\alpha}r_{E_i}^{-\eta}|\tilde{g}_{E_i}|^2 + \rho^{-1}}, \tag{6.6}$$

and the SINR for the SIC decoding of the refining layer is given by

$$\gamma^B_{E_i,r} = \rho\bar{\alpha} r_{E_i}^{-\eta} |\tilde{g}_{E_i}|^2. \tag{6.7}$$

Similarly, the SINR of the RU in decoding of the base layer, considering the higher layer as interference is

$$\gamma^B_{R_j,b} = \frac{\alpha r_{R_j}^{-\eta} |\tilde{g}_{R_j}|^2}{\bar{\alpha} r_{R_j}^{-\eta} |\tilde{g}_{R_j}|^2 + \rho^{-1}} \tag{6.8}$$

The set of $m \in [1 : M]$ successful AUs in decoding base and refining messages in the broadcast phase is denoted by $\mathcal{B}^s_E$ and similarly the set of successful RUs is denoted by $\mathcal{B}^s_R$. the set of failed EUs and RUs is denoted by

$$\mathcal{B}^f_E = \{1, 2, ..., M\} \backslash \mathcal{B}^s_E, \tag{6.9}$$

$$\mathcal{B}^f_R = \{1, 2, ..., N\} \backslash \mathcal{B}^s_R. \tag{6.10}$$

During the cooperative phase, every $E_i \in \mathcal{B}^s_E$ serves as relay and transmits the messages s_b and s_r in its respective time slot with the same power $P_r = \beta P_s, 0 \leq \beta \leq 1$, hence the transmit signal for each relying node in cooperative phase is given by

$$x_C = \sqrt{\alpha P_r} s_b + \sqrt{\bar{\alpha} P_r} s_r \tag{6.11}$$

For the EU $E_k \in \mathcal{B}^f_E$, the received signal in time slot i is given by

$$y^i_{E_k} = g_{E_k,E_i} x_c + n^i_{E_k}, k \in \mathcal{B}^f_E, i \in \mathcal{B}^s_E \tag{6.12}$$

For the decoding process, we propose a max ratio combining strategy, where the received messages of both broadcast and cooperation phases are combined. The received vector at the failed EU E_k is given by

$$\mathbf{y}^C_{E_k} = [y^b_{E_k}, y^1_{E_k}, ..., y^m_{E_k}]^T. \tag{6.13}$$

Similarly for the $R_j \in \mathcal{B}^f_R$, the received signals in the cooperation phase is given by

$$y^i_{R_j} = g_{R_j,E_i} x_c + n^i_{R_j}, j \in \mathcal{B}^f_R, i \in \mathcal{B}^s_E \tag{6.14}$$

and the received vector is

$$\mathbf{y}^C_{R_j} = [y^b_{R_j}, y^1_{R_j}, ..., y^m_{R_j}]^T. \tag{6.15}$$

6.4 Outage Analysis

Now we proceed to analyze the outage probability of the proposed distributed cooperative multicast NOMA scheme for EU and RU nodes. Firstly, the outage event of the broadcast phase is analyzed. For EU $E_i, i \in [1:M]$, given the distance r_i, the mutual information in broadcast phase of the base layer is given by

$$I^B_{E_i,b} = \frac{1}{M} I(y^B_{E_i}; s_b | r_i) \tag{6.16}$$

$$= \frac{1}{M} \log(1 + \gamma^B_{E_i,b}), \tag{6.17}$$

and for the refining layer deploying SIC, is given by

$$I^B_{E_i,r} = \frac{1}{M} I(y^B_{E_i}; s_r | s_b, r_i) \tag{6.18}$$

$$= \frac{1}{M} \log(1 + \gamma^B_{E_i,r}), \tag{6.19}$$

where $\gamma^B_{E_i,b}$ and $\gamma^B_{E_i,r}$ are given in (6.6) and (6.7) respectively. For the RU nodes the mutual information is given by

$$I^B_{R_j,b} = \frac{1}{M} I(y^B_{R_j}; s_b | r_i) \tag{6.20}$$

$$= \frac{1}{M} \log(1 + \gamma^B_{R_j,b}), \tag{6.21}$$

where $\gamma^B_{R_j,b}$ is given in (6.8). Assuming the target rate pair (R_b, R_r) for the layers, and given the distance r_i, the outage event for EU E_i is given by

$$P_{\mathcal{O}^B_{E_i}|r_i} = Pr[I^B_{E_i,b} < R_b \cup I^B_{E_i,r} < R_r | r_i] \tag{6.22}$$

$$= Pr[\gamma^B_{E_i,b} < 2^{MR_b} - 1 \cup \gamma^B_{E_i,r} < 2^{MR_r} - 1] \tag{6.23}$$

denoting $\phi_b = 2^{MR_b} - 1$, $\phi_r = 2^{MR_r} - 1$ and

$$\phi_{EU} = \max\{\frac{\phi_b}{1 - \bar{\alpha}\phi_b}, \phi_b\} \tag{6.24}$$

averaging over the distance variable r_i and further simplification we have

$$P_{\mathcal{O}^B_{E_i}} = Pr[\gamma^B_{E_i,b} < \phi_b \cup \gamma^B_{E_i,r} < \phi_r] \tag{6.25}$$
$$= 1 - Pr[\gamma^B_{E_i,b} \geq \phi_b, \gamma^B_{E_i,r} \geq \phi_r] \tag{6.26}$$
$$= 1 - Pr[r_i^{-\eta}|\tilde{g}_{E_i}|^2 \geq \phi_{EU}.\rho^{-1}] \tag{6.27}$$
$$= 1 - \int_{r_i=0}^{R_E} e^{-r_i^{\eta}\phi_{EU}\rho^{-1}} f(r_i)dr_i \tag{6.28}$$
$$= 1 - \frac{2}{\eta R^2_{E_i}}(\frac{\rho}{\phi_{EU}})^{\frac{1}{\eta}}\Gamma(\frac{2}{\eta}, \frac{\phi_{EU}R^{\eta}_{E_i}}{\rho}), \tag{6.29}$$

where $\Gamma(s,x) = \int_0^x t^{s-1}e^{-t}dt$ is the lower incomplete Gamma function [95]. Similarly, for the RU nodes, it can be shown that

$$P_{\mathcal{O}^B_{R_j}} = 1 - \frac{2}{\eta R^2_{R_j}}(\frac{\rho}{\phi_b})^{\frac{1}{\eta}}\Gamma(\frac{2}{\eta}, \frac{\phi_b R^{\eta}_{R_j}}{\rho}), \tag{6.30}$$

The set of successfully decoded EUs and RUs in the broadcast phase is given by

$$\mathcal{B}^s_E = \{i|\gamma^B_{E_i,b} \geq \phi_b, \gamma^B_{E_i,r} \geq \phi_r, i \in [1:M]|\mathbf{L}_E\} \tag{6.31}$$
$$\mathcal{B}^s_R = \{j|\gamma^B_{R_j,b} \geq \phi_b, j \in [1:N]|\mathbf{L}_R\} \tag{6.32}$$

As the decoding process for each node is independent of the other nodes, the probability of achieving m successful AUs in broadcast phase, $|\mathcal{B}^s_E| = m$, which acts as relaying nodes in the cooperative phase is given by

$$Pr(\mathcal{B}^s_E, \mathcal{B}^f_E) = \prod_{i\in\mathcal{B}^s_E}(1 - P_{\mathcal{O}^B_{E_i}}) \times \prod_{i\in\mathcal{B}^f_E} P_{\mathcal{O}^B_{E_i}} \tag{6.33}$$

Now we proceed to analyze the outage event for cooperative phase. Conditioned on m successful EUs in the broadcast phase and given the location vector $\mathbf{L}_E$ of the nodes, considering the received signal vector (6.15), the mutual information of base layer in cooperative phase is computed as

$$\frac{1}{M}I(\mathbf{y}^C_{E_j}; s_b|\mathbf{L}_E) = \frac{1}{M}\log(1 + \gamma^C_{E_{j,b}}) \tag{6.34}$$

where

$$\gamma^{C}_{E_{j,b}} = \frac{\alpha r^{-\eta}_{E_j} |\tilde{g}_{E_j}|^2 + \alpha\beta \sum_{i=1}^{m} r^{-\eta}_{E_j,E_i} |\tilde{g}_{E_j,E_i}|^2}{\bar{\alpha} r^{-\eta}_{E_j} |\tilde{g}_{E_j}|^2 + \bar{\alpha}\beta \sum_{i=1}^{m} r^{-\eta}_{E_j,E_i} |\tilde{g}_{E_j,E_i}|^2 + \rho^{-1}} \tag{6.35}$$

and for the refining layer is

$$\frac{1}{M} I(\mathbf{y}^{C}_{E_j}; s_r | s_b, \mathbf{L}_E) = \frac{1}{M} \log(1 + \gamma^{C}_{E_{j,r}}), \tag{6.36}$$

where

$$\gamma^{C}_{E_{j,r}} = \bar{\alpha} r^{-\eta}_{E_j} |\tilde{g}_{E_j}|^2 \rho + \bar{\alpha}\beta \sum_{i=1}^{m} r^{-\eta}_{E_j,E_i} |\tilde{g}_{E_j,E_i}|^2 \rho. \tag{6.37}$$

Hence conditional outage event for user $j \in \mathcal{B}^{f}_{E}$, given $\mathbf{L}_E$ and the set $(\mathcal{B}^{s}_{E}, \mathcal{B}^{f}_{E})$, is

$$\begin{aligned} &P_{\mathcal{O}^{C}_{E_j} | \mathbf{L}_E} = \\ &Pr\big[I(\mathbf{y}^{C}_{E_j}; s_1 | \mathbf{L}_E) < MR_b \cup I(\mathbf{y}^{C}_{E_j}; s_2 | s_1, \mathbf{L}_E) < MR_r\big]. \end{aligned} \tag{6.38}$$

With further manipulation it can be shown to be

$$\begin{aligned} &P_{\mathcal{O}^{C}_{E_j} | \mathbf{L}_E} = \\ &= 1 - Pr(r^{-\eta}_{E_j} |\tilde{g}_{E_j}|^2 + \beta \sum_{i=1}^{m} r^{-\eta}_{E_j,E_i} |\tilde{g}_{E_j,E_i}|^2 \qquad (6.39) \\ &\qquad\qquad \geq \max\{\frac{\phi_b}{1 - \bar{\alpha}\phi_b}, \frac{\phi_r}{\bar{\alpha}}\}.\rho^{-1}) \qquad (6.40) \end{aligned}$$

We define random variables $\{u_i\}_{i=0}^{m}$ as

$$\begin{aligned} u_0 &= r^{-\eta}_{E_j} |\tilde{g}_{E_j}|^2, \\ u_i &= \beta r^{-\eta}_{E_j,E_i} |\tilde{g}_{E_j,E_i}|^2, \end{aligned} \tag{6.41}$$

where $u_i, i \in [0:m]$ is an exponential random variable with parameters $\lambda_0 = r^{\eta}_{E_j}$ and $\lambda_i = \beta^{-1} r^{\eta}_{E_j E_i}$. Defining the random variable s_m as $s_m = \sum_{i=0}^{m} u_i$, the outage probability can be written as

$$P_{\mathcal{O}^{C}_{E_i} | \mathbf{L}_E} = 1 - Pr(s_m \geq \max\{\frac{\phi_b}{1 - \bar{\alpha}\phi_b}, \frac{\phi_r}{\bar{\alpha}}\}.\rho^{-1}) \tag{6.42}$$

where s_m is a hypo exponential random variable with probability distribution function [95],

$$p_{s_m}(x) = \prod_{i=0}^{m} \lambda_i \sum_{j=0}^{m} \frac{e^{-\lambda_j x}}{\prod\limits_{\substack{k=1 \\ k\neq j}}^{m} (\lambda_k - \lambda_j)}. \tag{6.43}$$

The outage event probability of cooperative phase, $P_{\mathcal{O}^C_{E_j}|\mathbf{L}_E}$, denoting $r_{E_j} = r_{E_jE_0}$ and $\beta_0 = 1$ and considering ϕ_{ER} defined in (6.24) can be calculated as

$$\begin{aligned}
P_{\mathcal{O}^C_{E_j}} &= \int_{\mathbf{L}_E} P_{\mathcal{O}^C_{E_j}|\mathbf{L}_E}.f(\mathbf{L}_E).d\mathbf{L}_E && (6.44)\\
&= \int_{\mathbf{L}_E} P_{s_m}(\phi_{ER}.\rho^{-1}).f(\mathbf{L}_E).d\mathbf{L}_E && (6.45)\\
&= \int_{\mathbf{L}_E} P_{s_m} \int_{x=o}^{\phi_{ER}.\rho^{-1}} p_{s_m}(x) f(\mathbf{L}_E) d\mathbf{L}_E dx && (6.46)\\
&= \prod_{i=0}^{m} \beta_i^{-1} r_{E_j,E_i}^{\eta}. \\
&\sum_{l=0}^{m} \int_{\mathbf{r}_E} \frac{1 - e^{-\beta_l^{-1} r_{E_j,E_l}^{\eta} \phi_{ER}.\rho^{-1}}}{\beta_l^{-1} r_{E_j,E_l}^{\eta} \prod\limits_{\substack{k=1 \\ k\neq l}}^{m+1} (\beta_k^{-1} r_{E_j,E_k}^{\eta} - \beta_l^{-1} r_{E_j,E_l}^{\eta})} \mathbf{r}_E d_{\mathbf{r}_E}. && (6.47)
\end{aligned}$$

By averaging over the set $(\mathcal{B}_E^s, \mathcal{B}_E^f)$, and considering the broadcast outage probability given in (6.29), The probability of outage for user $E_i, i \in [1:M]$ is given by

$$P_{\mathcal{O}_{E_i}}(m) = P_{\mathcal{O}^C_{E_i}} \times \prod_{j\in\mathcal{B}_E^s} (1 - P_{\mathcal{O}^B_{E_j}}) \times \prod_{k\in\mathcal{B}_E^f - \{i\}} P_{\mathcal{O}^B_{E_k}} \tag{6.48}$$

and finally, the probability of outage event averaged over all EU nodes for the proposed scheme is

$$P_{\mathcal{O}_E} = \frac{1}{M} \sum_{m=0}^{M} \sum_{i\in\mathcal{B}_E^f} P_{\mathcal{O}^C_{E_i}}. \prod_{j\in\mathcal{B}_E^s} (1 - P_{\mathcal{O}^B_{E_j}}). \prod_{k\in\mathcal{B}_E^f - \{i\}} P_{\mathcal{O}^B_{E_k}}, \tag{6.49}$$

where closed form expressions for $P_{\mathcal{O}^B_{E_i}}$ and $P_{\mathcal{O}^C_{E_i}}$ are given in (6.29) and (6.47) respectively. Similar analysis for outage probability of RUs is carried out to derive $P_{\mathcal{O}^C_{R_j}}$ and $P_{\mathcal{O}_{R_j}}$.

6.5 Diversity order analysis

In order to get deeper insight into the outage behavior of the proposed coding we provide an asymptotic analysis in high SNR regime and identify the diversity order of the set of EU and RU nodes.

Considering $P_{\mathcal{O}^C_{E_j}|\mathbf{L}_E}$ of (6.47), the cooperative phase outage event $P_{\mathcal{O}^C_{E_j}|\mathbf{L}_E}$ given in (6.38) can be upper bounded by

$$P_{\mathcal{O}^C_{E_i}} = Pr[\sum_{k=0}^{m} u_k < \frac{\phi_b}{1-\bar{\alpha}\phi_b}.\rho^{-1} \cup \sum_{k=1}^{m} u_k < \frac{\phi_r}{\bar{\alpha}}.\rho^{-1}] \tag{6.50}$$

$$\leq Pr[\sum_{k=0}^{m} u_k < \frac{\phi_b}{1-\bar{\alpha}\phi_b}.\rho^{-1}] + Pr[\sum_{k=1}^{m} u_k < \frac{\phi_r}{\bar{\alpha}}.\rho^{-1}], \tag{6.51}$$

where exponential random variables $\{u_i\}_{i=0}^m$ is defined in (6.41) and parameters λ_i is given there. We deploy the following lemma for high SNR approximation of terms given in (6.51).

[35, Claim 1]: Let $u_k, k = 1, 2, ..., m$ be independent exponential random variables with parameter λ_k, then

$$\lim_{\epsilon\to 0} \frac{1}{e^m} Pr[\sum_{k=1}^{m} u_k < \epsilon] = \frac{1}{m!} \prod_{k=1}^{m} \lambda_k. \tag{6.52}$$

hence in high SNR we can write

$$\lim_{\rho\to\infty} P_{\mathcal{O}^C_{E_i}} = \frac{\phi_b.\rho^{-(m+1)}}{(1-\bar{\alpha}\phi_b)(m+1)!} \prod_{k=0}^{m} \lambda_k + \frac{\phi_r.\rho^{-(m+1)}}{\bar{\alpha}(m+1)!} \prod_{k=0}^{m} \lambda_k \tag{6.53}$$

$$= \frac{\rho^{-(m+1)}}{(m+1)!} (\frac{\phi_b}{(1-\bar{\alpha}\phi_b)} + \frac{\phi_r}{\bar{\alpha}}) \prod_{k=0}^{m} \lambda_k \tag{6.54}$$

$$= C_m \rho^{-(m+1)}, \tag{6.55}$$

where C_m isolates parameters other than ρ. Now we examine the broadcast phase outage probability of (6.47) in high SNR regime.

$$\prod_{j\in\mathcal{B}^s_E} (1 - P_{\mathcal{O}^B_{E_i}}) \times \prod_{k\in\mathcal{B}^f_E - \{i\}} P_{\mathcal{O}^B_{E_k}} = \tag{6.56}$$

$$\prod_{k\in\mathcal{B}^s_E} e^{-r_j^{\eta}\phi_{EU}.\rho^{-1}}. \prod_{k\in\mathcal{B}^f_E - \{i\}} 1 - e^{-r_k^{\eta}\phi_{EU}.\rho^{-1}}, \tag{6.57}$$

in high SNR it reduces to

$$= \prod_{j \in \mathcal{B}_E^s} (1 - r_j^{\eta} \phi_{EU} . \rho^{-1}) . \prod_{k \in \mathcal{B}_E^f - \{i\}} r_k^{\eta} \phi_{EU} . \rho^{-1} \tag{6.58}$$

$$= D_m . \rho^{-(M-m-1)} \tag{6.59}$$

combining (6.55) and (6.59), we have

$$\lim_{\rho \to \infty} \frac{\log P_{\mathcal{O}_{E_i}}(m)}{\rho} = -(m+1) - (M-m-1) \tag{6.60}$$

$$= -M. \tag{6.61}$$

Hence it is proved that diversity order of M is achievable for all of the enhanced users which shows the outage probability for the proposed cooperative multicast scheme decays asymptotically proportional to $1/\rho^M$. Similar analysis is carried out for the RU nodes which demonstrates diversity order of $M+1$ is achieved by every regular user and is omitted.

6.6 Simulations results and Discussions

In this section we provide simulation results to analyze the outage event for both the RU and EU nodes deploying the proposed distributed cooperative NOMA layered multicast code and compare with several counterpart multicast schemes. We consider a cellular network depicted in Fig. 6.1. R_E is set to 10, $R_R = 15$ and $R_D = 20$. We assume 5 EU and 3 RU nodes, hence $M = 5$ and $N = 3$. the path loss exponent, η , is set to 3. We use fixed power allocation of $\alpha = 0.5$ and we assume that the ratio of power at relays to the BS is $\beta = 0.1$. Rate of layers is fixed at $R_b = 1$ and $R_r = 0.3$ bits per channel use.

For comparison we consider the following schemes. In all the cooperating schemes given in below, the first phase where the BS broadcasts the NOMA code to the users is the same, and different cooperating strategies is deployed in the second phase.

- Direct NOMA: In this scheme the BS directly broadcast to all nodes during the whole channel block and no cooperation scheme is performed.
- DC-NOMA [8]: The best available cooperative scheme when CSI is not available at the BS. All the successful EU nodes simultaneously transmit the received signals in second phase with no space-time coordination.

– F-BUS [75]: A fixed-power scheme where the best user among the $\mathcal{B}_E^s$ is selected based on a max min scheme. CSI is needed at the EUs to determine the optimal objective value to solve the best user selection (BUS) criteria.

– BARS [80]: similar to F-BUS a user among the successful EUs is selected to forward the messages in the second phase. Best average reception selection (BARS) is employed in this scheme. CSI is needed at the EUs to perform the selection process.

– OC-NOMA [8]: The best available cooperative scheme in the case of CSI at the transmitting nodes. A two-step selection criterion is used to determine the best relaying EU among the successful nodes in first phase.

In Fig. 6.2 and Fig. 6.3, we compare the outage event probability of the EU and RU nodes receptively. The proposed scheme is compared with the above counterparts. It can be seen that the cooperative schemes dominantly improve upon the direct NOMA due to distributed diversity gain. The capability of the cooperative schemes in utilizing the available diversity gain in the system determines the performance of the scheme. As can be seen for both of the RU and EU nodes, the DC-NOMA scheme given in [8] performs poorly as it is not able to exploit the full diversity gain available in the network and achieves diversity gain of 2. We proved in section IV that diversity order of M for EU nodes and $M+1$ for RU nodes is achievable by the proposed scheme, which makes it superior to the OC-NOMA codes. As can be seen in the Fig. 6.2 and Fig. 6.3 the outage performance of the proposed scheme is close to the schemes deploying CSI including OC-NOMA, F-BUS and BARS. Considering low SNRs, the CSI schemes enjoys two-fold gains over the non CSI scheme; first is the power gain due to the possible power allocation based on the CSI and second gain comparing to the proposed scheme is that they have higher spectral efficiency due to longer broadcast phase. Considering the high SNR regime for both the RU and EU nodes the proposed scheme is achieving the full diversity gain and is in fact optimal in term of diversity order. Our results demonstrates that the full diversity order is achievable for cooperative NOMA codes in the case of no CSI at transmitting side. Although the proposed coding scheme is optimal in term of diversity order for both the EU and RU nodes, comparing Fig. 6.2 and Fig. 6.3 demonstrates that the proposed coding performance has faster convergence to CSI schemes in case of EUs comparing to the RUs. This observation is due to the refining layer decoding at the EU nodes which increases the spectral efficiency and enhance the outage performance.

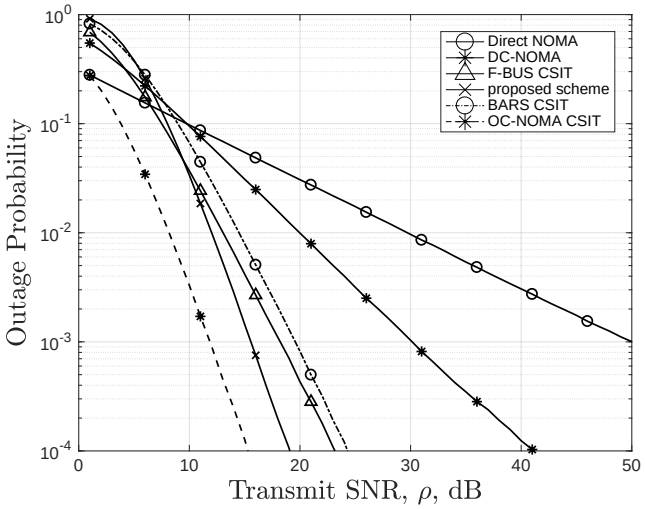

Figure 6.2: Outage event for the enhanced users (EU).

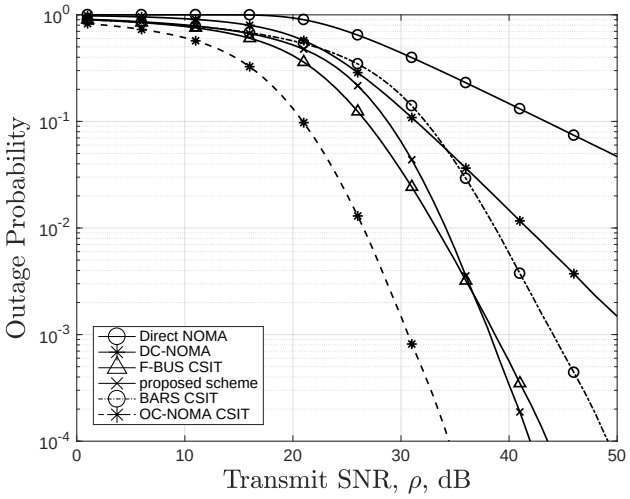

Figure 6.3: Outage event for the regular users (RU).

6.7 Conclusions

In this chapter a distributed cooperative layered multicasting NOMA code is proposed over downlink cellular network for spatially random users located in two groups of enhanced

users and regular users. The outage probability analysis is provided for both group of users. High SNR analysis demonstrates that the proposed coding achieves optimal diversity order for both groups. Simulation results confirms the close performance of the proposed coding in no CSIT setting, similar to the counterparts' codes with CSIT assumption.

Chapter 7

Conclusions and Future Work

7.1 Conclusions

Efficient provisions for multimedia multicast/broadcast and the machine type communications for IoT networks, are two key requirements of 5G radio access networks. NOMA codes and scalable layered source codes are two key technologies to address this requirements. In this dissertation we proposed novel coding techniques by matching these two technologies over several cooperative scenarios. For each considered network, we analyzed the system performance by studying several key performance indicators including outage probability, expected distortion, layered diversity-multiplexing gain, diversity order and distortion exponent.

First we studied a multi-relay network and applied the layered coding scheme over an NAF relaying protocol. We proposed proper power and rate allocation among the layers with the assumption of no CSI at the transmitting node. We analyzed the outage event and layered DMT curve of the network. Further the achievable distortion exponent as the end to end performance metric is derived. We proved the regions on bandwidth ratio where the proposed coding achieves the MISO upper bound in asymptotic regime of infinite number of layers hence we proved the proposed coding is optimal in these regions. We also considered limited feedback case where partial CSI is available at the transmitting node and compared the results with the layered coding with no CSI. We further extend the coding scheme to multihop MIMO network with DF relaying strategy.

Next we extended the layered coding scheme to uplink NOMA codes with application to IoT communication of 5G uplink network. An achievable lower bound on the distortion

exponent is derived by designing a cooperative scheme, and proper rate and power allocation among the layers for a symmetric channel. We have shown that the proposed layered cooperative NAF coding achieve the optimal DE performance of the MISO upper bound in the limit of infinite number of layers.

Next we focused on a simpler network of a single relay channel to analyze the system performance in general SNR regime. We proposed a layered coding scheme based on CF relaying scheme and optimized the end to end expected distortion performance over a two-state fading channel.

Finally considering a multicast scenario over a distributed cooperative downlink network, we implemented a non-orthogonal layered scheme to enhance the multicasting performance for users with diverse channel conditions. We analytically derived the outage probability performance over such network. In the high SNR regime the diversity order performance analysis is carried out and it is shown that the full diversity gain is achieved for both the cooperating nodes and cell edge user is achievable.

7.2 Directions for Future Work

The application of non-orthogonal layered codes over cooperative networks with applications of multicasting of multimedia content and machine type communications is an ongoing research direction for new releases of 5G networks and beyond. In this dissertation we mainly focused on theoretical limits of such techniques by deriving end to end performance measures for several network settings and cooperative schemes. There are several assumptions in our work which enabled us to analytically solve the resource allocations and derive end to end performance measures. First we assumed that the source and channel code lengths are asymptotically long enough where rate-distortion functions, diversity-multiplexing curves and channel capacity are well defined and achievable. We have assumed Gaussian random codes and joint typicality decoding rules. In fact our results serves as an upper bound for the proposed coding and protocols in finite code length. One direction for future work is to consider practical code design for finite length coding and practical ML decoders.

Secondly due to complexity of resource allocation optimization problems in general SNR values as in 2.27, we have considered a high SNR regime, where DE analysis is employed to derive the system performance. Sub optimal optimization algorithms given for SISO channels in [9], [13] and [17] can be devised for general SNR values of cooperative NAF scheme of chapter 3.

As we have indicated even for simple network architectures the proposed schemes serve as an achievable lower bounds on the network capacity. Indeed more efficient and more complex cooperative scheme like dynamic DF can and sequential slotted AF be studied as the cooperative scheme. The analysis for CF relaying scheme in chapter 5 can be extended to continuous fading channels and for other relaying scheme. For all the proposed non-orthogonal layered schemes, perfect SIC decoders are assumed. The impact of imperfect SIC and impaired decoders is of practical importance and can be further studied.

The cooperative uplink NOMA code proposed in chapter 4 is shown to achieve the MISO upper bound in the asymptotic of infinite number of layers. It has been also evaluated that considerable gains is achieved for limited number of layers. This results are derived for symmetric channel where all the nodes are constrained by the same power level and are transmitting as the same rate. Extension to more general asymmetric network is an open problem.

Multicasting over downlink scheme has been an active of area of research in the context of multicasting over 5G networks. We studied a novel cooperative scheme which can be extended in different directions. User clustering/grouping is an important technique, where efficient grouping of the user can directly affect the diversity order achieved by the users. We considered a fixed clustering method based on relative location of the users and more dynamic methods can be envisioned. The fixed time slot assignment for the broadcast phase and cooperation phase can be extended to adaptive cooperation phase assignment which can further improving the system throughput. Cooperative multicasting over massive MIMO setup is an interesting network architecture for further research, where several issues of beamforming, antenna selection, power allocation is needed to be addressed to optimize the system throughput and reliability.

References

[1] G. A. Akpakwu, B. J. Silva, G. P. Hancke, A. M. Abu-Mahfouz, "A Survey on 5G Networks for the Internet of Things: Communication Technologies and Challenges," *IEEE Access*, vol. 6, no. 12, pp. 3619-3647, Dec 2017.

[2] C. Bockelmann, N. K. Pratas, G. Wunder, S. Saur, M. Navarro, D. Greg,"Towards Massive Connectivity Support for Scalable mMTC Communications in 5G Networks," *IEEE Access*, vol. 6, no. 5, pp. 28969-28992, May 2018.

[3] A. Ijaz, L. Zhang, M. Grau, A. Mohamed, S. Vural, A. U. Quddus, M. A. Imran, C. H. Foh, R. Tafazolli, "Enabling Massive IoT in 5G and Beyond Systems: PHY Radio Frame Design Considerations," *IEEE Access*, vol. 4, no. 6, pp. 3322-3339, Jun. 2016.

[4] P. Popovski, K. F. Trillingsgaard, O. Simeone, G. Durisi, "5G Wireless Network Slicing for eMBB, URLLC, and mMTC: A Communication-Theoretic View," *IEEE Access*, vol. 6, no. 9, pp. 55765-55779, Sep. 2018.

[5] L. Zhang, M. Xiao, G. Wu, M. Alam, Y.-C. Liang, and S. Li, "A survey of advanced techniques for spectrum sharing in 5G networks," *IEEE Wireless Commun.*, vol. 24, no. 5, pp. 44-51, Oct. 2017.

[6] L. Dai, B. Wang, Y. Yuan, S. Han, C. -L. I, Z. Wang, "Non-orthogonal multiple access for 5G: solutions, challenges, opportunities, and future research trends," *IEEE Commun. Mag.*, vol. 53, no. 9, pp. 74-81, Sep 2015.

[7] Z. Ding, M. Peng, H. V. Poor, "Cooperative Non-Orthogonal Multiple Access in 5G Systems," *IEEE Commun. Lett.,* vol. 19, no. 8, pp. 1462-1465, Aug. 2015.

[8] L. Yang, Q. Ni, L. Lv, J. Chen, H. Xue, H. Zhang, H. Jiang, "Cooperative Non-Orthogonal Layered Multicast Multiple Access for Heterogeneous Networks," *IEEE Trans. Commun.*, vol. 67, no. 2, pp. 1148-1163, Feb. 2019.

[9] C. Tian, A. Steiner, S. Shamai, and S. Diggavi, "Successive refinement via broadcast: Optimizing expected distortion of a Gaussian source over a Gaussian fading channel," *IEEE Trans. Inf. Theory*, vol. 54, no. 7, pp. 2903-2918, Jul. 2008.

[10] W. Equitz and T. Cover, "Successive refinement of information," *IEEE Trans. Inf. Theory*, vol. 37, no. 2, pp. 269-275, Feb. 1991.

[11] K. Azarian, H. El Gamal, and P. Schniter,"On the Achievable Diversity-Multiplexing Tradeoff in Half-Duplex Cooperative Channels," *IEEE Trans. Inf. Theory*, vol. 51, no. 12, pp. 4152-4172, Dec 2005.

[12] L. Zheng, and D. N. C. Tse, "Diversity and Multiplexing: A Fundamental Tradeoff in Multiple-Antenna Channels," *IEEE Trans. Inf. Theory*, vol. 49, no. 5, pp. 1073-1096, May 2003.

[13] S. Shamai and A. Steiner, "A broadcast approach for a single-user slowly fading MIMO channel," *IEEE Trans. Inf. Theory*, vol. 49, no. 10, pp. 2617-2635, Oct. 2003.

[14] C. T. K. Ng, , D. Gunduz, A. J. Goldsmith, and E. Erkip, "Distortion Minimization in Gaussian Layered Broadcast Coding With Successive Refinement," *IEEE Trans. Inf. Theory*, vol. 55, no. 11, pp. 5074-5086, Nov. 2009.

[15] J. N. Laneman, E. Martinian, G. W. Wornell, and J. G. Apostolopoulos, "Source-Channel Diversity for Parallel Channels," *IEEE Trans. Inf. Theory*, vol. 51, no. 10, pp. 3518-3539, Oct. 2005.

[16] S. Sesia, G. Caire, and G. Vivier, "Lossy Transmission over Slow-Fading AWGN Channels: A Comparison of Progressive and Superposition and Hybrid Approaches," *Proc. IEEE Int. Symp. Inf. Theory*, pp. 224-228, Sep. 2005.

[17] F. Etemadi, H. Jafarkhani, "Optimal Layered Transmission Over Quasi-Static Fading Channels," Proc. IEEE Int. Symp. Information Theory, pp. 1051–1055, Sep 2006.

[18] G. Gunduz, D. Deniz, and E. Erkip, "Joint Source-Channel Codes for MIMO Block-Fading Channels," *IEEE Trans. Info. Theory*, vol. 54, no. 1, pp. 116-134, Jan 2008.

[19] K. Bhattad, K. R. Narayanan, and G. Caire, "On the Distortion SNR Exponent of Some Layered Transmission Schemes," *IEEE Trans. on Info. Theory* vol. 54, no. 7 pp. 2943-2958, Jul 2008.

[20] G. Gunduz and E. Erkip, "Source and channel coding for cooperative relaying," *IEEE Trans. Inf. Theory Special Issue on Models, Theory, and Codes for Relaying and Cooperation in Communication Networks*, vol. 53, no. 10, pp. 3453-3475, Oct. 2007.

[21] K. Seddik, A. Kwasinski, and K.J. Ray Liu, "Asymptotic Distortion Performance of Source-Channel Diversity over Multihop and Relay Channels," *IEEE Trans. Mobile Computing*, vol. 9, no. 2, pp. 270-287, Feb 2010.

[22] J. Wang, J. Liang, and S. Muhaidat, "On the Distortion Exponents of Layered Broadcast Transmission in Multi-Relay Cooperative Networks," *IEEE Trans. Signal Process.*, vol. 58, no. 10, pp. 5340-5352, Oct. 2010.

[23] J. Laneman, D. Tse, and G. Wornell, "Cooperative diversity in wireless networks: Efficient protocols and outage behavior," *IEEE Trans. Inf. Theory*, vol. 50, no. 12, pp. 3062-3080, Dec. 2004.

[24] J. Wang, J. Soo, Y. H. Kim, I. Song, P.C. Cosman, and L.B. Milstein, "Cooperative Relaying of Superposition Coding with Simple Feedback for Layered Source Transmission," *IEEE Trans. Commun.*, vol. 61, no. 11, pp. 4448-4461, Nov 2013.

[25] T. T. Kim, M. Skoglund, and G. Caire, "On Source Transmission Over MIMO Channels With Limited Feedback," *IEEE Trans. Signal Process.*, vol. 57, no. 1, pp. 324-341, Jan 2009.

[26] J. Wang, J. Liang, and S. Muhaidat, "Distortion Exponents for Multi-Relay Cooperative Networks with Limited Feedback," *IEEE Trans. Veh. Technol.*, vol. 59, no. 7, pp. 3417-3426, Sep 2010.

[27] J. Wang, and J. Liang, "Distortion Exponents of Two-Way Relay Networks," *IEEE Trans Signal Process.*, vol 59, no. 9, pp. 4424-4437, Sep 2011.

[28] E. Aguerri, I. Estella , and D. Gunduz, "Distortion Exponent in MIMO Fading Channels With Time-Varying Source Side Information," *IEEE Trans. Info. Theory*, vol. 62, no. 6 pp. 3597-3617, June 2016.

[29] S. Zhao, D. Tuninetti, R. Ansari, and D. Schonfeld, "On Achievable Distortion Exponents for a Gaussian Source Transmitted Over Parallel Gaussian Channels With Correlated Fading and Asymmetric SNRs," *IEEE Trans. Info. Theory*, vol. 62, no. 7, pp. 4135-4153, Jul. 2016.

[30] T. Cover and A. El Gamal, "Capacity theorems for the relay channel," *IEEE Trans. Inf. Theory*, vol. 25, no. 5, pp. 572-584, May 1979.

[31] B. Rimoldi, "Successive Refinement of Information: Characterization of the Achievable Rates," *IEEE Trans. Inf. Theory*, vol. 40, no. 1, pp. 253-259, Jan. 1994.

[32] F. Etemadi, H. Jafarkhani, "Joint Source-Channel Coding for Quasi-Static Fading Channels with Quantized Feedback," *Proc. IEEE Int. Symp. Information Theory*, pp. 2241-2245, Jun. 2005.

[33] Y. Sheng, J. -C. Belfiore, "Optimal space-time codes for the MIMO amplify-and-forward cooperative channel," *IEEE Trans. Inf. Theory,* vol.53, no.2 PP. 647-663, Feb. 2007.

[34] U. Sethakaset, T. Quek, and S. Sun, "Joint Source-Channel Optimization over Wireless Relay Networks," *IEEE Trans. Commun.*, vol. 59, no. 4, pp. 1114-1122, Apr. 2011.

[35] J. N. Laneman, G. W. Wornell, "Distributed space-time-coded protocols for exploiting cooperative diversity in wireless networks," *IEEE Trans. Inf. Theory*, vol. 49, no. 10, pp. 2415-2425, Oct. 2003.

[36] G. Caire, and K. Narayanan, "On the Distortion SNR Exponent of Hybrid Digital-Analog Space-Time Coding," *IEEE Trans. Info. Theory*, vol. 53, no. 8, pp. 2867-2878, Aug. 2007.

[37] J. She, J. Ho, Z. Chen, and P.-H. Ho, "Logical Superposition Coded Video Multicast/Broadcast," *IEEE Trans. Veh. Technol.*, vol. 66, no. 2, pp. 1379-1392, Feb. 2017

[38] J. Ho and P. -H. Ho, "On Transmission of Multiresolution Gaussian Sources over Noisy Relay Networks," *IEEE Trans. Wireless Commun.*, vol. 12, no. 7, pp. 3170-3179, Jul. 2013.

[39] P. Padidar, P. -H. Ho, Y. Ji, W. Duan, "A Deep Study on Layered Multi-Relay Non-Orthogonal Amplify-Forward Networks," *IEEE Trans. Wireless Commun.,* vol. 19, no. 1, pp. 354-366, Jan. 2020.

[40] R. U. Nabar, H. Bolcskei, F. W. Kneubuhler, "Fading relay channels: Performance limits and space-time signal design," *IEEE J. Select. Areas Commun.*, vol. 22, no. 6, pp. 1099-1109, Aug. 2004.

[41] D. Tse and P. Viswanath, *Fundamentals of wireless communication.* Cambridge, UK; New York: Cambridge University Press, 2005.

[42] T. Cover and J. Thomas, *Elements of information theory*, John Wiley Sons, 2005.

[43] A. El Gamal and Y-H Kim, *Network information theory*, Cambridge University Press, 2011.

[44] S. Boyd, and L. Vandenberghe. *Convex Optimization.* Cambridge: Cambridge University Press, 2004.

[45] T. Cover, "Broadcast channels," *IEEE Trans. Inf. Theory*, vol. 18, no. 1, pp. 2-14, Jan. 1972.

[46] P. Padidar, P. -H. Ho, and J. Ho, "Superposition Transmission of Layered Encoded Sources over Non-Orthogonal Amplify-Forward Relay Networks," *Proc. IEEE Wireless Commun. and Networking Conf.,* Istanbul, Turkey, pp. 1326-1331, Apr, 2014.

[47] J. She, F. Hou, P.-H. Ho, and L.-L. Xie, "IPTV over WiMAX: Key Success Factors, Challenges and Solutions," *IEEE Commun. Mag.*, vol. 45, no. 8, pp. 87-93, Aug. 2007.

[48] J. She, X. Yu, P.-H. Ho and E.-H. Yang, "A Cross-Layer Design Framework for Robust IPTV Services over IEEE 802.16 Networks," *IEEE J. Sel. Areas on Commun.*, vol. 27, no. 2, pp. 235-245, Feb. 2009.

[49] P. Padidar, P. -H. Ho, and J. Ho, "Layered Sources in Non-Orthogonal Amplify-Forward Relay Networks," *Proc. IEEE Wireless Commun. and Networking Conf.*, Shanghai, China, pp. 3260-3264, Apr. 2013.

[50] P. Padidar, P. -H. Ho, L. Peng, A. Haque,"A Novel Multi-layer Non-Orthogonal Amplify-and-Forward (NAF) Cooperative NOMA Codes for Internet of Things (IoT)," submitted to *IEEE Internet Things J.*

[51] Z. Ding, Z. Yang, P. Fan, and H. V. Poor, "On the performance of non-orthogonal multiple access in 5G systems with randomly deployed users," *IEEE Signal Process. Lett.*, vol. 21, no. 12, pp. 1501-1505, Dec. 2014.

[52] Z. Ding, P. Fan, H. V. Poor, "Impact of User Pairing on 5G Nonorthogonal Multiple-Access Downlink Transmissions,"*IEEE Trans. Veh. Technol.*, vol. 65, no. 8, pp. 6010-6023, Aug. 2016.

[53] B, Kimy, S. Lim, H. Kim, S. Suh, J. Kwun, S. Choi, C. Lee, S. Lee, D. Hong, "Non-orthogonal multiple access in a downlink multiuser beamforming system," *Proc. IEEE Military Commun. Conf. (MILCOM)*, pp. 1278-1283, Nov. 2013.

[54] A. Pastore and M. Navarro, "A Fairness-Throughput Tradeoff Perspective on NOMA Multiresolution Broadcasting," *IEEE Trans. Broadcast.*, vol. 65 , no. 1, pp. 179-186, Mar.2018.

[55] X. Wang, J. Wang, L. He, J. Song, "Spectral Efficiency Analysis for Spatial Modulation Aided Layered Division Multiplexing Systems With Gaussian and Finite Alphabet Inputs," *IEEE Trans. Broadcast.*, vol. 64, no. 4, pp. 909-914, Dec. 2018.

[56] Y. Zhang, J. Ge, and E. Serpedin, "Performance Analysis of Non-Orthogonal Multiple Access for Downlink Networks with Antenna Selection Over Nakagami-m Fading Channels," *IEEE Trans. Veh. Technol.*, vol. 66, no. 11, pp. 10590-10594, Nov. 2017.

[57] Z. Ding, F. Adachi, H. V. Poor, " The Application of MIMO to Non-Orthogonal Multiple Access," *IEEE Trans. Wireless Commun.*, vol. 15, no. 1, pp 537-552, Jan. 2016.

[58] Z. Ding, R. Schober, H. V. Poor, "A General MIMO Framework for NOMA Downlink and Uplink Transmission Based on Signal Alignment," *IEEE Trans. Wireless Commun.*, vol. 15, no. 6, pp 4438-4454,, Mar. 2016.

[59] J. Choi, "On the Power Allocation for MIMO-NOMA Systems With Layered Transmissions, " *IEEE Trans. Wireless Commun.*, vol. 15, no. 5, pp 3226-3237, May 2016.

[60] Z. Ding, Z. Zhao, M. Peng, H. V. Poor, "On the Spectral Efficiency and Security Enhancements of NOMA Assisted Multicast-Unicast Streaming," *IEEE Trans. Commun.*, vol. 65, no. 7, pp. 3151-3163, Jul. 2017.

[61] J. Choi, "Minimum Power Multicast Beamforming With Superposition Coding for Multiresolution Broadcast and Application to NOMA Systems," *IEEE Trans. Commun.*, vol. 63, no. 3, pp. 791-800, Mar. 2015.

[62] J. -B. Kim, I. -H. Lee, "Capacity Analysis of Cooperative Relaying Systems Using Non-Orthogonal Multiple Access," *IEEE Commun. Lett.,* vol. 19, no. 11, pp. 1949-1952, Nov. 2015.

[63] J. -B. Kim, I.-H. Lee, "Non-Orthogonal Multiple Access in Coordinated Direct and Relay Transmission," *IEEE Commun. Lett.,* vol. 19, no. 11, pp. 2037-2040, Nov. 2015.

[64] J. Men, J. Ge, and C. Zhang, "Performance Analysis of Nonorthogonal Multiple Access for Relaying Networks over Nakagami-m Fading Channels," *IEEE Trans. Veh. Technol.,* vol. 66, no. 2, pp. 1200-1208, Feb. 2017.

[65] R. Jiao, L. Dai, J. Zhang, R. MacKenzie, and M. Hao, "On the Performance of NOMA-Based Cooperative Relaying Systems over Rician Fading Channels," *IEEE Trans. Veh. Technol.*, vol. 66, no. 12, pp. 11409-11413, Dec. 2017.

[66] D. Zhang, Y. Liu, Z. Ding, Z. Zhou, A. Nallanathan, and T. Sato, "Performance Analysis of Non-Regenerative Massive-MIMO-NOMA Relay Systems for 5G," *IEEE Trans. Commun.,* vol. 65, no. 11, pp. 4777-4790, Nov. 2017.

[67] Z. Ding, H. Dai, and H. V. Poor, "Relay Selection for Cooperative NOMA," *IEEE Wireless Commun. Lett.*, vol. 5, no. 4, pp. 416-419, Apr. 2016.

[68] X. Liang, Y. Wu, D. W. K. Ng, Y. Zuo, S. Jin and H. Zhu, "Outage Performance for Cooperative NOMA Transmission with an AF Relay," *IEEE Commun. Lett.,* vol. 21, no. 11, pp. 2428-2431, Nov. 2017.

[69] L. Zhang, J. Liu, M. Xiao, G. Wu, Y.-C. Liang, and S. Li, "Performance analysis and optimization in downlink NOMA systems with cooperative full-duplex relaying," *IEEE J. Select. Areas Commun.*, vol. 35, no. 10, pp. 2398-2412, Oct. 2017.

[70] J. So, Y. Sung, "Improving Non-Orthogonal Multiple Access by Forming Relaying Broadcast Channels," *IEEE Commun. Lett.,* vol. 20, no. 9, pp. 1816-1819, Sep. 2016.

[71] P. Padidar, P. -H. Ho, J. Ho, "End-to-end distortion analysis of multicasting over orthogonal receive component decode-forward cooperative broadcast channels," *Proc. IEEE WCNC'16.*

[72] , Z. Ding, Y. Liu, J. Choi, Q. Sun, M. Elkashlan, C. -L. I, H. V. Poor, "Application of Non-Orthogonal Multiple Access in LTE and 5G Networks," vol. 55, no. 2, pp. 185-191, Feb. 2017.

[73] P. Padidar, , P. -H. Ho, L. Peng, "End-to-end Distortion Analysis of Non-orthogonal Layered Coding over Relay-Assisted Networks," *IEEE Syst. J.*, 2020.

[74] Z. Zhang, Z. Ma, X. Lei, M. Xiao, C.-X. Wang, and P. Fan, "Power Domain Non-Orthogonal Transmission for Cellular Mobile Broadcasting: Basic Scheme, System Design, and Coverage Performance," *IEEE Wireless Commun.*, vol. 25, no. 2, pp. 90-99, Apr. 2018.

[75] L. Yang, J. Chen, Q. Ni, J. Shi, X. Xue, "NOMA-Enabled Cooperative Unicast-Multicast: Design and Outage Analysis," *IEEE trans. Wireless Commun.,* vol. 16, no. 12, pp. 7870-7889, Dec. 2017.

[76] L. Lv, J. Chen, Q. Ni, Z. Ding, "Design of Cooperative Non-Orthogonal Multicast Cognitive Multiple Access for 5G Systems, User Scheduling and Performance Analysis," *IEEE Trnas. Commun.,* vol. 65, no. 6, pp. 2641-2656, Jun. 2017.

[77] , P. Padidar, P. -H. Ho, L. Peng, A. Haque, "On the Performance of NOMA-based Distributed Cooperative Multi-layer Multicast with spatially random users," submitted to *IEEE GLOBECOM* 2020.

[78] Z. Zhang, Z. Ma, Y. Xiao, M. Xiao, G. K. Karagiannidis, P. Fan, "Non-Orthogonal Multiple Access for Cooperative Multicast Millimeter Wave Wireless Networks," *IEEE J. Sel. Areas Commun.*, vol. 35, no. 8, pp. 1794-1808, Aug. 2017.

[79] Y. Gao, B. Xia, K. Xiao, Z. Chen, X. Li, and S. Zhang, "Theoretical analysis of the dynamic decode ordering SIC receiver for uplink noma systems," *IEEE Commun. Lett.*, vol. 21, no. 10, pp. 2246-2249, Oct. 2017.

[80] Y. Chen, L. Wang, and B. Jiao, "Cooperative multicast non-orthogonal multiple access in cognitive radio," *Proc. IEEE ICC*, Paris, France, pp. 1–6, May 2017.

[81] H. V. Zhao, W. Su, "Cooperative wireless multicast: performance analysis and power/location optimization," *IEEE Trans. Wireless Commun.*, vol. 9, no. 6, pp. 2088-2100, Jun. 2010.

[82] M. Al-Imari, P. Xiao, M. A. Imran, and R. Tafazolli, "Uplink nonorthogonal multiple access for 5G wireless networks," *Proc. 11th Int. Symp. Wireless Commun. Syst. (ISWCS),* pp. 781-785, Aug. 2014.

[83] N. Zhang, J. Wang, G. Kang, Y. Liu, "Uplink Nonorthogonal Multiple Access in 5G Systems,"*IEEE Commun. Lett.,* vol. 20, no. 3, pp. 458-461, Jan. 2015.

[84] Y. Liu, M. Derakhshani, S. Lambotharan, "Outage Analysis and Power Allocation in Uplink Non-Orthogonal Multiple Access Systems," *IEEE Commun. Lett.,* vol. 22, no. 2, pp. 336-339, Feb. 2018.

[85] J. Choi, "On power and rate allocation for coded uplink NOMA in a multicarrier system," *IEEE Trans. Commun.*, vol. 66, no. 6, pp. 2762-2772, Jun. 2018.

[86] H. Tabassum, M. S. Ali, E. Hossain, M. J. Hossain, D. I. Kim, "Uplink vs. downlink NOMA in cellular networks: Challenges and research directions," *Proc. IEEE Veh. Technol. Conf. (VTC Spring)*, pp. 1-7, Jun. 2017.

[87] Y. Endo, Y. Kishiyama, and K. Higuchi, "Uplink non-orthogonal access with MMSE-SIC in the presence of inter-cell interference," *Proc. IEEE ISWCS*, Paris, France, Aug. 2012.

[88] Z. Zhang, H. Sun, and R.Q. Hu, "Downlink and uplink nonorthogonal multiple access in a dense wireless network," *IEEE J. Sel. Areas Commun.*, vol. 35, no. 17, pp. 2771-2784, Dec. 2017.

[89] M. F. Kader and S. Y. Shin, "Coordinated direct and relay transmission using uplink NOMA," *IEEE Wireless Commun. Lett.*, vol. 7, no. 8, pp. 400-403, Jun. 2018.

[90] H. Liu, N. I. Miridakis, T. A. Tsiftsis, K. J. Kim, K. S. Kwak, "Coordinated uplink transmission for cooperative NOMA systems", *Proc. IEEE Global Commun. Conf. (Globecom)*, pp. 1-6, Dec. 2018.

[91] W. Mei and R. Zhang, "Uplink cooperative NOMA for cellular-connected UAV," *IEEE J. Sel. Topics Signal Process.*, vol. 13, no. 3, pp. 644-656, Jun. 2019

[92] S. Abdel-Razeq, S. Zhou, R. Bansal, M. Zhao, "Uplink NOMA transmissions in a cooperative relay network based on statistical channel state information," *IET Commun.,* vol. 13, no. 4, pp. 371-378, Mar. 2019.

[93] Y. Zhang, Z. Yang, Y. Feng, and S. Yan, "Performance analysis of a novel uplink cooperative NOMA system with full-duplex relaying," *IET Communications*, vol. 12, no. 19, pp. 2408-2417, 2018.

[94] W. Shin, H. Yang, M. Vaezi, J. Lee, H. V. Poor, "Relay-aided NOMA in uplink cellular networks", *IEEE Signal Process. Lett.*, vol. 24, no. 12, pp. 1842-1846, Dec. 2017.

[95] W. Feller, *An introduction to probability theory and its applications*, John Wiley & Sons, 1968.

List of Publications

[1] **P. Padidar**, P. -H. Ho, Y. Ji, W. Duan, "A Deep Study on Layered Multi-Relay Non-Orthogonal Amplify-Forward Networks," *IEEE Trans. Wireless Commun.*, vol. 19, no. 1, pp. 354-366, Jan. 2020.

[2] **P. Padidar**, P. -H. Ho, L. Peng, A. Haque,"A Novel Multi-layer Non-Orthogonal Amplify-and-Forward (NAF) Cooperative NOMA Codes for Internet of Things (IoT)," submitted to *IEEE Internet Things J.*

[3] **P. Padidar**, , P. -H. Ho, L. Peng, "End-to-end Distortion Analysis of Non-orthogonal Layered Coding over Relay-Assisted Networks," *IEEE Syst. J.*, 2020.

[4] P. -H. Ho, **P. Padidar**, L. Peng, A. Haque,"Distortion Exponent Analysis of Successive Refinement Source Code over Layered Multi-Relay Non-Orthogonal Amplify-Forward Networks," The 35th ACM/SIGAPP Symposium On Applied Computing, 2020.

[5] W. Duan, Y. Ji, M. Wen, **P. Padidar**, P. -H. Ho, "Spectral Efciency Enhanced Cooperative Device-to-Device Systems with Non-orthogonal Multiple Access for IoT," *IEEE Internet Things J*, 2020.

[6] **P. Padidar**, P. -H. Ho, L. Peng, A. Haque, "On the Performance of NOMA-based Distributed Cooperative Multi-layer Multicast with spatially random users," submitted to *IEEE GLOBECOM*, 2020.

[7] **P. Padidar**, P. -H. Ho, J. Ho, "End-to-end distortion analysis of multicasting over orthogonal receive component decode-forward cooperative broadcast channels," *Proc. IEEE WCNC'16*.

[8] Z. Chen, P. -H. Ho, J. She, **P. Padidar**, "Energy optimal multi-resolution multicast with asynchronous relaying," *Proc. IEEE WCNC'16*.

[9] Z. Chen, P. -H. Ho, J. She, K. Naik, **P. Padidar**,"Optimal joint source-relay multi-resolution multicast networks,"*Proc. IEEE WCNC'16*.

[10] **P. Padidar**, P. -H. Ho, J. Ho,"Superposition transmission of layered encoded sources over non-orthogonal amplify-forward relay networks," *Proc. IEEE WCNC'14*.

[11] **P. Padidar**, P. -H. Ho, J. Ho,"Layered sources in non-orthogonal amplify-forward

relay networks, *Proc. IEEE WCNC'13*.

Appendix A

Proofs of Theorems from chapter 3

A.1 Proof of Theorem 3.3.1

Considering the M-layer non-orthogonal layered code over NAF network model of (3.20), assuming lower layers $[1:k-1]$ are decoded and subtracted from the received signal and considering the higher layers $[k+1:M]$ as interference term to the received signal of layer k, the outage event O_k for layer k is defined as

$$O_k = \{G : \mathcal{I}^k < R_k\} \tag{A.1}$$

$$= \{G : \frac{1}{2L} I(\mathbf{x}_k; \mathbf{y}_k) < R_k\}, \tag{A.2}$$

where $I(\mathbf{x}_k; \mathbf{y}_k)$ is given in (3.22). Replacing β_j with the value given in (3.11), and assuming the high SNR regime, where $\rho \to +\infty$, the mutual information term of (3.22) can be written as

$$I(\mathbf{x}_k;\mathbf{y}_k) = \tag{A.3}$$

$$\sum_{j=1}^{L} \log \frac{(1+g_{d,s}^2\bar{\rho}_k)^2(1+g_{j,s}^2)+g_{j,s}^2 g_{d,j}^2 \bar{\rho}_k}{(1+g_{d,s}^2\bar{\rho}_{k+1}^2)^2(1+g_{j,s}^2)+g_{j,s}^2 g_{d,j}^2 \bar{\rho}_{k+1}}. \tag{A.4}$$

Let vector $\mathbf{u} = \big(u, \{v_j\}_{j=1}^L, \{w_j\}_{j=1}^L\big)$, be the exponential order of channel gain vector

$$\big(\frac{1}{|g_{d,s}|^2}, \{\frac{1}{|g_{j,s}|^2}\}_{j=1}^L, \{\frac{1}{|g_{d,j}|^2}\}_{j=1}^L\big). \tag{A.5}$$

Considering r_k, the multiplexing gain of each layer, defined as $R_k = r_k \log \rho$. Assuming the aggregate power allocation coefficients in (4.31), the power allocated to each layer k is the difference of two consecutive aggregate power gains,

$$\rho_k = \rho^{\gamma_k} - \rho^{\gamma_{k+1}}, k = 1, ..., M-1, \tag{A.6}$$
$$\rho_M = \rho^{\gamma_M}. \tag{A.7}$$

Letting $\rho \to \infty$, the high SNR outage event of layer k denoted by O'_k is

$$O'_k = \big\{\mathbf{u} : \mathcal{I}^k < R_k\big\} \tag{A.8}$$
$$= \big\{\mathbf{u} : I(\mathbf{x}_k; \mathbf{y}_k) < 2Lr_k \log \rho\big\}. \tag{A.9}$$

Deploying the power allocation of (A.6), the high SNR outage event O'_k, in terms of the exponential order vector and the aggregate power allocation coefficients is

$$O'_k = \big\{\mathbf{u} : \sum_{j=1}^{L} \log \frac{(1+\rho^{\gamma_k - u})^2(1+\rho^{-v_j}) + \rho^{\gamma_k - v_j - w_j}}{(1+\rho^{\gamma_{k+1} - u})^2(1+\rho^{-v_j}) + \rho^{\gamma_{k+1} - v_j - w_j}} < 2Lr_k \log \rho\big\}. \tag{A.10}$$

The outage event can be written as

$$O'_k = \big\{\mathbf{u} : \frac{(1+\rho^{\gamma_k - u})^{2L}}{(1+\rho^{\gamma_{k+1} - u})^{2L}} < \rho^{2Lr_k}, \sum_{j=1}^{L} \frac{1+\rho^{\gamma_k - v_j - w_j}}{1+\rho^{\gamma_{k+1} - v_j - w_j}} < \rho^{2Lr_k}\big\}, \tag{A.11}$$

and we have

$$O'_k = \big\{\mathbf{u} : 1 + \rho^{\gamma_k - u} - \rho^{r_k + \gamma_{k+1} - u} < \rho^{r_k}, 1 + \rho^{L\gamma_k - \sum_{j=1}^{L} v_j + w_j} - \rho^{2Lr_k + L\gamma_{k+1} - \sum_{j=1}^{L} v_j + w_j} < \rho^{2Lr_k}\big\}. \tag{A.12}$$

We define $\gamma_k, k \in [1 : M]$, the exponents of the aggregate power allocation coefficient in (A.6) recursively as

$$\gamma_{k+1} = \gamma_k - 2r_k - \epsilon,$$
$$\gamma_1 = 1 - \epsilon, \tag{A.13}$$

for some $\epsilon > 0$. Plugging into (A.12), the high SNR layered outage event can be written as

$$O'_k = \big\{\mathbf{u} : \gamma_k - u < r_k, \\ L\gamma_k - \sum_{j=1}^{L} v_j + w_j < 2Lr_k\big\}. \tag{A.14}$$

Consequently the following lower bounds on the channel gains' SNR exponents for $\mathbf{u} \in \mathcal{O}'_k$, can be derived

$$\begin{cases} u > \gamma_k - r_k, \\ \sum_{j=1}^{L} v_j + w_j > L\gamma_k - 2Lr_k. \end{cases} \tag{A.15}$$

Provided the recursive power allocation coefficients given in (A.13), the power allocation exponents for each layer in terms of the multiplexing gains is

$$\gamma_k = 1 - 2\sum_{i=1}^{k-1} r_i - k\epsilon. \tag{A.16}$$

The probability of outage is defined as

$$P_{O'_k} = \int_{O'_k} p_{\mathbf{u}}(\mathbf{u}) d\mathbf{u}. \tag{A.17}$$

We follow similar steps of identifying the typical outage event, used in [11] and [12] to calculate the outage probability $P_{O'_k}$. the following lemma is used to derive the integral in (A.17).

[11, Result 5]: Assuming a Gaussian random variable g and denoting $-u$ as the exponential order of $|g|^2$. The probability density function of u can be shown to be,

$$p_U(u) = \lim_{\rho \to +\infty} \ln(\rho) \rho^{-u} \exp\left(-\rho^{-u}\right). \tag{A.18}$$

For independent random variables $\{u_j\}_{j=1}^{M}$ distributed identically to u, the probability P_O that $(u_1, ..., u_M)$ belongs to set O can be characterized

$$P_O = d^{-d_o}, \text{ for } d_o = \inf_{(u_1,u_2,...,u_M) \in O^+} \sum_{j=1}^{M} u_j. \tag{A.19}$$

This lemma identifies the typical outage event, which has the dominant probability. We deploy this lemma for the SNR exponent computation of the outage probability in high SNR. The probability of high SNR outage event (A.17) can be derived as

$$P_{O'_k} \doteq \rho^{-d_k(r_k)}, \tag{A.20}$$

where $d_k(r_k)$ is the SNR exponent of outage event and is given by

$$d_k(r_k) = \inf_{\mathbf{u}\in O'_k} u + \sum_{j=1}^{L}(v_j + w_j). \tag{A.21}$$

Considering the lower bounds on the exponent order of channel gains, given in (A.15), replacing the power allocation coefficients in (A.15) with the values in (A.16), the $d_k(r_k)$ in (A.21) can be calculated as

$$d_k(r_k) = (1 - 2\sum_{i=1}^{k-1} r_i - r_k) + L(1 - 2\sum_{i=1}^{k} r_i)^+. \tag{A.22}$$

This completes the proof of theorem 3.3.1. □

A.2 Proof of Theorem 3.3.2

Similar to the proof of theorem 3.3.1 given in previous section, and assuming having 1-bit feedback to the source per each relaying link, considering the outage event of (A.12), and having $\gamma_1 = 1 - \epsilon$, we apply the adaptive power allocation

$$\begin{cases} \gamma_{k+1} & = \gamma_k - 2r_k - \epsilon, \\ & \quad 2(\gamma_k - u) \geq \gamma_k - 1/L \sum_{j=1}^{L} (v_j + w_j), \\ \gamma_{k+1} & = \gamma_k - r_k - \epsilon, \text{ other wise,} \end{cases} \tag{A.23}$$

based on the received 1-bit feedback and identifying the dominant link between the direct link and the relayed link. Hence the lower bounds on the channel gains exponent vector $\mathbf{u}$ becomes

$$\begin{cases} u > 1 - \sum_{i=1}^{k-1} r_i - k\epsilon \\ \sum_{j=1}^{L} v_j + w_j > 1 - 2L \sum_{i=1}^{k-1} 2r_i \end{cases} \tag{A.24}$$

Following similar steps to the proof of theorem 3.3.1, the outage event probability in high SNR regime can be calculated. Deploying the power allocation given in (A.23), will lead to the diversity gain of (3.33) for the network with 1-bit feedback link.

This completes the proof of theorem 3.3.2. □

A.3 Proof of Lemma 3.4.1

We intend to optimize the expected distortion in (3.35) by assigning the optimal multiplexing gains. The optimization problem can be written as

$$-\min -b\sum_{i=1}^{M} r_i \tag{A.25}$$

$$\text{s.t. } b\sum_{i=1}^{M} r_i \leq d(r_k) + b\sum_{i=1}^{k} r_i, k \in [0:M]. \tag{A.26}$$

We form the Lagrangian

$$L = -b\sum_{i=1}^{M} r_i + \sum_{k=0}^{M} \mu_k \big(b\sum_{i=k+1}^{M} r_i - d(r_k)\big). \tag{A.27}$$

The optimization problem (A.25) is a linear programming problem and we solve it by setting the gradient of L equal to zero. Applying the KKT conditions [44], we have

$$\begin{cases} \nabla L = 0 \\ \mu_k \big(b\sum_{i=k+1}^{M} r_i - d(r_k)\big) = 0, k \in [0, M] \\ \mu_k \geq 0, k \in [0, M]. \end{cases} \tag{A.28}$$

Solving $\partial L/\partial r_i = 0$ for $i \in [0, M]$, the coefficients μ_k are

$$\mu_{k+1} = \frac{b-1}{1+2L}\mu_k, \tag{A.29}$$

where $\mu_0 = \frac{b}{1+b^3}$. Hence for $b > 1$ the $\mu_k, k \in [0, M]$ are strictly positive. Therefore for the minimizer $(r_1, r_2, ..., r_M)$, we have

$$b\sum_{i=k+1}^{M} r_i - d(r_k) = 0, k \in [1, M]. \tag{A.30}$$

This completes the proof of lemma 3.4.1. □

A.4 Proof of Theorem 3.4.2

Based on the result of lemma 3.4.1, the exponent for each $k \in [0 : M]$ in (3.37) is

$$d(r_k) + b(r_1 + ... + r_{k+1}), \tag{A.31}$$

Replacing the value of diversity gain of each layer with the optimal value of (3.31), given by theorem 3.3.1 and putting the terms equal to each other, we get $M+1$ cases for multiplexing gain assignment. For the case $k \in [1 : M+1]$, we assume

$$1 - 2r_1 - ... - 2r_{k-1} \geq 0, \tag{A.32}$$
$$1 - 2r_1 - ... - 2r_k < 0. \tag{A.33}$$

For $i = 0...k-2$, we have

$$r_1 = (\frac{2L+1}{b-1})^{k-2} r_{k-1}. \tag{A.34}$$

For $i = k-1, ..., M$, we have

$$r_M = (b-1)^{M-k} r_k. \tag{A.35}$$

Setting the two terms of $i = k-2$ and $i = k-1$ equal to the last term in (A.31), the values for r_{k-1} and r_k can be find as

$$r_{k-1} = \frac{1 + L(1 + bC_k)}{(bC_k + 1)(b-1) + 2A_{k-1}(1 + L(bC_k + 1))}, \tag{A.36}$$
$$r_k = \frac{b-1}{(bC_k + 1)(b-1) + 2A_{k-1}(1 + L(bC_k + 1))}. \tag{A.37}$$

where A_k and C_k are given in (3.40). Distortion exponent is given by

$$\Delta = b(r_1 + ... + r_n) \tag{A.38}$$
$$= b(r_1 + ... + r_{k-1}) + b(r_k + ... + r_n) \tag{A.39}$$
$$= bA_{k-1}r_{k-1} + bC_k r_k. \tag{A.40}$$

Replacing the r_{k-1} and r_k with values of (A.36) gets to the result of DE given in (3.39). This completes the proof for theorem 3.4.2. $\square$

A.4.1 Proof of Theorem 3.4.5

We follow similar steps to the proof of Theorem 3.4.2. Having derived the diversity gains of layered code for the 1-bit feedback network, in Theorem 3.3.2, we replace the $d_k(r_k)$ in (A.31) with the values of (3.33). Hence the rates of each layer is

$$r_i = (\frac{2L+1}{b})^{k-1-i} r_{k-1}, \tag{A.41}$$

for $1 \leq i < k-1$ and is

$$r_i = b^{M-k} r_k, \tag{A.42}$$

for $k < i \leq M$, where for layer k we have

$$1 - 2r_1 - ... - 2r_{k-1} \geq 0, \tag{A.43}$$

$$1 - 2r_1 - ... - 2r_k < 0. \tag{A.44}$$

Hence the diversity gain of layer $k-1$ and layer k can be computed as

$$r_k = \frac{b + A_{k-1}L}{(1+bC_k)(b + A_{k-1} + 2LA_{k-1}) - A_{k-1}bC_k}, \tag{A.45}$$

$$r_{k-1} = \frac{1 + L + LbC_k}{(1+bC_k)(b + A_{k-1} + 2LA_{k-1}) - A_{k-1}bC_k}, \tag{A.46}$$

where A_k and C_k are defined in (3.45). Having derived the values for $r_i, i \in [1:M]$ given in (A.41) and (A.42), the distortion exponent can be written as

$$\Delta_{fb} = b(r_1 + ... + r_M) \tag{A.47}$$

$$= b\sum_{i=1}^{k-1} (\frac{2L+1}{b})^{k-1-i} r_{k-1} + b\sum_{i=k}^{M} b^{i-k} r_k \tag{A.48}$$

Replacing the values for r_k and r_{k-1} given in (A.45), we derive the value given in (3.43) for Δ_{fb} and this completes the proof of theorem 3.4.3. □

A.5 Proof of Lemma 3.4.5

The expected distortion for the case of Q-level feedback is given in equation (3.50), where the cumulative distribution function is given by

$$F(y_i) = Pr\{G : I^{SL}(G) < y_i\}. \tag{A.49}$$

Hence $F(y_i)$ is equivalent to outage event if the rate is set to y_i. In high SNR regime, we define $y_i = r_i \log \rho$ where r_i is the corresponding multiplexing rate. Hence $ED^{SL-fb}(Q)$ in high SNR can be written as

$$ED^{SL-fb}(Q) = \sum_{i=0}^{Q} \left(P_{O_i} - P_{O_{i-1}}\right).2^{-br_{i-1}}. \tag{A.50}$$

As

$$\lim_{\gamma\to\infty} (P_{O_i} - P_{O_{i-1}}) = P_{O_i}, \tag{A.51}$$

(A.50) is simplified to

$$\lim_{\gamma\to\infty} ED^{SL-fb}(Q) = \sum_{i=0}^{Q} P_{O_i}.\rho^{-br_{i-1}}, \tag{A.52}$$

$$= \sum_{i=0}^{Q} \rho^{-d_{r_i}}.\rho^{-br_{i-1}} \tag{A.53}$$

Similar to the proof of lemma 3.4.1 it can be shown that the dominant term in the above summation is the term with minimum exponent, hence the ED^{SL-fb} is maximized if all the exponents $d_{r_i} + br_{i-1}$ are set equal to each other for $i \in [1 : Q]$. A system of linear equations with Q variable is formed. Applying the optimal multiplexing gain assignment to (A.52) achieves the DE given in (3.51). This completes the proof of lemma 3.4.5. □

A.5.1 Proof of Lemma 3.5.1

For the multi-hop MIMO setting, the probability of outage of layer k, assuming the lower layers are decoded, can be written as

$$P_{O_k} = (1 - P_{O_{k,r}}).P_{O_{k,d}} + P_{O_{k,r}}, \tag{A.54}$$

where $P_{O_{k,r}}$ is the outage event for layer k at relay node and $P_{O_{k,d}}$ is the outage event for layer k at destination. Given the αN channel uses for the source node and knowing the MIMO layered DMT as given in [18], applying the rate splitting with parameter α, we have

$$P_{O_{k,r}} \doteq \rho^{-d_{k,r}} \tag{A.55}$$

where

$$d_{k,r}(r_k) = mn_r(1 - \sum_{i=1}^{k-1} r_i) - (m + n_r - 1)\frac{r_k}{\alpha}. \tag{A.56}$$

Similarly for the $(1-\alpha)N$ channel uses of the relay node

$$d_{k,r}(r_k) = mn_r(1 - \sum_{i=1}^{k-1} r_i) - (m + n_r - 1)\frac{r_k}{1-\alpha}. \tag{A.57}$$

In high SNR regime

$$P_{O_k} \doteq (1 - \rho^{-d_{k,r}}).\rho^{-d_{k,s}} + \rho^{-d_{k,r}} \tag{A.58}$$

and can be simplified as

$$P_{O_k} \doteq \rho^{-d_{k,s}} + \rho^{-d_{k,r}} \tag{A.59}$$

P_{O_k} is dominated by the minimum of $\rho^{-d_{k,s}}$ and $\rho^{-d_{k,r}}$. Hence the optimum channel allocation, α, is the solution to equation (3.61). For the case of $n_s = n_d = m$, we set $d_{k,r}(r_k)$ given in (A.57) equal to $d_{k,d}(r_k)$ given in (A.56) to get the maximization solution to equation (3.61). It leads to a quadratic equation with optimizing solution $\alpha^* = 0.5$. Replacing α^* in (3.61) leads to (3.62). This completes the proof for 3.5.1. □

A.6 Proof of Lemma 3.5.2

The proof for DE optimization of multi-hop MIMO follows the steps of proofs of theorem 4.2 and theorem 4.3, hence we briefly give an outline.

The exponent term of expected distortion for each layer given in (3.35), considering the layered diversity gain of (3.62) is

$$mn_r(1 - \sum_{i=1}^{k-1} r_i) - 2(m + n_r - 1)r_k + b\sum_{i=1}^{k-1} r_i, \tag{A.60}$$

for $1 \leq k \leq M$. In order to minimize the expected distortion exponent, we set the terms given in (A.60) for the M layers equal to each other which leads to a system of linear

equation with M variables. For the case of $b < mn_r$, the following assignment of values can be shown as the solution,

$$r_1 = \frac{(mn_r - b)(mn_r)A^{M-1}}{(mn_r - b)A^M + b(A^M - C^M)}, \tag{A.61}$$

$$r_i = \big(1 + \frac{b - mn_r}{2(m+n-1)}\big)^{i-1} r_1, \ 2 \leq i \leq M, \tag{A.62}$$

where A and C are given in (3.64). For the case of $b > mn_r$, the optimal rate assignment can be solved to be

$$r_1 = \frac{mn_r}{bM + 2(m+n-1)}, \ 1 \leq i \leq M. \tag{A.63}$$

Applying the above assignment for $\{r_1\}_{i=1}^M$, leads to the optimal DE given in (3.63). This completes the proof for lemma 3.5.2. $\square$